Final report to DOE Terrestrial Ecosystem Sciences Program (TES), Office of Biological and Environmental Research (BER)

Water-carbon Links in a Tropical Forest: How Interbasin Groundwater Flow Affects Carbon Fluxes and Ecosystem Carbon Budgets

DE-SC0006703

David P. Genereux (PI), Christopher L. Osburn, Diana Oviedo Vargas
Department of Marine, Earth, and Atmospheric Sciences, NC State University, Raleigh, NC

Steven F. Oberbauer, Diego Dierick
Department of Biological Sciences, Florida International University, Miami, FL

Contents

Chapter 1: A connection to deep groundwater alters ecosystem carbon fluxes and budgets: example from a Costa Rican rainforest, page 2

Chapter 2: The effect of regional groundwater on carbon dioxide and methane emissions from a lowland rainforest stream in Costa Rica, page 15

Chapter 3: Chamber measurements of high CO_2 emissions from a rainforest stream receiving old C-rich regional groundwater, page 49

Chapter 4: Extreme effects of regional groundwater and storms on the quality and export of DOM in tropical streams, page 74

Chapter 5: Deep groundwater-derived CO_2 as a source for plant photosynthetic uptake in a Costa Rican rainforest, page 106

Chapter 1: A connection to deep groundwater alters ecosystem carbon fluxes and budgets: example from a Costa Rican rainforest

Key Points

- Discharge of regional groundwater can greatly alter ecosystem C concentrations and fluxes
- C chemical, isotopic, and flux signals in groundwater, surface water, and air are affected
- Effects may be critical in assessing the C budget & source/sink status of ecosystems from data

Abstract

Field studies of watershed carbon fluxes and budgets are critical for understanding the carbon cycle, but the role of deep regional groundwater is poorly known and field examples are lacking. Here we show that discharge of regional groundwater into a lowland Costa Rican rainforest has a major influence on ecosystem carbon fluxes. This influence is observable through chemical, isotopic, and flux signals in groundwater, surface water, and air. Not addressing the influence of regional groundwater in the field measurement program and data analysis would give a misleading impression of the overall carbon source or sink status of the rainforest. In quantifying a carbon budget with the traditional "small watershed" mass-balance approach, it would be critical at this site and likely many others to consider watershed inputs or losses associated with exchange between the ecosystem and the deeper hydrogeological system on which it sits.

Introduction

Quantitative understanding of carbon cycling in ecosystems is a topic of ongoing interest to geochemists, ecologists, and hydrologists, with important links to climate change [Battin et al. 2008; Cole et al. 2007]. The fundamental questions of whether some ecosystems operate as net sources or sinks of CO_2 to the atmosphere, and whether or when they may flip from sink to source upon warming, remain the focus of active inquiry and sometimes conflicting results. These questions are significant because ecosystems operating as net sources represent a positive feedback on warming.

A watershed is often used as a convenient subset of an ecosystem for organizing measurements and analysis of the carbon budget. Watersheds have long been used as practical field units for determination of water and solute fluxes and budgets [e.g., Likens and Bormann 1995], and doing so for carbon is in keeping with growing awareness of the critical connections between terrestrial water and carbon fluxes [Cole et al. 2007]. A potentially large but relatively unstudied factor in ecosystem carbon fluxes is the discharge of regional groundwater that is often high in dissolved carbon.

Interbasin groundwater flow (IGF), groundwater flow beneath surface topographic divides from one basin or watershed to another, is the natural hydrogeological process responsible for long-distance movement of regional groundwater from upland recharge areas to streams and wetlands in lowland watersheds [Tóth 2009]. Schaller and Fan [2009] argued for the importance of IGF to climate modeling efforts, on the basis of the water and heat energy transported. Here we focus on the carbon transported by IGF and its role in the watershed carbon budget. The fundamental motivating questions include: What field data are needed to know whether a rainforest (or other ecosystem) is a net source or sink of carbon, can regional groundwater be important, what measurable ecosystem signals (chemical, isotopic, or flux) are available to help decide, what are the implications for carbon fluxes in streams, and what are the potential errors if regional groundwater is important but ignored?

We assessed the influence of IGF on carbon fluxes and budgets in two small adjacent watersheds at La Selva Biological Station in the lowland tropical rainforest of Costa Rica (Fig. 1). The watersheds are identical or nearly so in all major features (rainfall, temperature, forest cover, soils, etc.), with one exception: the Arboleda watershed receives a significant influx of 3000-4000 year-old regional groundwater via IGF, while the Taconazo does not [Genereux et al. 2009, 2005]. The Taconazo has only young local groundwater several years or less in age [Solomon et al. 2010]. We utilized multiple chemical and isotopic signals for carbon, combined with hydrologic data to estimate fluxes.

Methods

Stream discharge (m^3/s) was measured every 15 minutes at V-notch weirs on the two watersheds during 2006-2009 (data are available at http://www.ots.ac.cr/meteoro/default.php?pestacion=2). Precipitation was measured at two tipping bucket rain gauges (one above the forest canopy on a tower and one about 2 m above ground in a forest clearing). Water samples for chemical analysis were collected on a weekly basis at the weirs, supplemented with additional event-based sampling. Details are in Zanon [2011], Nagy [2012], and Zanon et al. [2013]. Carbon export by stream flow was estimated using the flow-weighted mean concentration approach [Walling and

Webb 1985; Birgand et al. 2010]. Measurements of the CO_2 content of riparian air were made with gas analyzers (a LI-840 from LI-COR Inc, Lincoln, NE USA, and GMT 222 from Vaisala, Helsinki, Finland), simultaneous with collection of air samples for isotopic measurement in Exetainer sample vials (Labco, Buckinghamshire, England) using a 30 ml syringe. Carbon isotopic measurements were made at the NOSAMS facility at the Woods Hole Oceanographic Institution (DIC), at the University of California at Davis (CO_2 in air samples), and at NC State University (DOC).

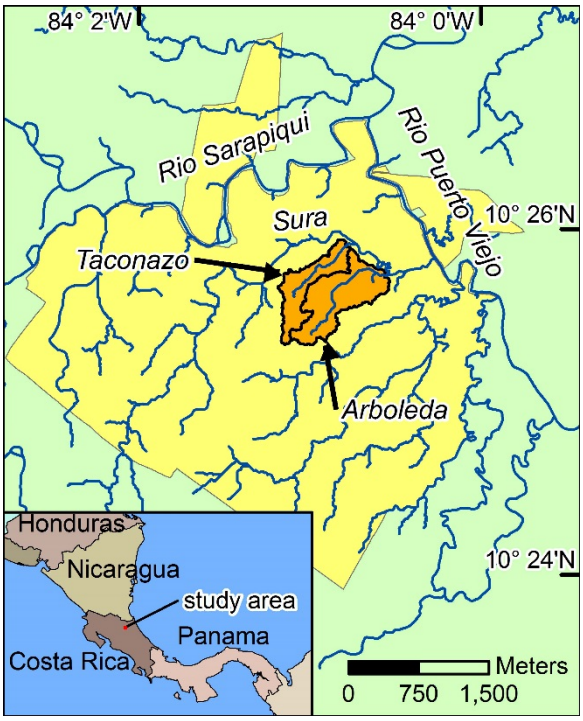

Figure 1. The Arboleda and Taconazo watersheds at La Selva Biological Station, Costa Rica.

Results

Comparing between the Taconazo and Arboleda streams (at the weirs), IGF increases the concentration of DIC by a factor of about 12, and stream export of DIC by a factor of about 70 (Table 1). IGF lowers the stream DOC concentration (old regional groundwater is lower in DOC than young groundwater), but increases DOC export by a factor of 3.5 (because of the large additional water throughput from IGF). The Taconazo DOC and DIC export values fall within published ranges for other small watersheds, while the Arboleda values augmented by IGF are higher (Fig. 2, Table 2).

Elevated DIC concentration and DIC and DOC export in the Arboleda are due to the large IGF into the Arboleda (about 10 m^3 of water per m^2 of watershed per year, or 10 m per year), much of which is high-DIC (14 mM) regional groundwater. The carbon input to the Arboleda by IGF was estimated to be about 870 gC/m^2yr, a value that is 24-32% of the magnitude of whole ecosystem respiration at La Selva [Cavaleri et al. 2008; Loescher et al. 2003]. The IGF carbon input is also at the upper end of the range for net ecosystem exchange (NEE) of CO_2 with the

atmosphere at La Selva: -5 to 800 gC/m^2yr (a positive value indicates an ecosystem sink), depending on the year and method of NEE estimation [Loescher et al. 2003]. In other words, the net carbon input to the Arboleda watershed "from below" (by IGF) is at least as large as the net input "from above" (NEE).

Parameter	Taconazo watershed	Arboleda watershed
area (ha)	27.9	46.1
air temperature[A,B] (°C)	25.1	25.1
precipitation[A,B] (mm/yr)	4341	4341
stream discharge[B] (mm/yr)	2390	12,725
stream DIC[B] (mM)	0.40	4.73
DIC export by stream[B] (gC/m^2yr)	9.6	683
stream DOC[C] (mM)	0.14	0.093
DOC export by stream[C] (gC/m^2yr)	4.0	14.1
$\delta^{13}C$ of stream DIC[C] (‰)	-22.35	-4.39
$\delta^{13}C$ of stream DOC[E] (‰)	-30.21	-27.85
^{14}C of stream DIC[C] (% modern)	108.7	17.7
CO_2 degassing from stream[B,D] (gC/m^2yr)	130	550
$\delta^{13}C$ of CO_2 in air above stream[E] (‰)	-14.8	-11.6
CO_2 in air just above stream[E] (ppm)	624	1081
DOM absorbance slope ratio S_R[C,E]	0.778	1.12

Table 1. Comparison of lowland rainforest watersheds with (Arboleda) and without (Taconazo) interbasin groundwater flow (IGF) of old regional groundwater, La Selva Biological Station, Costa Rica. All fluxes normalized by areas of watersheds.
superscripts: A = assumed equal for small adjacent watersheds, B = mean of 2007-2009 data, C = 2006 data, D = see assumptions in text, E = 2012 data

The low ^{14}C and high $\delta^{13}C$ of the DIC reaching the Arboleda from below are strongly consistent with the isotopic signature of magmatic CO_2 [Genereux et al. 2009 and references therein]. That is, the carbon entering the Arboleda in association with the water from IGF is from a geological source and not a result of any modern ecosystem process that differs between the Arboleda and the Taconazo.

Degassing of CO_2 from surface water has been shown to be a potentially significant carbon flux for terrestrial ecosystems [Oquist et al. 2009; Johnson et al. 2008; Teodoru et al. 2009; Richey et al. 2002; Hope et al. 2001]. We expect that the degassing flux from streams is much larger in the presence of IGF. An estimate of this flux based on the measured aqueous CO_2 concentrations in the Taconazo and Arboleda streams, the approximate stream surface areas, and an estimate of 75 day^{-1} for the first-order degassing rate constant (a reasonable value for small shallow streams; Hope et al. 2001; Genereux and Hemond 1992) suggests about 4 times more CO_2 degassing from the Arboleda stream than the Taconazo stream. Measurements of CO_2 concentration and the $\delta^{13}C$ of CO_2 in air just above the streamwater surface are consistent with an enhanced flux of isotopically-heavy CO_2 from the Arboleda stream. We sampled air above streams in the early morning (March, June, July, October, and November 2012) before daytime mixing of the canopy air began and found higher CO_2 concentration and heavier $\delta^{13}C$-CO_2 in air above the Arboleda stream compared to air above the Taconazo (Table 1). Concentrations of

CO_2 were highest in the Arboleda weir splash zone, but isotopically heavier CO_2 was also found above more quiescent streamwater about 150 m upstream of the Arboleda weir.

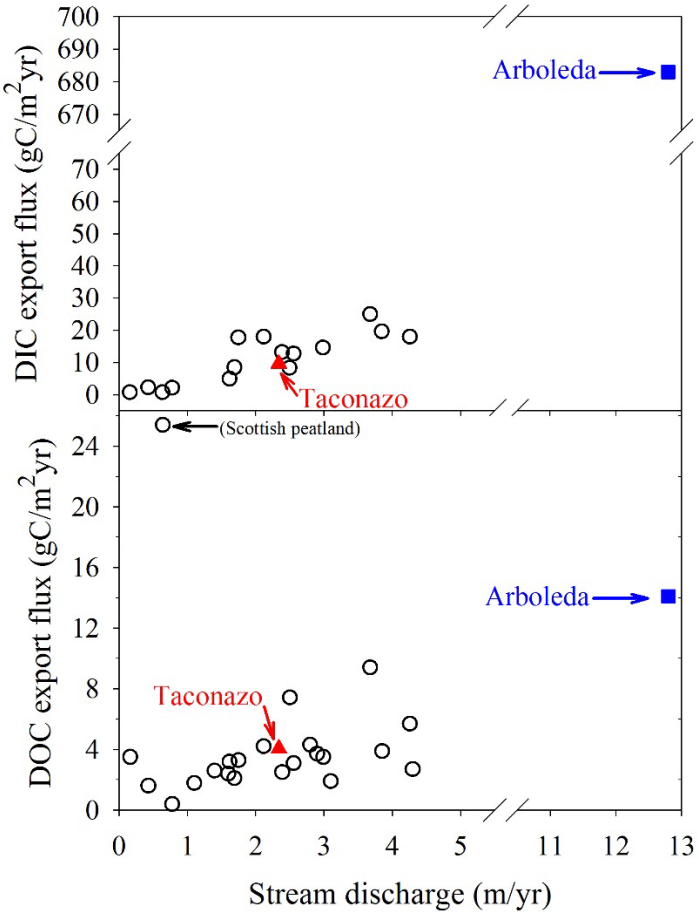

Figure 2. Annual DIC and DOC export vs. annual stream discharge for previous studies on watersheds <20 km^2 in area (open black circles), the Taconazo watershed (red triangle), and the Arboleda watershed (blue square). See Table 2.

Measurements of UV-visible light absorbance by dissolved organic matter (DOM) suggest that IGF of old groundwater alters the chemical nature of the DOM in streams as well as the concentration and export flux of its constituent carbon (DOC, Table 1). Slope ratio S_R was determined for the Taconazo and Arboleda stream DOM, and for groundwater from Guacimo Spring, a large spring discharging high-DIC regional groundwater. S_R is the ratio of the slope values from a linear fit, in two different wavelength ranges of light absorbance, of the logarithm of light absorbance vs. wavelength. Larger S_R values are associated with DOM that is relatively low in molecular mass and/or weakly-aromatic [Helms et al. 2008; Spencer et al. 2012]. With regard to S_R, the Arboleda was more variable than the Taconazo, and intermediate in magnitude between the Taconazo (local groundwater) and Guacimo Spring (regional groundwater), likely reflecting time-varying mixing of local and regional groundwaters (each with distinct DOM) in the Arboleda (Fig. 3).

S_R data indicate a qualitative difference in DOM chemistry between old regional groundwater and young local groundwater, likely that the former has become less aromatic and/or lower in molecular mass through partial microbial degradation during its long subsurface residence time.

We hypothesize that older degraded DOM from regional groundwater is less bioavailable in rainforest streams, compared to younger fresher DOM. If true this would suggest that IGF alters watershed export of DOC by two mechanisms: additional input of DOM to the watershed, and input of DOM that is less bioavailable and thus more likely to experience hydrologic export from the watershed and longer riverine transport. Also, given the similarity in δ^{13}C-DOC values between the Arboleda and Taconazo streams, it is unlikely that much of the geological DIC in the Arboleda is taken up there by photosynthesis. Uptake may occur downstream if streams receiving high-DIC IGF leave the rainforest where stream algae are light-limited [Pringle and Triska 1991] and enter pasture or other deforested areas.

Name	Location	Size (ha)	Precip (m/yr)	Runoff (m/yr)	pH	Alk (mN)	[DIC] (mM)	DIC Export (gC/m^2yr)	[DOC] (mM)	DOC Export (gC/m^2yr)
Taconazo[a]	Costa Rica	27.94	4.24	2.34	4.93	0.0205	0.4	9.62	0.14	4.05
Arboleda[a]	Costa Rica	46.14	4.24	12.8	6.11	2.25	4.73	683	0.09	14.1
Desbonnes[b]	Guadeloupe	550	1.79	0.78	7.11	0.372	0.436	2.1	0.09	0.4
Deshaies[b]	Guadeloupe	438	1.75	0.43	7.51	0.360	0.383	2.3	0.365	1.6
Moustique Sainte-Rose[b]	Guadeloupe	616	2.29	1.62	7.24	0.223	0.251	4.9	0.136	3.2
Bras-David[b]	Guadeloupe	1100	3.41	2.39	7.38	0.397	0.428	13.2	0.091	2.5
Corossol[b]	Guadeloupe	1252	--	--	7.75	0.393	0.407	12.5	0.123	3.3
Goyaves[b]	Guadeloupe	1440	3.45	2.56	7.51	0.423	0.447	12.8	0.103	3.1
Lostau[b]	Guadeloupe	804	2.74	1.69	7.74	0.607	0.630	8.5	0.156	2.1
Beaugendre[b]	Guadeloupe	817	2.72	2.12	7.42	0.672	0.712	18.0	0.168	4.2
Vieux-Habitants[b]	Guadeloupe	1910	3.83	3.85	7.71	0.397	0.412	19.6	0.093	3.9
Moustique Petit-Bourg[b]	Guadeloupe	1150	3.99	2.99	7.05	0.333	0.390	14.6	0.108	3.5
Capesterre[b]	Guadeloupe	1620	5.20	4.26	7.29	0.309	0.333	18.0	0.123	5.7
Icacos[c]	Puerto Rico	326	3.75	3.68	--	--	0.566	25.0	0.132	9.4
Sonadora[c]	Puerto Rico	262	3.75	2.5	--	--	0.278	8.34	0.177	7.43
Toronja[c]	Puerto Rico	16.2	3.75	1.75	--	--	0.844	17.7	0.113	3.3
Tempisquito[d]	Costa Rica	319	2.4	2.9	--	--	--	--	--	3.7
Tempisquito Sur[d]	Costa Rica	311	2.4	4.3	--	--	--	--	--	2.7
Kathia[d]	Costa Rica	264	2.4	3.1	--	--	--	--	--	1.9
Marilin[d]	Costa Rica	36	2.4	1.6	--	--	--	--	--	2.4
El Jobo[d]	Costa Rica	55	2.4	1.4	--	--	--	--	--	2.6
Zompopa[d]	Costa Rica	37	2.4	2.8	--	--	--	--	--	4.3
Black Burn[e]	Scotland	335	1.16	0.64	--	--	0.31	0.72	2.68	25.4
Igarape Asu[f]	Brazil	680	2.4	1.1	--	--	--	--	--	1.77
Mengong[g]	Cameroon	60	1.779	0.163	--	--	--	0.75	--	3.5

Table 2. Previous tropical studies of DIC and DOC export. [a]this study, [b]Lloret et al. (2011), [c]McDowell & Asbury (1994), [d]Newbold et al (1995), [e]Dinsmore et al. (2010), [f]Waterloo et al. (2006), [g]Brunet et al. (2009).

Discussion

IGF clearly alters carbon concentrations and fluxes, and the chemistry of DOM, in the Arboleda watershed at La Selva. Using La Selva as an example, a preliminary conceptual carbon flux diagram (Fig. 4) illustrates how knowledge of IGF could help avoid incorrect conclusions about the carbon source/sink status of a watershed.

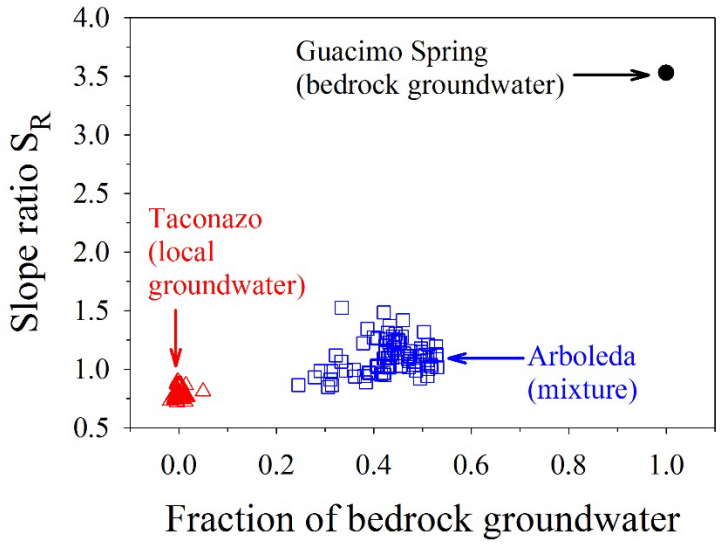

Figure 3. Slope ratio S_R vs. fraction of regional groundwater in the Taconazo stream (red triangles), Arboleda stream (blue squares), and Guacimo Spring (black circle). The fraction of regional groundwater in each sample was computed from its measured chloride concentration, taking Guacimo Spring (the highest-solute water at the study site) as 100% regional groundwater and average Taconazo streamwater as 0% regional groundwater (i.e., 100% young local groundwater).

Estimates of NEE at La Selva span a wide range from carbon-neutral to a strong ecosystem sink, depending on the year and calculation method used [Loescher et al. 2003]. On either watershed, considering direct CO_2 degassing from the stream separately from NEE (a possibility suggested for other sites by Dinsmore et al. [2010], Cole et al. [2007], Billet et al. [2004], and Hope et al. [2001]) could, at lower than average NEE values, shift the watershed from a net sink to a source of carbon. Bringing stream export of DIC and DOC into the budget picture does not have a major impact on source/sink status for the Taconazo, but it does for the Arboleda.

Summarizing for the Arboleda, in the presence of significant IGF:

1. assuming NEE alone represents the carbon budget would suggest that the watershed is on average a clear sink for CO_2, and
2. consideration of NEE, stream export, and stream degassing, without knowledge (based in part on the water budget) of the carbon input from IGF, would give the opposite conclusion, that the watershed is a clear source of CO_2.

Correct understanding of the watershed source/sink status requires (1) knowledge of the carbon input by IGF (which supports the large stream export flux of carbon), and (2) field estimation of all fluxes during the same time period (inter-annual variation may be large, as noted above for NEE).

Other examples of the importance of IGF to ecosystem carbon budgets are lacking in the literature, but the widespread occurrence of the two key factors (IGF, and elevated dissolved carbon in regional groundwater) gives strong reason to believe IGF may affect watershed carbon fluxes at other sites, with impacts ranging from small (and difficult to detect) to large (such as found at the Arboleda). Regional groundwater may acquire elevated dissolved carbon from magmatic outgassing, dissolution of carbonate minerals, dissolution-respiration-methanogenesis of sedimentary organic matter, or migration of carbon compounds from petroleum deposits. Even considering just magmatic outgassing alone, the extent of IGF-based effects on ecosystem carbon fluxes and budgets may be large, given that high topographic relief and active volcanism coincide over large areas (the entire Pacific rim, east Africa, parts of the northern Mediterranean, etc.). High DIC has been found in groundwater in many such areas, e.g., up to 45 mM [Evans et al. 2002] in the western U.S., up to 28 mM [Chiodini et al. 2000] in Italy, and up to 65 mM [Ohsawa et al. 2002] in Japan (the 14 mM from La Selva is not at the high end of the range globally).

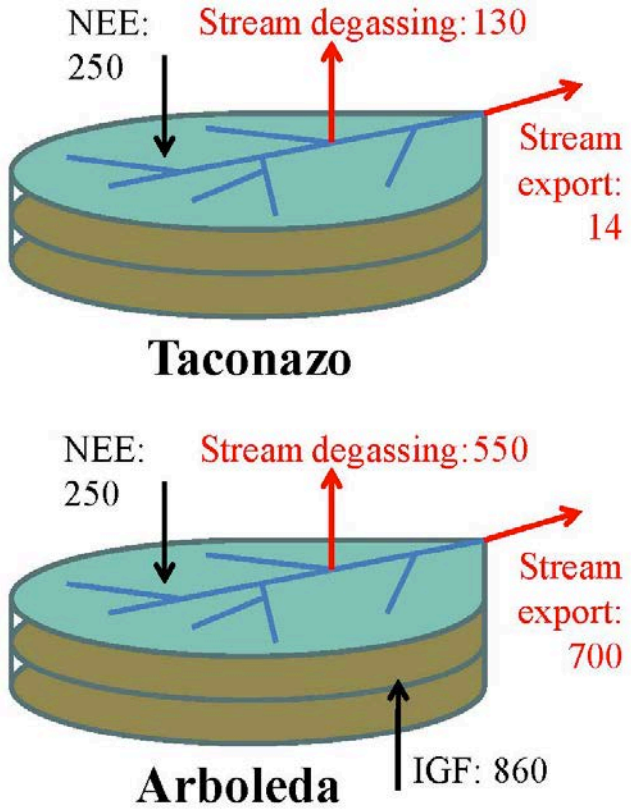

Figure 4. Carbon flux schematic for rainforest watersheds at La Selva with and without regional groundwater inputs by IGF (the Arboleda and Taconazo, respectively). Black arrows are inputs, red are outputs. Units are g C per m^2 of watershed per year. Stream export includes both DIC and DOC. NEE represents an average for 1998-2000 data (Loescher et al. 2003).

Elevated DIC is well known from carbonate rock aquifers, e.g., up to 5 mM in the Floridan aquifer of Florida [Plummer and Sprinkle 2001] and up to 15.9 mM in the Great Lakes region of the U.S. [McIntosh and Walter 2006]. Significant DIC, DOC, and/or dissolved methane occur in many primarily clastic regional aquifers in non-volcanic areas, such as the U.S. Atlantic coastal

plain, where DIC of 10-14 mM occurs in confined aquifers in the Carolinas [Chappelle and Lovley 1990; Kennedy and Genereux 2007], and lower but significant DIC (up to 3.3 mM) occurs in the Aquia aquifer of Maryland [Aeschbach-Hertig et al. 2002]. In the central U.S., Clark et al. [1998] found DIC up to 9 mM in the Dakota aquifer, and McMahon et al. [2004] found DIC up to 4.3 mM in the High Plains aquifer. Murphy et al. [1989] found DIC up to 14.2 mM, DOC up to 1.4 mM, and methane up to 13.3 mM in the Milk River aquifer, Canada. Aravena and Wassenaar [1993] found DOC up to 1.5 mM and methane up to 4.7 mM in the Alliston aquifer, Ontario, Canada.

Also, IGF is an expected part of the hydrologic cycle with a theoretical foundation in the relationship between topography and groundwater flowpaths at multiple spatial scales [e.g., Worman et al. 2007; Cardenas 2008; Tóth 2009]. IGF has been detected worldwide in both high- and low-relief topographic settings [e.g., Genereux et al. 2005 and references therein; Tóth, 2009; Kasper et al. 2010], though its global extent and magnitude are not fully known, in part because it can be costly to quantify, and perhaps in part because areas showing evidence of IGF may be avoided as long-term field research sites (IGF may be viewed as an unwanted complication in the determination of water or element fluxes and budgets in an experimental watershed). New research [e.g., Gleeson and Manning 2008; Frisbee et al. 2011; Gardner et al. 2011; Smerdon et al. 2012] continues to advance the hydrogeology of IGF and large-scale groundwater flowpaths to streams, but the significance for carbon budgets and fluxes remains relatively unexplored.

We suggest this is a significant gap, and an opportunity, in the study of carbon fluxes and the carbon source/sink status of watersheds and ecosystems. The connection between ecosystems and the deeper hydrogeological systems on which they sit may have strong relevance to understanding the carbon cycle and is ripe for further study.

Acknowledgements

Financial support from the U.S. National Science Foundation (awards 0421178 and 1029371) and U.S. Department of Energy (award DE-SC0006703) is gratefully acknowledged. Logistical support at the field site was provided by the Organization for Tropical Studies, especially William Ureña. Preparation of Figure 1 was by Carlo Zanon. Statements and opinions in this report are those of the authors and do not necessarily reflect the views of the sponsoring agencies.

References

Aeschbach-Hertig, W., M. Stute, J. F. Clark, R. F. Reuter, and P. Schlosser (2002), A paleotemperature record derived from dissolved noble gases in groundwater of the Aquia Aquifer (Maryland, USA), *GCA*, 66(5), 797-817.

Aravena, R., and L.I. Wassenaar. 1993. Dissolved organic carbon and methane in a regional confined aquifer, southern Ontario, Canada: Carbon isotopic evidence for associated subsurface sources. *App. Geochem.*, 8: 483-493.

Battin, T. J., L. A. Kaplan, S. Findlay, C. S. Hopkinson, E. Marti, A. I. Packman, J. D. Newbold, and F. Sabater (2008), Biophysical controls on organic carbon fluxes in fluvial networks, *Nature Geoscience*, 1, 95-100.

Billett, M. F., S. M. Palmer, D. Hope, C. Deacon, R. Storeton-West, K. J. Hargreaves, C. Flechard, and D. Fowler (2004), Linking land-atmosphere-stream carbon fluxes in a lowland peatland system, *Global Biogeochem. Cycles*, 18, GB1024, doi:10.1029/2003GB002058.

Birgand, F., C. Faucheux, G. Gruau, B. Augeard, F. Moatar, and P. Bordenave (2010), Uncertainties in assessing annual nitrate loads and concentration indicators: Part 1. Impact of sampling frequency and load estimation algorithms, *Trans. ASABE*, 53(2), 437-446.

Brunet, F., K. Dubois, J. Veizer, G. R. Nkoue Ndondo, J. R. Ndam Ngoupayou, J. L. Boeglin, and J. L. Probst (2009), Terrestrial and fluvial carbon fluxes in a tropical watershed: Nyong basin, Cameroon, *Chemical Geology*, 265, 563-572.

Cardenas, M. B. (2008), Surface water-groundwater interface geomorphology leads to scaling of residence times, *Geophysical Research Letters*, 35, L08402, doi:10.1029/2008GL033753.

Cavaleri, M. A., S. F. Oberbauer, and M. G. Ryan (2008), Foliar and ecosystem respiration in an old-growth tropical rain forest, *Plant, Cell, and Env.*, 31, 473-483.

Chappelle, F. H., and D. R. Lovley (1990), Rates of microbial metabolism in deep Coastal Plain aquifers, *Applied and Environ. Microbiol.*, 56(6), 1865-1874.

Chiodini, G., F. Frondini. C. Cardellini. F. Parello, and L. Peruzzi (2000), Rate of diffuse carbon dioxide earth degassing estimated from carbon balance of regional aquifers: The case of central Apennine, Italy, *JGR*, 105(B4), 8423-8434.

Clark, J. F., M. L. Davisson, G. Bryant Hudson, and P. A. Macfarlane (1998), Noble gases, stable isotopes, and radiocarbon as tracers of flow in the Dakota aquifer, Colorado and Kansas, *J. of Hydrol.*, 211, 151-167.

Cole, J. J., Y. T. Prairie, N. F. Caraco, W. H. McDowell, L. J. Tranvik, R. G. Striegl, C. M. Duarte, P. Kortelainen, J. A. Downing, J. J. Middelburg, and J. Melack (2007), Plumbing the global carbon cycle: Integrating inland waters into the terrestrial carbon budget, *Ecosystems*, 10, 171-184, doi:10.1007/s10021-006-9013-8.

Dinsmore, K. J., M. F. Billet, U. M. Skiba, R. M. Rees, J. Drewer, and C. Helfter (2010), Role of the aquatic pathway in the carbon and greenhouse gas budgets of a peatland catchment, *Global Change Biology*, doi:10.1111/j.1365-2486.2009.02119.x.

Evans, W.C., M.L. Sorey, A.C. Cook, B.M. Kennedy, D.L. Shuster, E.M. Colvard, L.D. White, and M.A. Huebner (2002), Tracing and quantifying magmatic carbon discharge in cold groundwaters: lessons learned from Mammoth Mountain, USA, *J. of Volcanology and Geothermal Research*, 114, 291-312.

Frisbee, M. D., F. M. Phillips, A. R. Campbell, F. Liu, and S. A. Sanchez (2011), Streamflow generation in a large, alpine watershed in the southern Rocky Mountains of Colorado: Is streamflow generation simply the aggregation of hillslope runoff responses?, *WRR*, 47, W06512, doi:10.1029/2010WR009391.

Gardner, W. P., G. A. Harrington, D. K. Solomon, and P. G. Cook (2011), Using terrigenic ^{4}He to identify and quantify regional groundwater discharge to streams, *WRR*, 47, W06523, doi:10.1029/2010WR010276.

Genereux, D. P., and H. F. Hemond (1992), Determination of gas exchange rate constants for a small stream on Walker Branch Watershed, Tennessee, *WRR*, 28(9), 2365-2374.

Genereux, D. P., M. T. Jordan, and D. Carbonell (2005), A paired-watershed budget study to quantify interbasin groundwater flow in a lowland rainforest, Costa Rica, *WRR*, 41, W04011, doi:10.1029/2004WR003635.

Genereux, D. P., M. Webb, and D. K. Solomon (2009), The chemical and isotopic signature of old groundwater and magmatic solutes in a Costa Rican rainforest: evidence from carbon, helium, and chlorine, *WRR*, 45, W08413, doi:10.1029/2008WR007630.

Gleeson, T., and A. H. Manning (2008), Regional groundwater flow in mountainous terrain: Three-dimensional simulations of topographic and hydrogeologic controls, *WRR*, 44, W10403, doi:10.1029/2008WR006848.

Helms, J. R., A. Stubbins, J. D. Ritchie, and E. C. Minor (2008), Absorption spectral slopes and slope ratios as indicators of molecular weight, source, and photobleaching of chromophoric dissolved organic matter, *Limnol. and Oceanog.*, 53(3), 955-969.

Hope, D., S. M. Palmer, M. F. Billet, and J. J. Dawson (2001), Carbon dioxide and methane evasion from a temperate peatland stream, *Limnol. and Oceanog.*, 46, 847–857.

Johnson, M. S., J. Lehmann, S. J. Riha, A. V. Krusche, J. E. Richey, J. P. H. B. Ometto, and E. G. Couto (2008), CO_2 efflux from Amazonian headwater streams represents a significant fate for deep soil respiration, *GRL*, 35, L17401, doi:10.1029/2008GL034619.

Kasper, J. W., J. M. Denver, T. E. McKenna, and W. J. Ullman (2010), Simulated impacts of artificial groundwater recharge and discharge on the source area and source volume of an Atlantic Coastal Plain stream, Delaware, USA, *Hydrogeol. J.*, 18, 1855-1866, doi:10.1007/s10040-010-0641-x.

Kennedy, C. D., and D. P. Genereux (2007), ^{14}C groundwater age and the importance of chemical fluxes across aquifer boundaries in confined Cretaceous aquifers of North Carolina, USA, *Radiocarbon*, 49(3), 1181-1203.

Likens, G. E., and F. H. Bormann (1995), *Biogeochemistry of a Forested Ecosystem*, 2nd ed., Springer, New York.

Lloret, E., C. Dessert, J. Gaillardet, P. Alberic, O. Crispi, C. Chaduteau, and M. F. Benedetti (2011), Comparison of dissolved inorganic and organic carbon yields and fluxes in the watersheds of tropical volcanic islands, examples from Guadeloupe (French West Indies), *Chemical Geology*, 280, 65-78.

Loescher, H. W., S. F. Oberbauer, H. L. Gholz, and D. B. Clark (2003), Environmental controls on net ecosystem level carbon exchange and productivity in a Central American tropical wet forest, *Global Change Biology*, 9, 396-412.

McDowell, W. H., and C. E. Asbury (1994), Export of carbon, nitrogen, and major ions from three tropical montane watersheds, *Limnology and Oceanography*, 39(1), 111-125.

McIntosh, J. C., and L. M. Walter (2006), Paleowaters in Silurian-Devonian carbonate aquifers: Geochemical evolutions of groundwaters in the Great Lakes region since the late Pleistocene, *GCA*, 70, 2454-2479.

McMahon, P. B., J. K. Bohlke, and S. C. Christenson (2004), Geochemistry, radiocarbon ages, and paleorecharge conditions along a transect in the central High Plains aquifer, southwestern Kansas, USA, *App. Geochem.*, 19, 1655-1686.

Murphy, E. M., S. N. Davis, A. Long, D. Donahue, and A. J. T. Jull (1989), Characterization and isotopic composition of organic and inorganic carbon in the Milk River Aquifer, *WRR*, 25(8), 1893-1905.

Nagy, L. (2012), *Effect of interbasin groundwater flow on optical properties of DOC and watershed export of DIC and DOC in a tropical rainforest, La Selva Biological Station, Costa Rica*, M.S. Thesis, Dept. of Marine, Earth, and Atmos. Sciences, N.C. State Univ., Raleigh, NC. http://repository.lib.ncsu.edu/ir/handle/1840.16/7736

Newbold, J. D., B. W. Sweeney, J. K. Jackson, and L. A. Kaplan (1995), Concentrations and export from six mountain streams in northwestern Costa Rica, *Journal of the North American Benthological Society*, 14(1), 21-37.

Ohsawa, S., K. Kazahaya, M. Yasuhara, T. Kono, K. Kitaoka, Y. Yusa, and K. Yamaguchi (2002), Escape of volcanic gas into shallow groundwater systems at Unzen Volcano (Japan): Evidence from chemical and stable isotope compositions of dissolved inorganic carbon, *Limnology*, 3, 169-173.

Oquist, M. G., M. Wallin, J. Seibert, K. Bishop, and H. Laudon (2009), Dissolved inorganic carbon export across the soil/stream interface and its fate in a boreal headwater system, *Env. Sci. and Tech.*, 43, 7364-7369.

Plummer, L. N., and C. L. Sprinkle (2001), Radiocarbon dating of dissolved inorganic carbon in groundwater from confined parts of the Upper Floridan aquifer, Florida, USA, *Hydrogeol. J.*, 9, 127–150.

Pringle, C. M., and F. J. Triska (1991), Effects of geothermal groundwater on nutrient dynamics of a lowland Costa Rican stream, *Ecology*, 72(3), 951-965.

Schaller, M., and Y. Fan (2009), River basins as groundwater exporters and importers: Implications for water cycle and climate modeling, *JGR*, 114, D04103, doi:10.1029/2008JD010636.

Smerdon, B. D., W. P. Gardner, G. A. Harrington, and S. J. Tickell (2012), Identifying the contribution of regional groundwater to the baseflow of a tropical river (Daly River, Australia), *J. of Hydrol.*, vol. 464-465, 107-115.

Solomon, D. K., D. P. Genereux, L. N. Plummer, and E. Busenberg (2010), Testing mixing models of old and young groundwater in a tropical lowland rainforest with environmental tracers, *WRR*, 46, W04518, doi: 10.1029/2009WR008341.

Spencer, R. G. M., K. D. Butler, and G. R. Aiken (2012), Dissolved organic carbon and chromophoric dissolved organic matter properties of rivers in the USA, *JGR*, 117, G03001, doi: 10.1029/2011JG001928 .

Teodoru, C. R., P. A. del Giorgio, Y. T. Prairie, and M. Camire (2009), Patterns in pCO_2 in boreal streams and rivers in northern Quebec, Canada, *Global Biogeochem. Cycles*, 23, GB2012, doi:10.1029/2008GB003404.

Tóth J. A. (2009), *Gravitational Systems of Groundwater Flow: Theory, Evaluation, Utilization*, Cambridge University Press, New York.

Walling, D. E., and B. W. Webb (1985), Estimating the discharge of contaminants to coastal waters by rivers: Some cautionary comments, *Marine Pollution Bulletin*, 16, 488-492.

Waterloo, M. J., S. M. Oliveira, D. P. Drucker, A. D. Nobre, L. A. Cuartas, M. G. Hodnett, I. Langedijk, W. W. P. Jans, J. Tomasella, A. C. Araujo, T. P. Pimentel, and J. C. Munera Estrada (2006), Export of organic carbon in run-off from an Amazonian rainforest blackwater catchment, *Hydrological Processes*, 20, 2581-2597.

Worman, A., A. I. Packman, L. Marklund, J. W. Harvey, and S. H. Stone (2007), Fractal topography and subsurface water flows from fluvial bedforms to the continental shield, *Geophysical Research Letters*, 34, L07402, doi:10.1029/2007GL029426.

Zanon, C. (2011), Watershed hydrologic modeling to assess interbasin groundwater flow in a tropical rainforest, M.S. Thesis, Dept. of Marine, Earth, and Atmos. Sciences, N.C. State Univ., Raleigh, NC.

Zanon, C., D. P., Genereux, and S. F. Oberbauer (2013), Use of a watershed hydrologic model to estimate interbasin groundwater flow in a Costa Rican rainforest, *Hydrol. Proc.*, in revision following initial review.

Chapter 2: The effect of regional groundwater on carbon dioxide and methane emissions from a lowland rainforest stream in Costa Rica

Diana Oviedo-Vargas[1*], David P. Genereux[1], Diego Dierick[2], Steven F. Oberbauer[2]
[1] Marine Earth and Atmospheric Sciences, North Carolina State University, Raleigh, NC
[2] Biological Sciences, Florida International University, Miami, FL

Key Points

- Regional groundwater input did not affect stream gas exchange velocity
- Regional groundwater input raised stream CO_2 concentration and degassing 7-8x
- Stream degassing of CO_2 from regional groundwater is a large ecosystem C flux

Abstract

In the tropical rainforest at La Selva Biological Station in Costa Rica, regional bedrock groundwater high in dissolved carbon discharges into some streams and wetlands, with the potential for multiple cascading effects on ecosystem carbon pools and fluxes. We investigated carbon dioxide (CO_2) and methane (CH_4) degassing from two streams at La Selva: the Arboleda, where ~1/3 of the streamflow is from regional groundwater, and the Taconazo, fed exclusively by local groundwater recharged within the catchment. The regional groundwater inflow to the Arboleda had no measurable effect on stream gas exchange velocity, dissolved CH_4 concentration, or CH_4 emissions but significantly increased stream CO_2 concentration and degassing. CO_2 evasion from the reach of the Arboleda receiving regional groundwater (lower Arboleda) averaged 5.5 mol C m^{-2} day^{-1}, ~7.5x higher than the average (0.7 mol C m^{-2} day^{-1}) from the stream reaches with no regional groundwater inflow (the Taconazo and upper Arboleda). Carbon emissions from both streams were dominated by CO_2; CH_4 accounted for only 0.06-1.70% of the total (average of both streams: $5x10^{-3}$ mol C m^{-2} day^{-1}). Annual stream degassing fluxes normalized by watershed area were 48 and 299 g C m^{-2} for the Taconazo and Arboleda, respectively. CO_2 degassing from the Arboleda is a significant carbon flux, similar in magnitude to the average net ecosystem exchange estimated by eddy covariance. Examining the effects of catchment connections to underlying hydrogeological systems can help avoid overestimation of ecosystem respiration and advance our understanding of carbon source/sink status and overall terrestrial ecosystem carbon budgets.

Keywords: carbon, greenhouse gases, streams, gas exchange, regional groundwater

1. Introduction

Streams and rivers are increasingly recognized as an important component in the carbon (C) cycle, from local to global scales [*Cole et al*., 2007; *Battin et al*., 2009; *Aufdenkampe et al.*, 2011]. Carbon dioxide (CO_2) and methane (CH_4) emissions from fluvial systems are a key consideration; omitting or miscounting them could result in incomplete C budgets for terrestrial ecosystems and incorrect estimates of net C sequestration [*Billett et al*., 2004; *Cole et al.*, 2007], and they can represent a positive feedback on global warming [*Battin et al*., 2009]. Sources of CO_2 and CH_4 to flowing waters include influx from the atmosphere, biological or chemical production in-situ (or in connected lakes and wetlands), and hydrologic inputs from the terrestrial ecosystem through overland and groundwater pathways. CO_2 and CH_4 transported to a stream by groundwater may originate within the catchment from a combination of soil root and microbial processes and bedrock weathering [*Schlesinger and Bernhardt*, 2013]; however, catchment connections to regional groundwater can constitute a source of C to fluvial systems that is external to the watershed and often overlooked [*Genereux et al*., 2013].

Regional groundwater flow is a natural hydrogeological process by which groundwater moves long distances beneath surface topographic divides, possibly recharging in one watershed and discharging in another many kilometers away [*Tóth*, 2009; *Schaller and Fan*, 2009; *Smerdon et al*., 2012; *Pacheco*, 2015], and thus creating the potential for relatively long-distance subsurface transport of C between watersheds and ecosystems. In addition to biogenic contributions from the surface, dissolved CO_2 and CH_4 in regional groundwater can originate from volcanic degassing, non-volcanic escape of gases from the upper mantle, intrusive magma chambers, carbonate bearing rocks in the crust, hydrocarbon accumulations [*Mörner and Ethiope*, 2002], and remineralization of ancient sedimentary organic matter [*Lovley and Anderson*, 2000; *Park et al*., 2009; *Liu et al*., 2014]. Aquifers transporting high concentrations of dissolved C have been identified in numerous places around the world, for example, Portugal [*Cruz and Amaral*, 2004], the Canary Islands [*Marrero et al*., 2008], the United States [*Evans et al*., 2009; *Kampman et al*., 2014], Japan [*Yamada et al*., 2011], Canada, Costa Rica, Italy [*Genereux et al*., 2013 and references therein], the Lesser Antilles [*Rivé et al.*, 2013], and the Slovak Republic [*Kucharič et al*., 2015]. However, little is known about the fate of that C once it discharges into surface waters, and its effects on C balances of the aquatic and surrounding terrestrial ecosystems.

Gas efflux from surface water to the atmosphere is a function of dissolved gas concentrations, thus increased stream concentrations of CO_2 or CH_4 resulting from regional groundwater influx may enhance C degassing from stream surfaces. Inputs of regional groundwater also have the potential to affect C degassing by modifying hydraulic characteristics of the stream (depth, velocity) that affect degassing. In recent years the number of studies quantifying C emissions from streams and rivers has increased steadily [e.g., *Hope et al*,. 2001; *Richey et al*., 2002; *Jonsson et al*., 2007; *Rasera et al*., 2008; *Wilcock and Sorrell*, 2008; *Koprivnjak et al*., 2010; *Rantakari et al*., 2010; *Butman and Raymond*, 2011; *Striegl et al*., 2012; *Crawford et al*., 2013; *Lundin et al*., 2013; *Campeau et al*., 2014; *Crawford et al*., 2014a; *Kokic et al*., 2015]. Some of these studies have highlighted the role of groundwater in altering stream concentrations of CO_2. *Crawford et al.* [2014b] found that "passage of groundwater through biologically active, organic-rich sediments and soils" was responsible for elevated CO_2 in stream water in northern Wisconsin, USA. *Dinsmore et al.* [2010] found that in stream water "CO_2 concentrations increased during periods of low flow when discharge was maintained primarily by inputs from groundwater and deep peat." A close similarity of CO_2 concentrations at

groundwater springs and in deep soil gas was found in one Amazonian catchment [*Johnson et al*., 2008]. However, the potential significance of regional groundwater flow and input to streams has been generally overlooked, and studies directly investigating its effect on stream CO_2 and CH_4 emissions are lacking. *Chiodini et al*. [1999] computed the molar loss of CO_2 by degassing from a stream in Italy receiving regional groundwater high in dissolved inorganic carbon (DIC), but the stream degassing flux was not reported.

In the present work we examined the effect of regional groundwater input on CO_2 and CH_4 emissions from a tropical rainforest stream and the significance for ecosystem C budgets. We measured C degassing from two streams at La Selva Biological Station in Costa Rica: one (the Taconazo) receiving only young local groundwater recharged within its watershed, and the other (the Arboleda) receiving both local groundwater and much older regional groundwater high in dissolved C [*Genereux et al*., 2009]. The scale of the regional bedrock groundwater system (tens of kilometers long and perhaps hundreds of meters thick) and long residence time of groundwater therein (roughly 3000 years) [*Genereux et al.*, 2005, 2009] differ from the shallow local groundwaters considered to date. To determine gas emissions from stream surfaces we measured air and aqueous CO_2 and CH_4 concentrations and estimated gas exchange rates by means of simultaneous releases of gaseous and conservative tracers (propane and sodium chloride, respectively) at each stream during the dry and the wet seasons. Results were used to estimate annual C stream degassing fluxes at the watershed level.

2. Study site

La Selva Biological Station is a 16 km^2 tropical rainforest reserve ranging in elevation from 35 to 130 m at the transition between the Caribbean lowland plains and the foothills of the Cordillera Central of Costa Rica. Average annual rainfall at La Selva from 1963 to 2013 was 4328 mm, with February, March, and April as the driest months and July, November, and December as the wettest. From 1982 to 2013, the mean air temperature was 25.0 °C and diurnal changes averaged 9.5 ºC (online meteorological data at http://www.ots.ac.cr/meteoro/default.php?pestacion=2). Annual evapotranspiration is about half or slightly more of precipitation [*Loescher et al*., 2005].

At higher elevations within La Selva, andesitic lava flows have weathered deeply to form reddish-brown clay soils [*Sollins et al.*, 1994]. At lower elevations the lava flows were later covered by alluvial and colluvial deposits of volcanic origin weathered to yellowish-brown clay soils. These two soils had been previously classified as Ultisols and Inceptisols respectively [*Sollins et al.*, 1994], and were recently both reclassified as Oxysols (Typic Haploperox) of different ages [*Veldkamp et al*., 2003]. The higher elevation clay soils are older and regarded as Pleistocene in age [*Sollins et al*., 1994].

Some streams and wetlands at La Selva receive inputs of both low-solute local groundwater recharged within the surrounding topographically-defined watershed, and high-solute regional bedrock groundwater recharged at high elevation upslope of La Selva in the Cordillera Central. The regional groundwater and local groundwater are estimated to have ages of 2400-4000 years and about 10 years or less, respectively [*Genereux et al*., 2009; *Solomon et al*., 2010]. We investigated C emissions from two streams at La Selva draining adjacent rainforest watersheds: the Taconazo (29.7 ha) and the Arboleda (46.1 ha) (Figure 1). These watersheds are very similar in terms of geology, soils, topography, land cover (100% forested), and climatic conditions, but in the Arboleda about 34% of the streamflow comes from regional bedrock groundwater, while the Taconazo stream is fed only by local young groundwater

recharged within the catchment [*Genereux et al.*, 2005; *Genereux and Jordan*, 2006]. $\delta^{13}C$ (-4.39‰) and $\Delta^{14}C$ (17% modern) of DIC in the water of the Arboleda show that the C input from regional groundwater dominates DIC in this stream [*Genereux et al.*, 2009; 2013]. Based on DIC data and water budget results, regional groundwater input to the Arboleda represents a large C flux, on a par with the net ecosystem exchange estimated by eddy covariance [*Genereux et al.*, 2009, 2013]. V-notch weirs were installed in 1998 in the Arboleda and Taconazo streams near their confluences with the Surá stream (Figure 1). Average annual stream discharge per unit area of watershed was approximately 2,500 and 13,000 mm for the Taconazo and Arboleda, respectively [*Zanon et al.*, 2014].

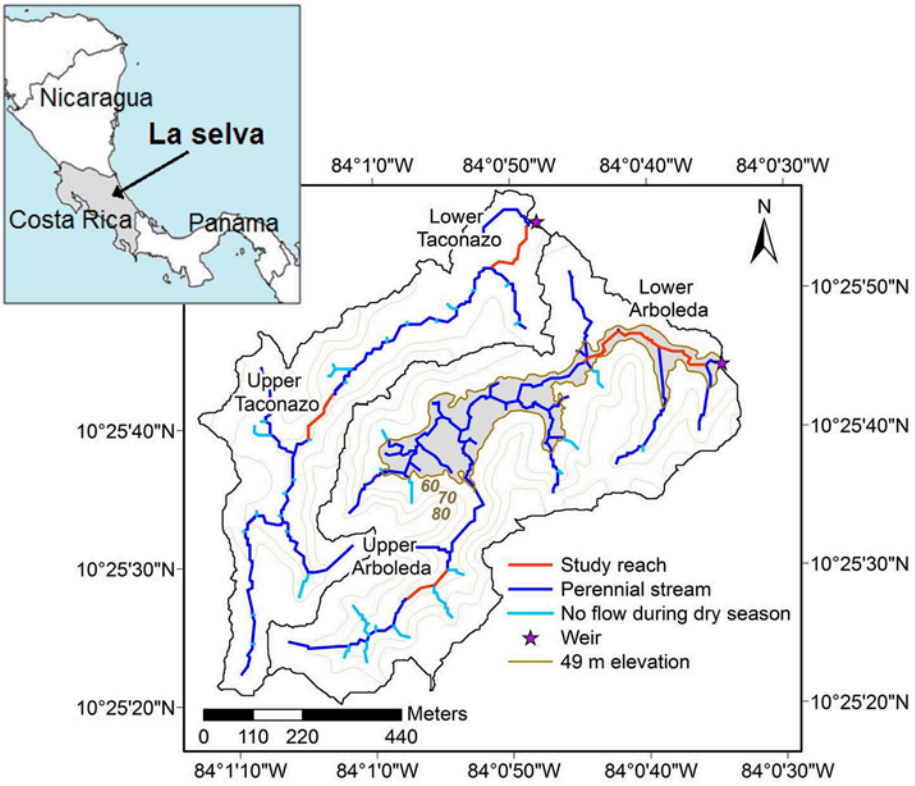

Figure 1. Stream channels in the Taconazo and Arboleda watersheds at La Selva Biological Station, Costa Rica. Gray shade indicates the area below the 49 m elevation contour, the approximate area in which C-rich regional groundwater discharges to streams in the Arboleda. "Study reach" refers to the four stream reaches in which the gas exchange work was done (upper and lower Taconazo and Arboleda).

3. Methods

3.1. Experimental design for gas exchange measurements

Gas exchange rate constant (k in day^{-1}) was measured using simultaneous injections of propane and NaCl [*Kilpatrick et al.*, 1989; *Genereux and Hemond*, 1992; *Wallin et al.*, 2011]. We selected two different reaches in the Arboleda stream, one near the headwaters where the stream is not affected by inputs of regional groundwater (upper Arboleda) and one downstream receiving significant inputs of regional groundwater (lower Arboleda) (Figures 1 and A1; figure and table numbers preceded by "A" indicate figures and tables found the Appendix). For the

Taconazo stream, a reach near the headwaters and one further downstream were also chosen (upper and lower Taconazo, respectively) (Figures 1 and A1).

We established four (three in the lower Arboleda) equally-spaced sampling stations in each reach. The reach length was defined by the most upstream and most downstream sampling station. Reach lengths ranged from 86 to 348 m (Table 1), and tracer injections and associated field measurements were generally completed within 4-6 hours for each reach. The dry season experiments were conducted in February-March 2014 and the wet season experiments in August 2014 (Figure 2). For each season, the experiments in the upper and lower Taconazo and the upper Arboleda were conducted once. Because the work in the lower Arboleda was more complex and uncertain due to the higher stream discharge, and critical as only this reach received regional groundwater, the experiments there were conducted twice within 2 or 3 days (Table 1).

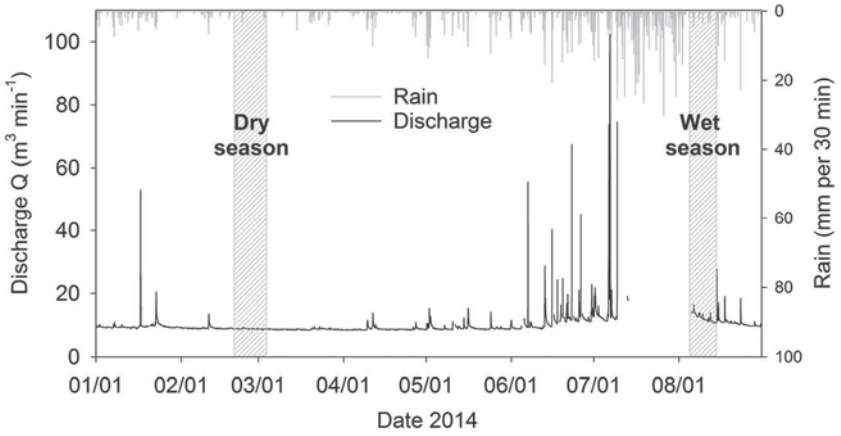

Figure 2. Hydrograph for January 2014 - August 2014 from the Arboleda weir. Shaded bars show the timing of the dry and wet season gas exchange measurements. The gap observed between 09 July 2014 and 05 August 2014 is due to data loss caused by large flooding events from 2 m of rainfall in July.

3.2. Techniques for the tracer injections

The propane and NaCl were injected at least 16 m upstream of the upstream measurement station (85-130 m in the case of the deeper and wider lower Arboleda) to allow for sufficient lateral mixing (Table 1). The propane (Praxair, 99.6% purity) was delivered into the stream using fine-pore diffusers (Sweetwater®) placed on the streambed. Floating plastic or styrofoam sheets were placed on the stream surface over the diffusers to increase contact time between propane bubbles and stream water and thereby maximize the dissolution of propane in the stream water (Figure A1).

We used both pulse injections and continuous injections [*Kilpatrick et al.*, 1989] for the NaCl. In the dry season, a Mariotte bottle was used to make continuous injections of a NaCl solution (approximate concentration 2.5 M, injection rate 70-75 mL min^{-1}) in the upper and lower Taconazo and the upper Arboleda reaches; pulse NaCl injections (6-8 kg NaCl dissolved in stream water) were used in the lower Arboleda. In the wet season we conducted all the NaCl injections using the pulse technique (Table 1). While steady NaCl injections offer the benefit of direct observation of a plateau conductivity in the stream once steady state is achieved, pulse injections require far less NaCl and simpler logistics.

During the experiments, specific conductivity (S) breakthrough curves were captured at all sampling stations using manual handheld conductivity meters and automated loggers (YSI

Table 1. Physicochemical characteristics of the study reaches at the time of the gas exchange experiments.

Reach	Upper Taconazo		Lower Taconazo		Upper Arboleda		Lower Arboleda[a]			
Season	Dry	Wet	Dry	Wet	Dry	Wet	Dry		Wet	
Date (2014)	22 Feb	14 Aug	20 Feb	11 Aug	25 Feb	9 Aug	1 Mar	4 Mar	4 Aug	6 Aug
NaCl injection	Continuous	Pulse	Continuous	Pulse	Continuous	Pulse	Pulse	Pulse	Pulse	Pulse
Reach length[b] (m)	90	86	132	132	100	100	175		348	
Mixing length[c] (m)	20	20	16	16	20	17	85		130	
Average width (m)	1.4	1.8	1.5	2.8	1.1	2.2	5.1		4.9	
Average depth (m)	0.083	0.138	0.086	0.197	0.078	0.190	0.88		0.82	
Travel time (min)	102	43	80	37	109.5	34.5	49	51	76	75.5
Water Velocity (m s^{-1})	0.015	0.033	0.027	0.059	0.015	0.048	0.066	0.062	0.076	0.077
Upstream Q (m^3 min^{-1})	0.066	0.491	0.194	1.699	0.040	0.730	9.7	9.1	14.2	14.1
Downstream Q (m^3 min^{-1})	0.087	0.595	0.236	1.830	0.064	0.926	10.2	10.1	18.0	16.8
[DIC] ± SE (µM)	212±19	148±7	292±7	224±8	244±23	116±3	2316±101	2377±104	2035±129	1991±44
$[CO_2]_{aq}$ ± SE (µM)	187±17	143±7	267±6	218±8	215±20	111±3	1078±47	1120±49	1248±79	1221±27
(µatm)	(5192)	(4011)	(7407)	(6128)	(5927)	(3125)	(34550)	(35426)	(34760)	(33948)
$[CH_4]_{aq}$ ± SE (µM)	0.9±0.3	2.5±0.5	1.1±0.1	2.7±0.1	0.6±0.1	0.6±0.1	0.82±0.03	0.85±0.02	1.6±0.1	1.60±0.04
(µatm)	(663)	(1788)	(781)	(1903)	(432)	(408)	(569)	(593)	(1131)	(1123)
Stream T ± SE (°C)	23.7±0.1	25.2±0.1	23.0±0.1	25.2±0.1	23.8±0.1	25.2±0.1	24.6±0.1	24.9±0.1	25.2±0.1	25.1±0.1

[a]Only reach receiving regional groundwater inputs

[b]From upstream to downstream measurement station

[c]From tracer injection station to first measurement station

Professional Plus multiparameter instrument, YSI EC300A conductivity meter, HOBO U24-001 conductivity data logger, and Hach 44600 conductivity meter). Because of its greater width (Table 1), in the lower Arboleda we measured *S* at each station in three locations across the stream (right side, center, and left side of the channel, at roughly 0.25, 0.5, and 0.75 of channel width). Breakthrough curves were used to quantify stream discharge and water/tracer travel time through each reach. Steady state was determined by the stabilization of *S* during the continuous NaCl injections, and was taken as at least 4 times the travel time from the injection point to the station in the case of the pulse additions of NaCl [*Kilpatrick et al*., 1989].

For continuous injections k_{C3H8} was calculated following *Genereux and Hemond* [1990]:

$$k_{C3H8} = \frac{1}{\tau}\ ln\left(\frac{[C_3H_8]_U \times [Cl^-]_D}{[C_3H_8]_D \times [Cl^-]_U}\right) \quad (1)$$

where τ represents travel time in the stream (in days) from the upstream (*U*) to downstream (*D*) station, $[C_3H_8]$ corresponds to the aqueous concentration of C_3H_8 (in µM) at steady state conditions at the station indicated in the subscript and $[Cl^-]$ corresponds to the background-corrected aqueous concentration of Cl^- (plateau concentration minus background concentration, in µM) at steady state at the station indicated in the subscript.

For pulse injections, k_{C3H8} was determined following *Kilpatrick et al*. [1989]:

$$k_{C3H8} = \frac{1}{\tau}\ ln\left(\frac{[C_3H_8]_U \times Q_U}{[C_3H_8]_D \times Q_D}\right) \quad (2)$$

where *Q* represents stream discharge (in $m^3\ min^{-1}$) at the station indicated in the subscript. For the pulse injections, *Q* at each station was calculated using the following equation [*Kilpatrick et al*., 1989]:

$$Q_{U,D} = \frac{m}{(A_c)_{U,D}} \quad (3)$$

where *m* represents the mass of NaCl (in mg) added to the stream as a pulse, and $(A_c)_{U,D}$ is the area under the $[Cl^-]$ vs. time curve collected at the station indicated in the subscript. For our experiments *S* was transformed to [*NaCl*] in $mg\ L^{-1}$ using calibration curves of [*NaCl*] vs. *S* prepared at La Selva laboratory facilities for each conductivity meter used. We used the trapezoidal approach for the computation of A_c.

Stream depth (*Z*) and width (*W*) were measured every 10 m approximately (12-25 m for the lower Arboleda) within each study reach 1-2 days before or after the injection experiment. The stream depths measured in the upper Arboleda and both Taconazo reaches were the maxima in the highly-variable stream cross-sections. Detailed work in 13 cross-sections showed that mean depth in a given cross-section was on average 0.7 of the maximum depth, intermediate between the 0.5 and 1.0 expected for triangular and rectangular channel cross-sections, respectively. Thus, the depth used in computing degassing flux from the upper Arboleda, upper Taconazo, and lower Taconazo reaches was 0.7x the mean of the maximum depth measurements every 10 m in the reach. The lower Arboleda reach is a more uniform and nearly rectangular channel, thus the degassing fluxes for this reach were calculated using the mean of the maximum depth measurements.

Stream gas exchange velocity for propane, (v_{C3H8}) was calculated as the product of k_{C3H8} and stream depth (*Z*).

3.3. Water and air sample collection and analysis

During each tracer release, an infrared gas analyzer sensor (Vaisala GMP343) was used to record the concentration of CO_2 in the air directly above the stream, $[CO_2]_{air}$, every minute.

The sensor was deployed ~30 cm above the stream, near the middle of each study reach, for the duration of each tracer release (Figure A1d). Before the tracer injections started, 60-mL air samples were collected in plastic syringes (n = 3 for the lower Arboleda, n = 1 for other three reaches) from each sampling station to determine concentrations of CH_4 in air directly above the stream surface, $[CH_4]_{air}$. $[CO_2]_{air}$ and $[CH_4]_{air}$ were used with Henry's Law constants for CO_2 and CH_4 (at the stream temperature) to calculate the aqueous concentrations of these gases that would be in equilibrium with the air, $[CO_2]_{eq}$ and $[CH_4]_{eq}$, respectively (needed for the gas flux calculations, as shown in the next section).

Before starting the tracer injections, we collected water samples (n = 3 for the lower Arboleda and n = 1-3 for the other reaches) at each sampling station for the determination of background dissolved gas concentration in stream water, $[G]_{aq}$ (where "*G*" represents either propane, CO_2 or CH_4). Also, we collected water samples (n = 9 for the lower Arboleda and n = 3 for the other reaches) for $[C_3H_8]_{aq}$ from each sampling station once steady was reached. Briefly, a known volume (~40.0 mL) of stream water was collected in 60-mL syringes fitted with three-way valves. Samples were collected carefully to avoid the formation of bubbles inside the syringe. Syringes were kept on ice until transported to the laboratory where they were kept at 4 °C overnight until analysis. In the laboratory, ~10.0 mL of nitrogen gas (N_2) was added to each syringe. To ensure the equilibration between the liquid and gas phases, the syringes were placed on a shaker table for 5 minutes and then left at rest for ~2 hours before the analysis. After the equilibration period the headspace was analyzed by gas chromatography using an SRI 8610C gas chromatograph equipped with a HayesSep D packed column, a flame ionization detector (FID) and a methanizer to convert CO_2 into CH_4 that allowed quantification of CO_2. $[G]_{aq}$ was calculated based on the concentration in the headspace ($[G]_{gas}$ in µM), the volume of stream water in the syringe (V_{water} in mL), and the volume of N_2 headspace (V_{N2} in mL) as follows:

$$[G]_{aq} = [G]_{gas}\left(\frac{1}{K_H} + \frac{V_{N2}}{V_{water}}\right) \quad (4)$$

where K_H is the dimensionless Henry's Law constant for gas *G* at the temperature of the equilibration (lab temperature).

At each sampling station, water samples (~ 15 mL) for determination of $[Cl^-]$ were collected pre-injection (n = 2-3) and at steady state (n = 9 for the lower Arboleda and n = 3 for the other reaches). Samples were filtered in the field or in the laboratory through 0.45 µm membranes and transported to North Carolina State University where concentrations were determined using an ion chromatograph (Dionex DX-500).

3.4. Fluxes of CO_2 and CH_4

Fluxes of CO_2 (f_{CO2}) and CH_4 (f_{CH4}) from the stream surface in a study reach at the time of the gas exchange experiment (mol C m^{-2} day^{-1}) were calculated as:

$$f_{CO2} = k_{CO2}Z([CO_2]_{aq} - [CO_2]_{eq}) \quad (5)$$

$$f_{CH4} = k_{CH4}Z([CH_4]_{aq} - [CH_4]_{eq}) \quad (6)$$

where k_{CO2} and k_{CH4} correspond to the gas exchange rate constants for CO_2 and CH_4, respectively, (day^{-1}), *Z* corresponds to the mean stream depth in the reach (m), and concentrations are given in mol C m^{-3}. k_{CO2} and k_{CH4} were calculated from k_{C3H8}:

$$k_{CO2} = k_{C3H8}\left(\frac{Sc_{C3H8}}{Sc_{CO2}}\right)^n \quad (7)$$

$$k_{CH4} = k_{C3H8}\left(\frac{Sc_{C3H8}}{Sc_{CH4}}\right)^n \quad (8)$$

where *Sc* corresponds to the Schmidt number of the gas indicated as a subscript [*Jähne et al.*, 1987a]. We assumed *n* to be 0.7 based on experimentally derived values from a range of systems [e.g. *Genereux and Hemond*, 1992; *Jähne and Haußecker*, 1998 and references therein, *Madsen et al*., 2007; *Striegl et al.*, 2012]. Sensitivity of gas flux *f* to a broader range of n values (0.5-0.9) was one component of the uncertainty analysis described below.

The *Sc* for a given gas was calculated as:

$$Sc = \frac{\mu}{\rho D} \quad (9)$$

where μ is the dynamic viscosity of water (Pa s), ρ is the density of water (kg m^{-3}), and *D* is the diffusion coefficient of the gas of interest (m^2 s^{-1}), all temperature dependent variables. We compiled literature data of *D* for CO_2, CH_4, and propane measured at 0-40 °C [*Thomas and Adams*, 1965; *Witherspoon and Saraf*, 1965; *Duda and Vrentas*, 1968; *Witherspoon and Bonoli*, 1969; *Maharajh and Walkley*, 1973; *Jähne et al*., 1987b; *Tamimi et al*., 1994; *Frank et al*., 1996; *Zeebe*, 2011; *Lu et al*., 2013] and used well known functions of μ [*Huber et al*., 2009] and ρ [*Tanaka et al*., 2001] vs. temperature (*T*) to estimate *Sc* at temperatures ranging from 0 to 40 °C. For each gas, cubic polynomial functions were then fitted to the *Sc* vs *T* values, similar to *Raymond et al.* [2012]:

$$Sc_{C3H8} = 3545.60 - 203.41\,T + 4.78\,T^2 - 0.0404\,T^3, \quad R^2 = 0.980 \quad (10)$$

$$Sc_{CO2} = 1686.02 - 89.66\,T + 2.07\,T^2 - 0.018\,T^3, \quad R^2 = 0.993 \quad (11)$$

$$Sc_{CH4} = 1517.5 - 58.30\,T + 0.8186\,T^2 - 0.003T^3, \quad R^2 = 0.978 \quad (12)$$

where *T* corresponds to stream temperature in ºC (Figure A2).

3.5. Upscaling from measured to annual C fluxes

3.5.1. Spatial scaling

Estimating annual watershed-scale stream degassing of CO_2 and CH_4 required that results from the gas exchange measurements be scaled up over space and time. Stream areas were estimated as the product of stream length and width (Table A2). Stream length was estimated using ArcGIS tools from a 5-m digital elevation model (DEM) created from LiDAR data [*Kellner et al*., 2009; *Zanon*, 2011]. We assumed that tributaries shorter than 100 m were flowing during the wet season but not the dry season (Figure 1), based on field observations of several tributaries. Perennial tributaries were assigned a width corresponding to 50% of the main channel width (based on field measurements made during the experiments, Table A2). We assumed that CO_2 and CH_4 fluxes measured in the upper Taconazo reach (f_{CO2}^{upper} and f_{CH4}^{upper}) were applicable to the upper 50% of the main channel (794 m, Table A2) and all its tributaries, and that fluxes measured in the lower Taconazo reach (f_{CO2}^{lower} and f_{CH4}^{lower}) were applicable to the lower 50% of the main channel and all its tributaries.

In its headwaters, the Arboleda stream is similar in width and depth to the Taconazo, but further downstream where regional groundwater enters it becomes significantly wider (about 5 m) and deeper (80-90 cm on average, Table 1). Because the Arboleda stream is not easily accessed over its full length through dense rainforest, the location of the transition from a small headwater stream to a much larger stream at lower elevation was not directly observed in the field and had to be estimated. Based on elevations at the Arboleda and Taconazo weirs (and the observation that there is no high-DIC regional groundwater at the latter, at an elevation of 49 m.a.s.l.), and elevations at the upper and lower Arboleda study reaches (the former above 49 m.a.s.l. and the latter below), we took the 49 m.a.s.l. elevation contour as a dividing line in the Arboleda watershed (Figure 1): stream channels above this elevation were considered to receive

no inputs of bedrock groundwater and to thus have C degassing similar to the upper Arboleda reach (f_{CO2}^{upper} and f_{CH4}^{upper}), while channels below 49 m.a.s.l. were considered to receive inputs of regional groundwater and to thus have C degassing similar to the lower Arboleda reach (f_{CO2}^{lower} and f_{CH4}^{lower}). In the dry season, 22% of the total stream surface area in the Arboleda watershed was above 49 m.a.s.l and 78% below 49 m.a.s.l; in the wet season the stream surface area above 49 m.a.s.l increased to 37% (Table A2).

3.5.2. Temporal scaling

We considered the f_{CO2} and f_{CH4} measured during the dry season to be representative of the full dry season from January 1st to April 30th (120 days) and the f_{CO2} and f_{CH4} measured during the wet season to be representative of the full wet season from May 1st to December 31st (245 days). Thus, annual stream C degassing fluxes (F) for each watershed normalized by watershed area (in g of C per m^2) were calculated as the sum of the seasonal fluxes as follows:

$$F = \frac{12.01\ g\ C}{mol\ C}\left[\left(120\ day\ \times\ F_{dry}\right) + \left(245\ day\ \times\ F_{wet}\right)\right] \quad (13)$$

where F_{dry} and F_{wet} correspond to the flux during the dry and wet seasons respectively.

For the Taconazo stream, F_{dry} was calculated as follows:

$$F_{dry} = \frac{\left\{\left[\alpha_{upper\ 50\%}\left(f_{CO2}^{upper} + f_{CH4}^{upper}\right)\right] + \left[\alpha_{lower\ 50\%}\left(f_{CO2}^{lower} + f_{CH4}^{lower}\right)\right]\right\}_{dry}}{A_{Taconazo}} \quad (14)$$

where α is the stream area for the given stream fraction (upper or lower 50%) in the dry season (Table A2), and A is the area of watershed (29.7 ha). F_{wet} was computed identically, with wet season α and f values. In the case of the Arboleda stream, F_{dry} and F_{wet} were calculated similarly using f values determined in the upper and lower Arboleda reaches, α as defined by the 49 m.a.s.l. contour line (Table A2), and the watershed area, A (46.1 ha).

3.6. Statistical analysis

To test the effect of regional groundwater input on $[CO_2]_{aq}$ and $[CH_4]_{aq}$ and to examine if this effect was seasonal (dry vs. wet), we used two-way analysis of variance (ANOVA) with reach and season as factors. A 10-base logarithmic transformation was used to normalize $[CO_2]_{aq}$ and $[CH_4]_{aq}$. Significant ANOVAs were followed by Tukey's honest significant difference (HSD) for multiple comparisons. Statistical analyses were performed in SPSS or SigmaPlot 11.1. Significance was tested at the 95% confidence level (P-value, P <0.05).

Uncertainty (Ω) at 95% confidence was calculated for k_{C3H8}, f_{CO2} and f_{CH4} following standard procedures for error propagation [*Ku*, 1966; *Miller and Miller*, 2005]:

$$\Omega_y = \sqrt{\left[\frac{\partial y}{dx_1} \times \Omega_{x1}\right]^2 + \left[\frac{\partial y}{dx_2} \times \Omega_{x2}\right]^2 + \cdots + \left[\frac{\partial y}{dx_n} \times \Omega_{xn}\right]^2} \quad (15)$$

where $y = f(x_1, x_2, \ldots x_n)$ and Ω is the uncertainty in the variable indicated by the subscript.

To constrain the annual fluxes and estimate their uncertainty we conducted Monte Carlo simulations of F in which Z, α, k_{C3H8}, n, Sc, and air and aqueous concentrations of CO_2 and CH_4 were allowed to vary within realistic ranges (Table A3). Each simulation was repeated 5000 times using Microsoft® Excel. For the stream reaches not affected by regional groundwater, k_{C3H8} in the Monte Carlo simulation was allowed to vary within the 95% confidence interval derived from equation 15, however for the lower Arboleda we used the 95% confidence interval derived from the four k_{C3H8} values obtained in the four experiments conducted in the lower Arboleda (see section 5.1 for further discussion).

4. Results

4.1. Stream concentrations of CO_2 and CH_4

At the lower Arboleda reach, $[CO_2]_{aq}$ was not significantly different between the dry and wet seasons (two-way ANOVA, Tukey's HSD, $P = 0.997$). In the dry season, $[CO_2]_{aq}$ in the lower Arboleda was 4-6x higher than in the reaches receiving only local groundwater (Table 1). A difference was also observed during the wet season, when $[CO_2]_{aq}$ was 6-11x higher in the lower Arboleda than in the other reaches. These differences were statistically significant for all reaches (two-way ANOVA, Tukey's HSD, $P<0.001$ for upper Taconazo, lower Taconazo, and upper Arboleda).

In the upper Taconazo, lower Taconazo, and upper Arboleda reaches, $[CO_2]_{aq}$ was significantly lower in the wet season than in the dry season (two-way ANOVA, Tukey's HSD, $P = 0.001$, 0.009, and 0.001, respectively). This seasonal difference was not significant in the lower Arboleda (two-way ANOVA, Tukey's HSD, $P = 0.880$). $[CH_4]_{aq}$ was significantly higher in the wet season in all reaches except the upper Arboleda (two-way ANOVA, Tukey's HSD, $P = 0.908$ for upper Arboleda and <0.001 for the other reaches). In both the dry and wet season experiments, $[CH_4]_{aq}$ did not differ significantly between the lower Arboleda and any of the reaches without regional groundwater (two-way ANOVA, Tukey's HSD, $P > 0.05$).

4.2. Gas exchange rates

First-order gas exchange rate coefficients (k_{C3H8}) measured during the dry season were comparable among the reaches receiving only local groundwater, ranging from 22.0±0.8 day^{-1} in the upper Taconazo to 27.2±3.6 day^{-1} in the lower Taconazo (Table 2). k_{C3H8} at the upper Taconazo and upper Arboleda was higher during the wet season than during the dry season, in contrast, at the lower Taconazo, k_{C3H8} was lower in the wet season (Table 2). In the lower Arboleda, where stream flow consisted of both local and regional groundwater, there was no distinguishable difference in k_{C3H8} between the wet and dry seasons (Table 2). k_{C3H8} in the lower Arboleda was lower than in the other reaches: 5-7x lower in the dry season and 3-13x lower in the wet season (Table 2). Gas exchange velocity v_{C3H8} was not greatly different between the lower Arboleda and the other reaches (Table 2), as lower k_{C3H8} in the lower Arboleda was mostly offset by greater depth.

4.3. Carbon fluxes

The f_{CO2} measured in the reaches receiving only local groundwater ranged from 0.4 in the upper Taconazo (dry season) to 1.1 mol C m^{-2} day^{-1} in the upper Arboleda (wet season) (Table 2, Figure 3). In the dry season, the lower Arboleda reach (average of two experiments) had f_{CO2} 7-15x higher than in the reaches without regional groundwater input. In the wet season this difference was 4-8x (Table 2, Figure 3). Within season, f_{CH4} was similar across all reaches. In the dry season f_{CH4} ranged from 2 mmol C m^{-2} day^{-1} in the upper Taconazo and upper Arboleda, to 4 mmol C m^{-2} day^{-1} in the lower Arboleda (average of two experiments) (Table 2, Figure 3). For all reaches, f_{CH4} in the wet season was consistently higher than in the dry season, ranging from 6 mmol C m^{-2} day^{-1} in the lower and upper Arboleda to 15 mmol C m^{-2} day^{-1} in the upper Taconazo (Table 2, Figure 3). Across reaches f_{CH4} was lower than f_{CO2} (Table 2, Figure 3) and represented only a very small fraction of the total C degassing flux: 0.06 to 0.5% in the dry season and 0.12 to 1.7% in the wet season (Table 2).

Annual fluxes normalized by watershed area were estimated to average 299 and 48 g C m^{-2} for the Arboleda and Taconazo, respectively. Confidence intervals (95%) of F from Monte

Table 2. Gas exchange coefficient k for propane (day^{-1}), gas exchange velocity v for propane ($m\ day^{-1}$), and measured C degassing fluxes f (per unit surface area of stream) with corresponding 95% uncertainty (Ω), at each stream reach. Under f_{CH4}, the values in parentheses correspond to the percent of the total C degassing flux as CH_4. Unless otherwise indicated Ω was calculated using equation 15.

Stream Reach	k_{C3H8}±Ω day^{-1}		v_{C3H8}±Ω $m\ day^{-1}$		f_{CO2}±Ω $mol\ C\ m^2\ day^{-1}$		f_{CH4}±Ω $mmol\ C\ m^2\ day^{-1}$ (% of total C flux)	
	Dry Season	Wet Season	Dry Season	Wet Season	Dry Season	Wet Season	Dry Season	Wet Season
Upper Taconazo	22.0±0.8	31.8±7.2	1.7±0.5	4.4±1.5	0.4±0.2	0.8±0.3	2±2 (0.50%)	15±8 (1.70%)
Lower Taconazo	27.2±3.6	10.2±4.2	2.4±1.1	2.1±0.9	0.9±0.4	0.6±0.3	3±2 (0.40%)	7±4 (1.19%)
Upper Arboleda	23.0±2.3	42.9±7.0	1.9±0.7	8.2±1.9	0.6±0.3	1.1±0.3	2±1 (0.33%)	6±2 (0.53%)
Lower Arboleda 1	5.5±4.0	3.8±3.2	4.8±3.7	3.1±2.7	8.8±7.0	5.6±5.0	5±4	7±6
Lower Arboleda 2	2.5±4.3	2.7±4.1	2.2±3.5	2.3±7.9	3.6±5.7	4.0±5.6	2±4	5±7
Lower Arboleda average[a]	4.0±2.1	3.3±0.8	3.5±1.8	2.7±0.6	6.2±0.9	4.8±0.5	4±1 (0.06%)	6±1 (0.12%)
Lower Arboleda overall average[b]	3.6±2.1		3.1±1.9					

[a]Average of the two experiments of the season, Ω corresponds to one standard deviation from the mean.
[b]Average of the four experiments conducted in the Lower Arboleda stream reach. Ω corresponds to the 95% CI calculated from the variation of the four values with respect to the mean.

Carlo simulations were 91-599 g C m^{-2} and 26-78 g C m^{-2} for the Arboleda and Taconazo, respectively. Of these annual fluxes, in the Arboleda, 0.14% (0.41 g C m^{-2}) were in the form of CH_4 and the remaining 99.86% (298.77 g C m^{-2}) in the form of CO_2. In the Taconazo, CH_4 contributed 1.22% (0.59 g C m^{-2}) and CO_2 98.77% (47.48 g C m^{-2}).

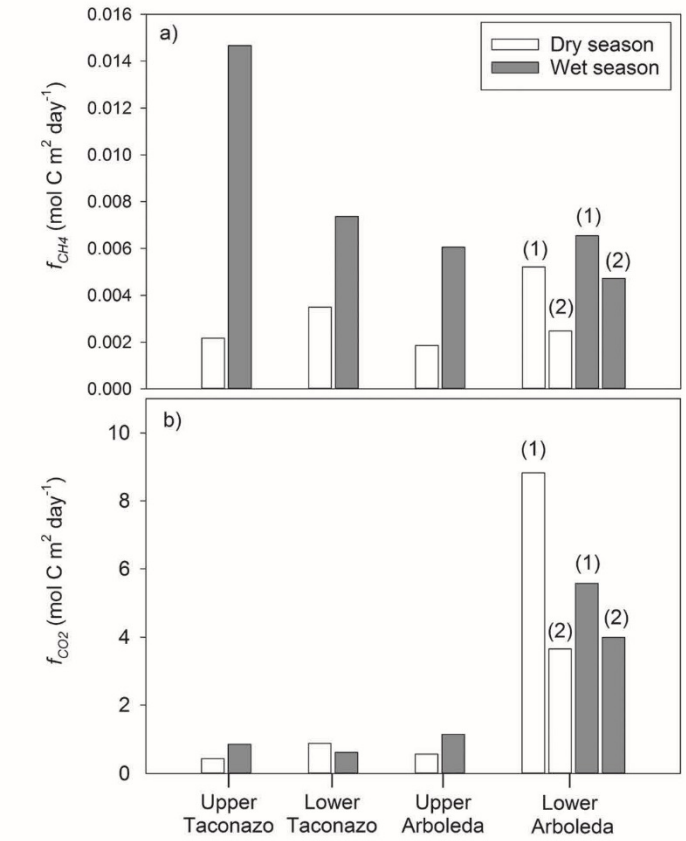

Figure 3. Measured C degassing fluxes *f* (mol C m^{-2} of stream surface day^{-1}) from each of the study reaches for (a) CH_4 and (b) CO_2 during the dry (white bars) and wet (gray bars) seasons. (1) and (2) indicate experiment 1 and 2, respectively, for the lower Arboleda.

4.4 Sources of uncertainty in annual C fluxes

The uncertainty in F (Ω_F) was derived from Monte Carlo simulations in which variables controlling F were allowed to vary within realistic ranges (Table A3). In the dry season, most of Ω_F for the Taconazo originated from the variability in Z in the lower section (±0.05 m, Table A3) which contributed 32% (Table A4) followed by the uncertainty in α (13%, Table A4). In the wet season the uncertainty in k_{C3H8} in the lower section of the stream (±4.3 day^{-1}, Table A3) was the largest contributor to Ω_F (18%, Table A4) followed by the uncertainty in α and Z from the lower reach (10% each, Table A4). In the case of the Arboleda, the largest source of Ω_F was the uncertainty in k_{C3H8} from the lower Arboleda (±2.1 day^{-1}, Table A3), for both dry (47%) and wet (43%) seasons (Table A4). The second largest contributor was the uncertainty in Z (±0.2 m, Table A3) in the lower reach (16%, Table A4). For both the Taconazo and Arboleda the uncertainty in Sc_{CO2}, Sc_{CH4}, $[CO_2]_{eq}$, $[CH_4]_{aq}$, and $[CH_4]_{eq}$ had a marginal contribution to Ω_F, while the uncertainty in n and Sc_{C3H8} contributed 9% and 12-14% respectively, to Ω_F (Table A4).

5. Discussion

5.1. Uncertainty in parameters controlling *F*

Uncertainties in stream depth (*Z)*, stream surface area (α), and gas exchange coefficient (k_{C3H8}) were the most important contributors to Ω_F for both study streams. Depth is small but highly variable in shallow pool-and-riffle streams like the Taconazo and upper Arboleda (Figure A3). The uncertainty in α is based on observed differences in stream width (*W*) within and between seasons and the assumptions made about stream length variation between seasons. Since *W* and *Z* depend largely on *Q*, other studies [e.g. *Butman and Raymond*, 2011; *Raymond et al.*, 2012; *Crawford et al*., 2013] have employed hydraulic geometry relationships [*Leopold and Maddock*, 1953] to estimate temporal variation in these parameters from continuous data on *Q*. However, the data on *Z* and *W* in the study reaches at La Selva do not show well defined relationships with *Q*. Also, studies extrapolating C flux measurements to larger areas often use remotely sensed land surface imaging to estimate α [e.g., *Richey et al*., 2002; *Rasera et al*., 2008], but this is not feasible for small densely forested watersheds like the Arboleda and Taconazo.

With no clear trend in k_{C3H8} of the lower Arboleda between the dry and wet seasons (Table 2), it is reasonable to view the four k_{C3H8} values as replicates and take the 95% CI of the mean (3.6±2.1 day^{-1}) as input to the Monte Carlo analysis of uncertainty in annual stream C emission, *F*. The variation among the four values is mainly due to the relatively small groundwater input and small amount of degassing within the lower Arboleda reach (the overall input of regional groundwater is large, but most of the input must have occurred upstream of the upstream-most measurement station). With respect to equation 1, $[C_3H_8]_U/[C_3H_8]_D$ and Q_U/Q_D were both close to 1 for the lower Arboleda (0.8 to 1.4 for the four experiments), which increases uncertainty in k_{C3H8}. Relative to the dry season, the longer reach length used in the wet season improved the reproducibility in k_{C3H8} in the lower Arboleda (Table 2). Overall, the coefficient of variation (CV) among the four lower Arboleda k_{C3H8} values (37%) was within the range of published CV values for replicate *k* measurements in the same stream reach (Table 3).

5.2. Effects of regional groundwater on dissolved C concentrations

The inflow of regional groundwater to the lower Arboleda significantly increased $[CO_2]_{aq}$ but did not have a distinguishable effect on $[CH_4]_{aq}$. Isotopic characterization of DIC, helium, and chloride in streams receiving regional groundwater at La Selva Biological Station indicates that high concentrations of C derive from mantle outgassing and/or weathering of volcanic rock beneath the Cordillera Central [*Genereux et al*., 2009]. Considering the origin of the CO_2, little or no enrichment of regional groundwater with CH_4 is consistent with other results from the region. Dry gas composition in geothermal fields of Costa Rica is dominated by CO_2 (93.34 to 99.80%), while CH_4 accounts for 0.002 to 0.150% of the gas [*Snyder et al*., 2003]. Furthermore, the regional groundwater at La Selva is generally oxic [*Solomon et al.*, 2010] despite a long subsurface residence time of about 3000 years in volcanic rock [*Genereux et al.*, 2009]. Groundwater from regional aquifer systems of different geology may have more potential to influence stream CH_4; for example, aqueous CH_4 concentrations up to 4.7 mM [*Aravena and Wassenaar*, 1993] and 13.3 mM [*Murphy et al.*, 1989] have been found in the sedimentary Alliston and Milk River aquifers, respectively, in Canada (concentrations much larger than that in the regional groundwater at La Selva, which was about $2x10^{-4}$ mM when measured in 2006 [*Solomon et al*., 2010]).

Table 3. Summary of coefficient of variation (CV) of repeat measurements of gas exchange in the same stream reaches using the tracer injection method.

Author	Stream or River	Gas tracer (method)	Hydrologic tracer (method)	Reach	Average k (day^{-1})	Overall n[a]	Overall CV[b]	n at similar Q[c]	CV at similar Q[d]
Yotsukura et al. [1983]	Cowaselon Creek	Propane (continuous)	Rhodamine (pulse)	A	2.6	3	16%	2	3%
				B	2.6	3	17%	2	2%
Wilcock [1988]	Tarawera River	Methyl chloride (pulse)	Rhodamine (pulse)	A	7.2	6	11%	4	6%
Genereux and Hemond [1992]	Walker Branch	Propane (continuous)	NaCl (continuous)	A	114.1	3	26%	2	6%
				B	92.6	8	17%	2	42%
								2	9%
				C	86.9	8	26%	2	47%
								2	5%
				D	89.5	2	51%	2	51%
				E	79.5	2	45%	2	45%
				F	98.8	3	4%	2	0%
Hope et al. [2001]	Brocky Burn Stream	Propane (continuous)	NaCl (continuous)	A	74.4	3	83%	2	72%
				B	363.6	4	28%	2	48%
				C	144.0	2	38%	0	-
Reid et al. [2007]	Lagan River	Krypton, or krypton and xenon (pulse)	Rhodamine (pulse)	A	41.6	10	63%	4	83%
								2	11%
								2	11%
Jin et al. [2012]	Panther Stream	Propane (continuous)	NaCl (continuous)	A	28.9	3	33%	2	6%
	Ledbetter Stream			A	8.2	3	30%	2	41%

[a]Total number of occasions on which gas exchange coefficient *k* was measured in a given reach.

[b]Coefficient of variation (CV) of all *k* values reported for a given reach.

[c]Number of occasions on which *k* was measured under conditions of similar stream discharge (Q), i.e., <10% difference from the average.

[d]Coefficient of variation (CV) of *k* values obtained under similar Q.

The dissolved CO_2 measured in the study reaches without regional groundwater input (Table 1) was comparable to values published for other tropical streams and rivers. *Richey et al*. [2002] reported annual concentrations in major Amazon tributaries averaging 5,000±3,300 µatm. The primary source of CO_2 in these rivers appeared to be the respiration (in the terrestrial or the aquatic ecosystem) of organic C fixed on land and along river margins and mobilized into flowing waters as litterfall, CO_2, and dissolved organic C; each of these pools contributed 35, 25 and 15% of the stream CO_2 evasion, respectively [*Richey et al.*, 2002]. *Neu et al*. [2011] found pCO_2 ranging from 6,491 to 14,976 µatm in a first order Amazon tributary. A survey of tributaries to the Amazon (streams < 100 m wide, which were not included in *Richey et al*. [2002]) showed pCO_2 averaging 3,353±2,168 µatm [*Alin et al*., 2011]. Few examples in tropical systems show dissolved CO_2 as high as that observed in the lower Arboleda (Table 1). *Johnson et al*. [2008] reported pCO_2 averaging 47,300 µatm for groundwater springs feeding first order streams in the southern Amazon (calculated from 21.1 mg C L^{-1}, Table 1 in *Johnson et al*. [2008] assuming water temperature of 23 °C). The high concentrations observed in these springs originated mostly from deep soil microbial respiration [*Johnson et al*., 2008]. Data for CH_4 in tropical streams and rivers are scarce. *Neu et al*. [2011] reported pCH_4 ranging from 291 to 438 µatm, at the lower end of our results (400-1900 µatm, Table 1). In rivers of the Amazon basin *Sawakuchi et al*. [2014] measured similar or lower $[CH_4]_{aq}$ (0.02-0.5 µM) than what we found for the Taconazo and Arboleda (0.6-2.7 µM, Table 1).

Literature examples in which increased stream dissolved carbon concentration originates from groundwater inputs of recognized regional flow systems are scarce, despite the fact that both regional groundwater flow and elevated dissolved carbon in regional groundwater are ordinary aspects of hydrogeology [e.g., *Genereux et al*., 2013]. In Central Italy, a stream receiving regional groundwater enriched with deep CO_2 showed $[CO_2]_{aq}$ of 10,000 µM (or pCO_2 of 285,600 µatm assuming 23°C and 1 atm) [*Chiodini et al.*, 1999]. In the Oregon Cascades, springs discharging regional groundwater known to be in contact with CO_2 of magmatic origin showed elevated [DIC] ranging from 930 to 1240 µM (or pCO_2 from 26,600 to 35,400 µatm assuming 23°C and 1 atm) [*James et al.*, 1999]. There are of course other causes, besides deep crustal or mantle outgassing, of elevated dissolved carbon (organic and inorganic) in deep groundwater.

5.3. Regional groundwater enhanced CO_2 emissions but not CH_4 emissions

Lower gas exchange coefficients in the lower Arboleda (k_{C3H8} 3-4 day^{-1}, compared to 10-43 day^{-1} for other reaches) seem directly related to the regional groundwater discharge in the lower section of the Arboleda stream. A significantly larger water flux into the lower Arboleda [*Genereux et al*., 2005] creates a deeper channel that results in lower *k*. Although gas exchange coefficients in the lower Arboleda reach were lower, the significantly higher $[CO_2]_{aq}$ and stream depth translated into f_{CO2} values that were on average 8.5x higher than in any of the other reaches. This was not the case for f_{CH4} since $[CH_4]_{aq}$ was not increased by regional groundwater.

Normalized by watershed area, on an annual basis, the Arboleda emitted 6x more C than the Taconazo. In terms of global warming potential on a 100 year time horizon (i.e., GWP_{100}, for which 1 kg of CH_4 is equivalent to 28 kg of CO_2 [*Myhre et al*., 2013]), the annual CH_4 flux from the Taconazo and Arboleda was 22 and 15 g of CO_2 equivalents m^{-2} of watershed area, respectively. Although the C flux from both study streams was dominated by CO_2, for the Taconazo, CH_4 constitutes 11% of the total GWP_{100} emitted from this stream. Because the C inputs from regional groundwater to the Arboleda and C degassing from the lower Arboleda

were dominated by CO_2, in this stream the CH_4 flux represented only 1% of the GWP_{100} (and GWP_{100} of Arboleda gas emissions was 7x that of the Taconazo). Our estimates of CH_4 degassing may be conservative since they only account for diffusive processes, and ebullitive degassing may represent an important fraction of the total CH_4 degassing from streams and rivers [*Sawakuchi et al*., 2014]. Most studies in tropical systems have focused on CO_2 emissions, and the Taconazo results suggest that more attention should be directed to headwater stream CH_4 emissions [*Sawakuchi et al*., 2014].

Comparing stream to land surface CO_2 emissions, average stream f_{CO2} from the Taconazo and upper Arboleda was 2-3x higher than the CO_2 emissions from La Selva soils measured over a 2-year period: 117.3-184.2 mg C m^2 hr^{-1} or 0.23-0.37 mol C m^{-2} day^{-1} [*Schwendenmann et al*., 2003]; f_{CO2} from the lower Arboleda, influenced by regional groundwater, was 12-20x higher than the soil emissions. Soil CO_2 efflux data from 2014, the year of the stream degassing measurements, are similar to the earlier measurements by *Schwendenmann et al*. [2003] (*Dierick et al*., *unpub. data*). Assuming the average of the soil fluxes measured at La Selva (0.3 mol C m^2 day^{-1}) is representative of annual CO_2 emissions from the Arboleda and Taconazo watershed soils, annual stream C emissions from the Taconazo and the Arboleda would contribute 4 and 18%, respectively, of the cumulative watershed (land + stream) CO_2 efflux. Considering the relatively small surface area the streams occupy in the catchment (1.1-1.8% for the Taconazo, 1.3-1.9% for the Arboleda, Table A2), these estimates support the idea that fluvial systems can play a disproportionate role in landscape C budgets [*Aufdenkampe et al.*, 2011; *Butman and Raymond*, 2011], even more so in the case of systems such as the Arboleda. The same can be inferred when comparing stream C degassing fluxes to net ecosystem exchange (NEE) of CO_2 from eddy covariance. Normalized by the watershed area, stream C degassing from the Taconazo and Arboleda (48 and 299 g C m^{-2} y^{-1}, respectively, Table 4) were equivalent to 19 and 120%, respectively, of the mean NEE at la Selva: mean±SD was 250±312 g C m^{-2} for 1998-2000 [*Loescher et al*., 2003].

5.4. Seasonal differences in dissolved gas concentrations and fluxes

Generally, higher $[CH_4]_{aq}$ and lower $[CO_2]_{aq}$ were observed in the wet season (Table 1), likely reflecting soil microbial processes. During the wet season higher soil moisture might limit methanotrophy in aerobic soils, and/or promote anaerobic conditions that favor methanogenesis and inhibit aerobic respiration. Measurements of soil CH_4 exchange at La Selva Biological Station showed that in old growth forest soils CH_4 consumption was greatest during the dry season [*Keller et al.*, 1994]. A recurrent transition between net CH_4 consumption and production was observed between dry and wet seasons in the soils of an upland tropical forest in the Amazon [*Davidson et al*., 2008]. Decreases in diffusive CO_2 emissions from soils to the atmosphere at La Selva Biological Station were strongly driven by increases in soil water content, and emissions were lowest at the end of the wet season [*Schwendenmann et al.* 2003].

Unlike the reaches receiving only local groundwater, no significant seasonal change in $[CO_2]_{aq}$ was observed in the lower Arboleda reach. Any change associated with local soil factors is likely masked by the large and steady C flux into the lower Arboleda from regional groundwater. In all the study reaches, higher $[CH_4]_{aq}$ during the wet season (Table 1) resulted in higher f_{CH4} (Table 2). Relative to the dry season, f_{CH4} in the wet season was 575%, 111%, 225% and 47% higher for the upper Taconazo, lower Taconazo, upper Arboleda, and lower Arboleda, respectively. The difference in f_{CH4} between seasons was larger for the upper Taconazo and

Table 4. Comparison of studies investigating C emissions from tropical surface waters. NR indicates data not reported

Reference	System	Location	Watershed area (km^2)	Measured f_{CO2} ($\mu mol\ C\ m^{-2}\ s^{-1}$)[a]	Measured f_{CH4}	Annual C emissions ($g\ C\ m^{-2}$)[b]
This study	Reaches without regional groundwater	Costa Rica (Central America)	0.279	8.61[c]	0.069[c]	48[d]
This study	Lower Arboleda	Costa Rica (Central America)	0.461	63.75[e]	0.055[e]	299[f]
Richey et al. [2002]	Central Amazon Basin	South America	NR	2.19[g]	NR	77[h]
Abril et al. [2005]	Sinnamary River[i]	French Guyana (South America)	NR	0.35-5.33	0.005	NR
	Petit Saut Reservoir	French Guyana (South America)	NR	0.16-1.54	0.031-0.089	NR
Johnson et al. [2008]	Amazon 2nd order tributary	Brazil (South America)	6	NR	NR	36[j]
Mitsch et al. [2010]	La Selva Wetland	Costa Rica (Central America)	--	NR	0.23-0.34	--
	Palo Verde Wetland	Costa Rica (Central America)	--	NR	1.04	--
Neu et al. [2011]	Tanguro Ranch 1st order stream	Brazil (South America)	13.19	15.0-25.4[k]	1.4-3.2[k]	0.51 (10.8)[m]
Alin et al. [2011][n]	Amazon River tributaries	Brazil (South America)	NR	0.67-12.13	NR	NR
Alin et al. [2011][n]	Mekong River tributary	Cambodia (Southeast Asia)	NR	1.61	NR	NR
Sawakuchi et al. [2014]	Rivers in the Amazon basin	South America	NR	NR	0.0001-0.4660	NR

[a]Per m^2 of stream surface area.
[b]Normalized by watershed area.
[c]Average values for the Taconazo (dry and wet seasons, upper and lower) and upper Arboleda (dry and wet seasons).
[d]Taconazo watershed
[e]Average values for the lower Arboleda (dry and wet seasons).

[f]Arboleda watershed
[g]Calculated from 8.3 Mg C ha^{-1} y^{-1}, value reported by *Richey et al*. [2002] as the CO_2 flux over the annual mean flooded area of the central Amazon basin.
[h]Calculated from the 470 Tg C y^{-1} value reported by *Richey et al*. [2002] as the CO_2 export to the atmosphere extrapolated to the Amazon basin and 6 million km^2 as the total area of the Amazon basin.
[i]Above the Petit Saut reservoir.
[j]Calculated from the ~90% of stream CO_2 that evaded to the atmosphere within the stream headwaters and the 40 g C m^{-2} y^{-1} exported to the stream from the terrestrial ecosystem as CO_2 [*Johnson et al*., 2008].
[k]Approximated from Figure 4 of *Neu et al*. [2011].
[m]Value estimated when adding in CO_2 losses through deep groundwater [*Neu et al*., 2011].
[n]Rivers of width < 100 m

upper Arboleda reaches because both gas exchange rates and $[CH_4]_{aq}$ were higher in the wet season.

5.5. Flux estimates in the context of other tropical ecosystems

In the lower Taconazo f_{CO2} was comparable to values observed in other tropical streams and rivers (Table 4). In contrast, lower Arboleda f_{CO2} was higher than all values reported in the literature for other tropical systems (Table 4). Results for f_{CH4} in the lower Taconazo and Arboleda were similar to those measured by *Abril et al*. [2005] in a tropical reservoir but lower than results from tropical wetlands in Costa Rica [*Mitsch et al*., 2010] and in the lower end of the range reported for Amazon rivers [*Sawakuchi et al*., 2014] (Table 4). Normalized by watershed area, annual C emissions from the Taconazo (48 g C m^{-2}, Table 4) fall within fluxes observed in other tropical systems: 36 g C m^{-2} from a second order Amazon tributary [*Johnson et al*., 2008] and 77 g C m^{-2} from the whole Amazon basin [*Richey et al*., 2002] (Table 4). In contrast, fluxes from the Arboleda (299 g C m^{-2}, Table 4) were much higher.

Fluxes normalized by watershed area for a tributary of the Tanguro River in the Amazon [*Neu et al*., 2011] were much smaller than our results for both the Arboleda and Taconazo catchments (0.51 g C m^{-2}, Table 4). In the Tanguro River tributary, ~90% of the net rainfall (precipitation – evapotranspiration) within the studied catchment appeared to bypass the stream and be exported through deep regional groundwater flow [*Neu et al*., 2011]. This resulted in a much smaller fraction of stream area relative to watershed area (0.007% versus 1-2% in the Taconazo or Arboleda), and low stream C emissions (most of the hydrologic export or loss of dissolved C was as recharge to deep groundwater rather than discharge to a stream). This catchment seems to represent the type of system that must lie upgradient of La Selva: an ecosystem losing (instead of gaining) groundwater and carbon by regional interbasin groundwater flow. The Tanguro in Brazil and Arboleda in Costa Rica may together illustrate, at recharge and discharge respectively, how regional groundwater flow can alter ecosystem C fluxes and budgets.

6. Summary and Conclusions

We measured CO_2 and CH_4 degassing fluxes from two rainforest streams, the Arboleda and Taconazo, at La Selva Biological Station in Costa Rica. The lower Arboleda receives significant inputs (about 1/3 of stream discharge) of old regional bedrock groundwater that is high in DIC and recharged outside of the topographically-defined Arboleda basin. The upper Arboleda, and the lower and upper Taconazo, receive only young local groundwater recharged within the topographic watershed. Results make it clear that input of regional groundwater to streams, which was previously shown to increase downstream transport of DIC [*Genereux et al*., 2013], can also greatly increase stream degassing of CO_2. Comparing the lower Arboleda to the upper and lower Taconazo and upper Arboleda, regional groundwater inputs: (1) increased stream water CO_2 concentration by a factor of 4-6 in the dry season and 6-11 in the wet season (for an overall average increase of 7x), and (2) increased CO_2 degassing flux by a factor of 7-15 in the dry season and 4-8 in the wet season (for an average increase of 8.5x) (Tables 1, 2). Regional groundwater had no effect on stream CH_4 concentration or degassing flux. The additional water input from regional groundwater led to the lower Arboleda being much deeper than the other stream reaches (Table 1), and the first-order gas exchange coefficient ($time^{-1}$) being lower (Table 2). These two effects are offsetting resulting in no major effect of regional groundwater discharge on stream gas exchange velocity (Table 2).

Augmentation of stream C degassing by input of high-C regional groundwater to streams is a general hydrogeological and geochemical phenomenon that extends beyond tropical rainforests, and may occur worldwide wherever there is: (1) a topographic driving force for regional interbasin groundwater flow leading to discharge in inland fresh waters (rather than on the seafloor, where some regional groundwater discharge occurs), and (2) a source for elevated dissolved C in regional groundwater. The CO_2 degassing from the Arboleda stream was large; normalized for the full land area of the watershed it was about 300 g C m^{-2} yr^{-1}, about 1.2x the average NEE of CO_2 estimated from previous eddy covariance measurements [*Loescher et al.*, 2003]. Observing increased stream CO_2 degassing rates such as those in the Arboleda could suggest that an ecosystem has elevated respiration and is a net source (rather than sink) with respect to atmospheric CO_2. Knowing that elevated stream CO_2 degassing is supported and driven by a large input of non-biogenic CO_2 from regional groundwater helps to avoid an overestimation of ecosystem respiration and provides a more accurate picture of the C source/sink status of the ecosystem.

Appendix

a)

b)

c)

d)

e)

f)

Figure A1. Images of the Arboleda and Taconazo streams taken at or near the study reaches. (a) Sampling station in the upper Arboleda reach; (b) sampling station in the Lower Arboleda reach; (c) tracer injection site in the lower Arboleda reach (floating white Styrofoam sheet is 1 m x 2 m); (d) infrared gas analyzer (Vaisala GMP343) in the upper Taconazo reach; (e) tracer injection site in the lower Taconazo reach; and (f) V-notch weir in the Taconazo stream, ~30 m downstream of the lower Taconazo reach.

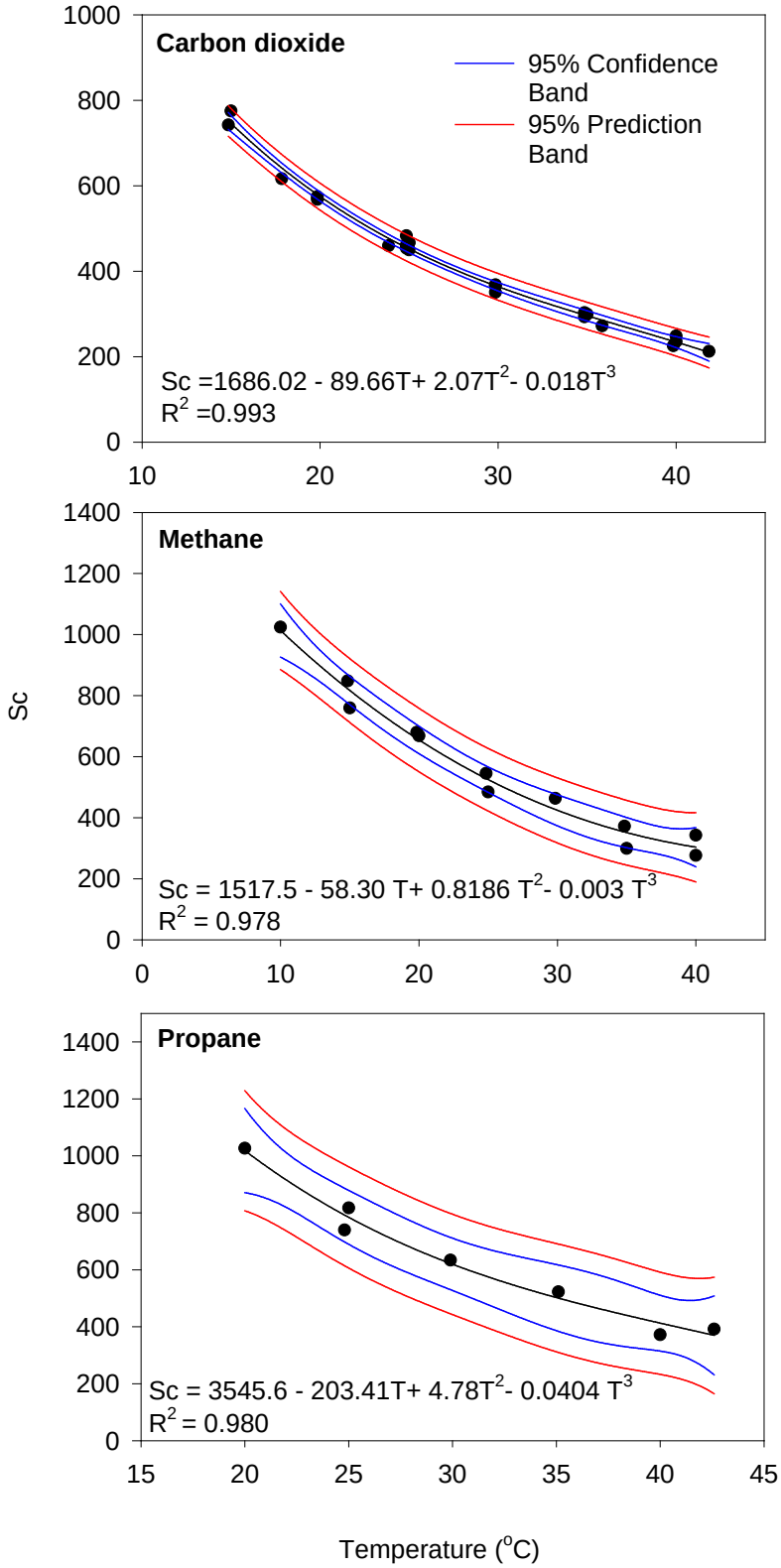

Figure A2. Schmidt numbers (*Sc*) as a function of temperature (*T*).

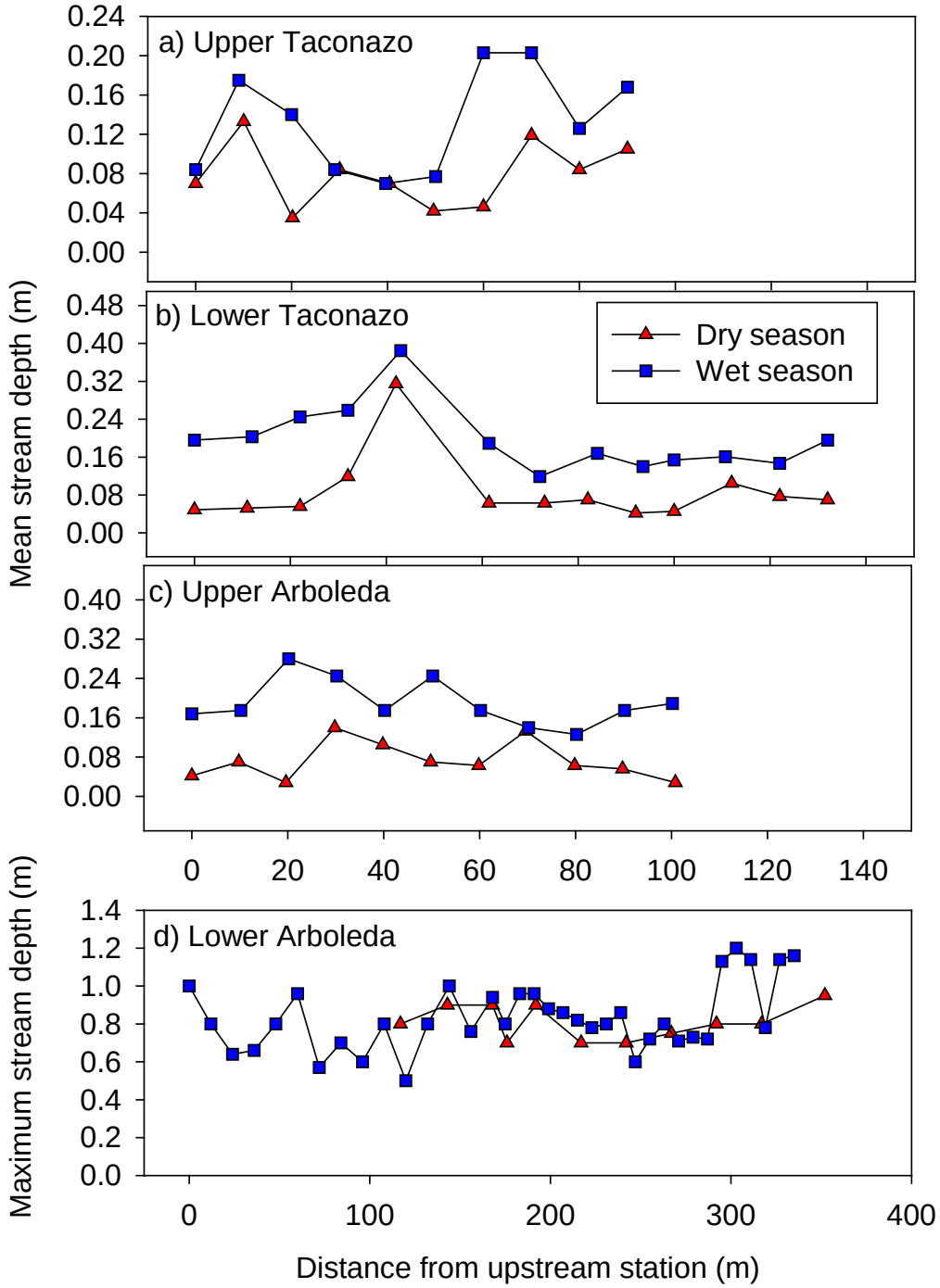

Figure A3. Mean stream depth calculated from maximum depth (see Section 3.2) as a function of distance from the upstream station for (a) the upper Taconazo, (b) lower Taconazo, and (c) upper Arboleda reaches at the time of the dry and wet season experiments. (d) Maximum stream depth as a function of distance for the upstream station for lower Arboleda reaches at the time of the dry and wet season experiments.

Reach	Season	Sub-reach	Sub-reach length (m)	k_{C3H8} (day^{-1})
Upper Taconazo	Dry season	A	30	37.4
		B	30	20.4
		C	30	14.2
	Wet season	A	30	46.0
		B	30	26.6
		C	26	23.6
Lower Taconazo	Dry season	A	42	19.1
		B	40	31.0
		C	50	37.4
	Wet season	A	43	15.4
		B	41	10.2
		C	48	17.4
Upper Arboleda	Dry season	A	40	8.8
		B	30	18.3
		C	30	48.8
	Wet season	A	40	49.7
		B	30	32.5
		C	30	37.6
Lower Arboleda	Dry season	Full reach exp 1	175	5.5
		Full reach exp 2	175	2.5
	Wet season	A exp 1	175	6.1
		A exp 2	173	2.4
		B exp 1	175	1.3
		B exp 2	173	3.2

Table A1. Propane gas exchange coefficients for sub-reaches located within the study reaches (Table 1). In addition to the upstream and downstream station defining each reach, intermediate stations defined sub-reaches (See section 3.2). Within the lower Arboleda study reach there were no intermediate stations in the dry season, and only one in the wet season which gave two sub-reaches (A and B). All other reaches had two intermediate stations forming three sub-reaches (A, B, and C).

Season	Stream section	Arboleda						Taconazo					
		Upper (above 49 m.a.s.l)			Lower (below 49 m.a.s.l)			Upper			Lower		
		L (m)	W (m)	α (m^2)	L (m)	W (m)	α (m^2)	L (m)	W (m)	α (m^2)	L (m)	W (m)	α (m^2)
Dry	Main channel	853	1.1	938	817	5	4083	794	1.4	1111	794	1.5	1191
	Tributaries	765	0.55	421	1483	0.5	742	487	0.7	341	487	0.75	365
	Total			**1358**			**4825**			**1452**			**1556**
	(% of the total)			**(22)**			**(78)**			**(48)**			**(52)**
Wet	Main channel	853	2.2	1876	817	5	4083	794	1.8	1429	794	2.8	2222
	Tributaries	1292	1.1	1422	1483	1	1483	596	0.9	536	596	1.4	834
	Total			**3297**			**5566**			**1965**			**3057**
	(% of the total)			**(37)**			**(63)**			**(39)**			**(61)**
Total dry season α					**6183**						**3008**		
(% of basin area)					**(1.3)**						**(1.1)**		
Total wet season α					**8863**						**5022**		
(% of basin area)					**(1.9)**						**(1.8)**		

Table A2. Estimated stream length (L), width (W), and area (α) for the upper and lower Arboleda and Taconazo stream networks (main channel plus tributaries) during the dry and wet seasons. Stream length was estimated using ArcGIS tools from a 5-m digital elevation model (DEM) created from LiDAR data [*Kellner et al*., 2009; *Zanon*, 2011]. The stream sections were classified as main channel, perennial tributaries (>100 m) and intermittent tributaries (<100 m). Intermittent tributaries were assumed to be dry during the dry season. For the Taconazo and the upper section of the Arboleda, the main channel was assigned a width based on field measurements within the study reach, and the flowing tributaries were assumed to be 50% narrower than the main channel. For the lower section of the Arboleda, the main channel was assigned a width based on field measurements within the study reach and the flowing tributaries were assumed to be 0.5 and 1 m wide during the dry and wet seasons, respectively. Surface area was calculated as the product of length and width.

Variable	Arboleda				Taconazo				Uncertainty is:
	Dry season		Wet season		Dry season		Wet season		
	Upper section	Lower section	Upper section	Lower section	Upper section	Lower section	Upper section	Lower section	
n	0.7±0.2	0.7±0.2	0.7±0.2	0.7±0.2	0.7±0.2	0.7±0.2	0.7±0.2	0.7±0.2	The interval between theoretical models: Surface renewal model (n = 0.5) and stagnant film model (n =1).
Sc_{CO2}	478±30	458±30	449±30	450±30	481±30	496±30	449±30	448±30	95% Prediction bands (Figure S2)
Sc_{C3H8}	833±175	795±175	777±175	780±175	839±175	867±175	778±175	776±175	95% Prediction bands (Figure S2)
Sc_{CH4}	553±100	531±100	520±100	522±100	556±100	572±100	521±100	520±100	95% Prediction bands (Figure S2)
k_{C3H8}	23±2.3	3.6±2.1	42.9±7.0	3.6±2.1	22±0.8	27.2±3.7	31.8±7.2	10.8±4.3	For Taconazo and upper section of Arboleda: 95% CI derived from error propagation of the calculation (equation 15). For the lower Arboleda: 95% CI derived from the four measurements obtained throughout the year.
$[CO_2]_{eq}$ (µM)	17.1±0.9	19.4±0.9	16.0±0.8	16.6±0.8	17.3±0.9	17.9±0.9	15.8±0.8	17.6±0.9	95% CI of variation in 1-min measurements made with the IRGA at the time of the experiment.
$[CO_2]_{aq}$ (µM)	215±30	1189±83	111±16	1235±86	187±26	267±37	143±20	219±31	95% CI of annual variation in CO_2 concentration estimated from weekly samples of dissolved inorganic carbon
$[CH_4]_{eq}$ (nM)	7.0±0.1	7.0±0.1	19.0±0.1	19.0±0.1	7.0±0.2	7.0±0.1	19.0±0.3	23.0±0.7	95% CI of variation in air samples collected during the experiment.
$[CH_4]_{aq}$ (µM)	0.7±0.2	0.8±0.1	0.6±0.1	1.6±0.1	0.9±0.6	1.1±0.3	2.5±1.1	2.7±0.3	95% CI of variation in water samples collected during the experiment.
Depth (m)	0.08±0.03	0.89±0.18	0.19±0.03	0.82±0.18	0.08±0.02	0.09±0.05	0.14±0.03	0.2±0.05	95% CI of variation in measurements taken at the time of the experiment.
Area (m^2)	1358±489	4825±193	3297±1187	5566±223	1452±131	1556±373	1965±177	3057±734	25% of the difference in α estimates between the dry and wet season.

Table A3. Best estimate for each of the parameters ± the uncertainty used in the Monte Carlo simulation to estimate the confidence interval (CI) for annual C degassing flux (F). Because the Schmidt number (Sc) is temperature dependent it can vary throughout the year, however the variation in water temperature between the dry and wet season was < 3°C; this variation would cause a change in Sc lower than the 95% prediction bands for equations [10], [11], and [12] (Figure S2). The regression prediction intervals from Figure S2 were used in the Monte Carlo simulation as the uncertainty associated with Sc. For $[CO_2]_{aq}$, variation in weekly measurements at the weirs was taken rather than variation during the gas exchange measurements, as a metric that is more relevant to scaling up over the year.

Factor in Montecarlo simulation	Arboleda dry season	Arboleda wet season	Taconazo dry season	Taconazo wet season
n	9.1%	9.0%	9.2%	9.0%
Sc_{CO2} in the upper section	0.1%	0.4%	1.2%	1.7%
Sc_{C3H8} in the upper section	0.3%	1.5%	4.0%	6.0%
Sc_{CH4} in the in the upper section	0.0%	0.0%	0.0%	0.1%
k_{C3H8} in the in the upper section	0.2%	1.5%	1.0%	8.5%
$[CO_2]_{eq}$ in the in the upper section	0.0%	0.1%	0.1%	0.2%
$[CO_2]_{aq}$ in the in the upper section	0.3%	1.5%	4.2%	5.8%
$[CH_4]_{eq}$ in the upper section	0.0%	0.0%	0.0%	0.0%
$[CH_4]_{aq}$ in the upper section	0.0%	0.0%	0.1%	0.3%
Depth in the upper section	0.8%	1.5%	6.5%	9.1%
Stream surface area in the upper section	0.8%	3.3%	2.4%	3.4%
Sc_{CO2} in the lower section	3.7%	3.4%	2.3%	2.1%
Sc_{C3H8} in the lower section	12.5%	11.5%	7.8%	7.1%
Sc_{CH4} in the in the lower section	0.0%	0.0%	0.0%	0.1%
k_{C3H8} in the in the lower section	47.1%	42.6%	7.4%	17.6%
$[CO_2]_{eq}$ in the in the lower section	0.1%	0.0%	0.2%	0.2%
$[CO_2]_{aq}$ in the in the lower section	5.7%	5.2%	8.3%	6.7%
$[CH_4]_{eq}$ in the lower section	0.0%	0.0%	0.0%	0.0%
$[CH_4]_{aq}$ in the lower section	0.0%	0.0%	0.1%	0.1%
Depth in the lower section	15.9%	15.6%	31.8%	11.2%
Stream surface area in the lower section	3.2%	2.9%	13.3%	10.7%

Table A4. Contribution of each input variable to the Monte Carlo-simulated uncertainty in annual C degassing flux (*F*).

Acknowledgments

The authors thank Emily Barnett, Daniel Rojas-Jimenez, Ruben Vargas, and William Ureña for their help with the field and laboratory tasks. This work was financed by the US Department of Energy (award DE-SC0006703). Logistical support at the field site was provided by the Organization for Tropical Studies. Supporting data are included in an SI file; any additional data may be obtained by contacting the corresponding author at doviedo@ncsu.edu. Statements and opinions in this report are those of the authors and do not necessarily reflect the views of the sponsoring agency.

References

Abril, G., F. Guérin, S. Richard, R. Delmas, C. Galy-Lacaux, P. Gosse, A. Tremblay, L. Varfalvy, M. A. Dos Santos, and B. Matvienko (2005), Carbon dioxide and methane emissions and the carbon budget of a 10-year old tropical reservoir (Petit Saut, French Guiana), *Global Biogeochem. Cycles*, *19*, GB4007, doi:10.1029/2005gb002457.

Alin, S. R., M. de F. F. L. Rasera, C. I. Salimon, J. E. Richey, G. W. Holtgrieve, A. V. Krusche, and A. Snidvongs (2011), Physical controls on carbon dioxide transfer velocity and flux in low-gradient river systems and implications for regional carbon budgets, *J. Geophys. Res. Biogeosci.*, *116*, G01009, doi:10.1029/2010jg001398.

Aravena, R., and L.I. Wassenaar (1993), Dissolved organic carbon and methane in a regional confined aquifer, southern Ontario, Canada: Carbon isotope evidence for associated subsurface sources, *Appl. Geochem., 8*, 483-493, doi:10.1016/0883-2927(93)90077-T.

Aufdenkampe, A. K., E. Mayorga, P. A. Raymond, J. M. Melack, S. C. Doney, S. R. Alin, R. E. Aalto, and K. Yoo (2011), Riverine coupling of biogeochemical cycles between land, oceans, and atmosphere, *Front. Ecol. Environ., 9*, 53-60, doi:10.1890/100014.

Battin, T. J., S. Luyssaert, L. A. Kaplan, A. K. Aufdenkampe, A. Richter, and L. J. Tranvik (2009), The boundless carbon cycle, *Nat. Geosci., 2*, 598-600, doi:10.1038/ngeo618.

Billett, M. F., S. M. Palmer, D. Hope, C. Deacon, R. Storeton-West, K. J. Hargreaves, C. Flechard, and D. Fowler (2004), Linking land-atmosphere-stream carbon fluxes in a lowland peatland system, *Global Biogeochem. Cycles, 18*, GB1024, doi:10.1029/2003gb002058.

Butman, D., and P. A. Raymond (2011), Significant efflux of carbon dioxide from streams and rivers in the United States, *Nat. Geosci., 4*, 839-842, doi:10.1038/ngeo1294.

Campeau, A., J.-F. Lapierre, D. Vachon, and P. A. Giorgio (2014), Regional contribution of CO_2 and CH_4 fluxes from the fluvial network in a lowland boreal landscape of Québec, *Global Biogeochem. Cycles, 28*, 57-69, doi:10.1002/2013GB004685.

Chiodini, G., F. Frondini, D. Kerrick, J. Rogie, F. Parello, L. Peruzzi, and A. Zanzari (1999), Quantification of deep CO_2 fluxes from Central Italy. Examples of carbon balance for regional aquifers and of soil diffuse degassing, *Chem. Geol., 159*, 205-222, doi:10.1016/S0009-2541(99)00030-3.

Cole, J., Y. Prairie, N. Caraco, W. McDowell, L. Tranvik, R. Striegl, C. Duarte, P. Kortelainen, J. Downing, and J. Middelburg (2007), Plumbing the global carbon cycle: integrating inland waters into the terrestrial carbon budget, *Ecosystems, 10*, 172-185, doi:10.1007/s10021-006-9013-8.

Crawford, J. T., R. G. Striegl, K. P. Wickland, M. M. Dornblaser, and E. H. Stanley (2013), Emissions of carbon dioxide and methane from a headwater stream network of interior Alaska, *J. Geophys. Res. Biogeosci., 118*, 482-494, doi:10.1002/jgrg.20034.

Crawford, J. T., E. H. Stanley, S. A. Spawn, J. C. Finlay, L. C. Loken, and R. G. Striegl (2014a), Ebullitive methane emissions from oxygenated wetland streams, *Global Change Biol., 20*, 3408-3422, doi:10.1111/gcb.12614.

Crawford, J. T., N. R. Lottig, E. H. Stanley, J. F. Walker, P. C. Hanson, J. C. Finlay, and R. G. Striegl (2014b), CO_2 and CH_4 emissions from streams in a lake-rich landscape: Patterns, controls, and regional significance, *Global Biogeochem. Cycles, 28*, 197-210, doi:10.1002/2013GB004661.

Cruz, J. V., and C. S. Amaral (2004), Major ion chemistry of groundwater from perched-water bodies of the Azores (Portugal) volcanic archipelago, *Appl. Geochem., 19*, 445-459, doi:10.1016/S0883-2927(03)00135-5.

Davidson, E. A., D. C. Nepstad, F. Y. Ishida, and P. M. Brando (2008), Effects of an experimental drought and recovery on soil emissions of carbon dioxide, methane, nitrous oxide, and nitric oxide in a moist tropical forest, *Global Change Biol., 14*, 2582-2590, doi:10.1111/j.1365-2486.2008.01694.x.

Dinsmore, K. J., M. F. Billett, U. M. Skiba, R. M. Rees, J. Drewer, and C. Helfter (2010), Role of the aquatic pathway in the carbon and greenhouse gas budgets of a peatland catchment, *Global Change Biol., 16*, 2750-2762, doi:10.1111/j.1365-2486.2009.02119.x.

Duda, J., and J. Vrentas (1968), Laminar liquid jet diffusion studies, *AIChE Journal, 14*, 286-294, doi:10.1002/aic.690140215.

Evans, W. C., D. Bergfeld, R. G. McGimsey, and A. G. Hunt (2009), Diffuse gas emissions at the Ukinrek Maars, Alaska: Implications for magmatic degassing and volcanic monitoring, *Appl. Geochem.*, *24*, 527-535, doi:10.1016/j.apgeochem.2008.12.007.

Frank, M. J., J. A. Kuipers, and W. P. van Swaaij (1996), Diffusion coefficients and viscosities of CO_2+H_2O, CO_2+CH_3OH, NH_3+H_2O, and NH_3+CH_3OH liquid mixtures, *J.Chem. Eng. Data*, *41*, 297-302, doi:10.1021/je950157k.

Genereux, D. P., and H. F. Hemond (1990), Naturally occurring radon 222 as a tracer for streamflow generation: Steady state methodology and field example, *Water Resour. Res.*, *26*, 3065–3075, doi:10.1029/WR026i012p03065.

Genereux, D. P., and H. F. Hemond (1992), Determination of gas exchange rate constants for a small stream on Walker Branch Watershed, Tennessee, *Water Resour. Res.*, *28*, 2365-2374, doi:10.1029/92WR01083.

Genereux, D. P., M. T. Jordan, and D. Carbonell (2005), A paired-watershed budget study to quantify interbasin groundwater flow in a lowland rain forest, Costa Rica, *Water Resour. Res.*, *41*, W04011, doi:10.1029/2004WR003635.

Genereux, D. P., and M. T. Jordan (2006), Interbasin groundwater flow and groundwater interaction with surface water in a lowland rainforest, Costa Rica: a review. *J Hydrol.*, *320*, 385-399, doi: 10.1016/j.jhydrol.2005.07.023.

Genereux, D. P., M. Webb, and D. K. Solomon (2009), Chemical and isotopic signature of old groundwater and magmatic solutes in a Costa Rican rain forest: Evidence from carbon, helium, and chlorine, *Water Resour. Res.*, *45*, doi:10.1029/2008WR007630.

Genereux, D. P., L. A. Nagy, C. L. Osburn, and S. F. Oberbauer (2013), A connection to deep groundwater alters ecosystem carbon fluxes and budgets: Example from a Costa Rican rainforest, *Geophys. Res. Lett.*, *40*, 2066-2070, doi:10.1002/grl.50423.

Hope, D., S. M. Palmer, M. F. Billett, and J. J. Dawson (2001), Carbon dioxide and methane evasion from a temperate peatland stream, *Limnol. Oceanogr.*, *46*, 847-857, doi:10.4319/lo.2001.46.4.0847.

Huber, M., R. Perkins, A. Laesecke, D. Friend, J. Sengers, M. Assael, I. Metaxa, E. Vogel, R. Mareš, and K. Miyagawa (2009), New international formulation for the viscosity of H_2O, *J. Phys. Chem. Ref. Data*, *38*, 101-125, doi:10.1063/1.3088050.

James, E. R., M. Manga, and T. P. Rose (1999), CO_2 degassing in the Oregon Cascades, *Geology*, *27*, 823-826, doi: 10.1130/0091-7613(1999)027<0823:CDITOC>2.3.CO;2

Jähne, B., K. O. Münnich, R. Bösinger, A. Dutzi, W. Huber, and P. Libner (1987a), On the parameters influencing air-water gas exchange, *J. Geophys. Res. Oceans (1978-2012)*, *92*, 1937-1949, doi:10.1029/JC092iC02p01937.

Jähne, B., G. Heinz, and W. Dietrich (1987b), Measurement of the diffusion coefficients of sparingly soluble gases in water, *J. Geophys. Res. Oceans (1978-2012)*, *92*, 10767-10776, doi:10.1029/JC092iC10p10767.

Jähne, B., and H. Haußecker (1998), Air-water gas exchange, *Ann. Rev. Fluid Mech.*, *30*, 443-468, doi:10.1146/annurev.fluid.30.1.443.

Jin, H.-S., D. White, J. Ramsey, and G. Kipphut (2012), Mixed tracer injection method to measure reaeration coefficients in small streams, *Water, Air, Soil Pollut.*, *223*, 5297-5306, doi:10.1007/s11270-012-1280-8.

Johnson, M. S., J. Lehmann, S. J. Riha, A. V. Krusche, J. E. Richey, J. P. H. B. Ometto, and E. G. Couto (2008), CO_2 efflux from Amazonian headwater streams represents a significant fate for deep soil respiration, *Geophys. Res. Lett.*, *35*, L17401, doi:10.1029/2008GL034619.

Jonsson, A., G. Algesten, A.-K. Bergström, K. Bishop, S. Sobek, L. J. Tranvik, and M. Jansson (2007), Integrating aquatic carbon fluxes in a boreal catchment carbon budget, *J. Hydrol.*, *334*, 141-150, doi:10.1016/j.jhydrol.2006.10.003.

Kampman, N., M.J. Bickle, A. Maskell, H.J. Chapman, J.P. Evans, G. Purser, Z. Zhou, M.F. Schaller, J.C. Gattacceca, P. Bertier, F. Chen, A.V. Turchyn, N. Assayag, C. Rochelle, C.J. Ballentine, A. Busch (2014), Drilling and sampling a natural CO_2 reservoir: Implications for fluid flow and CO_2-fluid-rock reactions during CO_2 migration through the overburden, *Chem. Geol.*, *369*, 51-82, doi:10.1016/j.chemgeo.2013.11.015.

Keller, M., and W. A. Reiners (1994), Soil-atmosphere exchange of nitrous oxide, nitric oxide, and methane under secondary succession of pasture to forest in the Atlantic lowlands of Costa Rica, *Global Biogeochem. Cycles*, *8*, 399-409, doi:10.1029/94GB01660.

Kellner, J. R., D. B. Clark, and M. A. Hofton (2009), Canopy height and ground elevation in a mixed-land-use lowland Neotropical rain forest landscape, *Ecology*, *90*, 3274-3274, doi:10.1890/09-0254.1.

Kilpatrick, F. A., R. Rathbun, N. Yotsukura, G. Parker, and L. DeLong (1989), *Determination of stream reaeration coefficients by use of tracers*, Techniques of Water Resources Investigations of the U.S. Geological Survey, report TWI 3-A18, 52 pages.

Kokic, J., M. B. Wallin, H. E. Chmiel, B. A. Denfeld, and S. Sobek (2015), Carbon dioxide evasion from headwater systems strongly contributes to the total export of carbon from a small boreal lake catchment, *J. Geophys. Res. Biogeosci.*, 2014JG002706, doi:10.1002/2014jg002706.

Koprivnjak, J. F., P. J. Dillon, and L. A. Molot (2010), Importance of CO_2 evasion from small boreal streams, *Global Biogeochem. Cycles*, *24*, GB4003, doi:10.1029/2009gb003723.

Ku, H. (1966), Notes on the use of propagation of error formulas, *J. Res. Nat. Bur. Stand.*, *70*, 263-273.

Kucharič, L. u., D. Bodiš, D. Panák, P. Liščák, and J. Božíková (2015), A contribution of CO_2 released from mineral springs into overall volume of annual CO_2 emissions in the Slovak Republic, *Environ. Earth Sci.*, *73*, 231-238, doi:10.1007/s12665-014-3418-z.

Leopold, L. B., and T. Maddock. (1953). *The hydraulic geometry of stream channels and some physiographic implications.* U.S. Government Printing Office, 57.

Liu, K., J. J. Jiao, and J.D. Gu (2014), Investigation on bacterial community and diversity in the multilayer aquifer-aquitard system of the Pearl River Delta, China, *Ecotoxicology*, *23*, 2041-2052, doi:10.1007/s10646-014-1311-x.

Loescher, H. W., S. F. Oberbauer, H. L. Gholz, and D. B. Clark (2003), Environmental controls on net ecosystem-level carbon exchange and productivity in a Central American tropical wet forest. *Global Change Biol.*, *9*, 396–412. doi:10.1046/j.1365-2486.2003.00599.x.

Loescher, H. W., H. Gholz, J. M. Jacobs, and S. F. Oberbauer (2005), Energy dynamics and modeled evapotranspiration from a wet tropical forest in Costa Rica, *J. Hydrol.*, *315*, 274-294, doi:10.1016/j.jhydrol.2005.03.040.

Lovley, D. R., and R. T. Anderson (2000), Influence of dissimilatory metal reduction on fate of organic and metal contaminants in the subsurface, *Hydrogeol. J.*, *8*, 77-88, doi:10.1007/PL00010974

Lu, W., H. Guo, I. Chou, R. Burruss, and L. Li (2013), Determination of diffusion coefficients of carbon dioxide in water between 268 and 473K in a high-pressure capillary optical cell with in situ Raman spectroscopic measurements, *Geochim. Cosmochim. Acta*, *115*, 183-204, doi:10.1016/j.gca.2013.04.010.

Lundin, E. J., R. Giesler, A. Persson, M. S. Thompson, and J. Karlsson (2013), Integrating carbon emissions from lakes and streams in a subarctic catchment, *J. Geophys. Res. Biogeosci.*, *118*, 1200-1207, doi:10.1002/jgrg.20092.

Madsen, H., J. Vollertsen, and T. Hvitved-Jacobsen (2007), Air-water mass transfer and tracer gases in stormwater systems. *Water Sci. Tech.*, *56*, 267-275, doi:10.2166/wst.2007.461 267

Maharajh, D. M., and J. Walkley (1973), The temperature dependence of the diffusion coefficients of Ar, CO_2, CH_4, CH_3Cl, CH_3Br, and $CHCl_2F$ in water, *Can. J. Chem.*, *51*, 944-952, doi:10.1139/v73-140.

Marrero, R., D. L. López, P. A. Hernández, and N. M. Pérez (2008), Carbon dioxide discharged through the Las Canadas Aquifer, Tenerife, Canary Islands, in *Terrestrial Fluids, Earthquakes and Volcanoes: The Hiroshi Wakita Volume III*, edited, pp. 147-172, Springer.

Miller, J. N., and J. C. Miller (2005), *Statistics and chemometrics for analytical chemistry*, 5th ed., Pearson Education, Ontario, Canada.

Mitsch, W. J., A. Nahlik, P. Wolski, B. Bernal, L. Zhang, and L. Ramberg (2010), Tropical wetlands: seasonal hydrologic pulsing, carbon sequestration, and methane emissions, *Wetl. ecol. manag.*, *18*, 573-586, doi:10.1007/s11273-009-9164-4

Mörner , N.-A., and G. Etiope (2002), Carbon degassing from the lithosphere, *Global. Planet. Change*, *33*, 185-203, doi:10.1016/S0921-8181(02)00070-X.

Murphy, E. M., S. N. Davis, A. Long, D. Donahue, and A. J. T. Jull (1989), Characterization and isotopic composition of organic and inorganic carbon in the Milk River Aquifer, *Water Resour. Res.*, *25*, 1893–1905, doi:10.1029/WR025i008p01893.

Myhre, G., D. Shindell, F.-M. Bréon, W. Collins, J. Fuglestvedt, J. Huang, D. Koch, J.-F. Lamarque, D. Lee, B. Mendoza, T. Nakajima, A. Robock, G. Stephens, T. Takemura and H. Zhang (2013), Anthropogenic and Natural Radiative Forcing, in: *Climate Change 2013: The Physical Science Basis. Contribution of Working Group I to the Fifth Assessment Report of the Intergovernmental Panel on Climate Change*, edited by T.F. Stocker, D. Qin, G.-K. Plattner, M. Tignor, S.K. Allen, J. Boschung, A. Nauels, Y. Xia, V. Bex and P.M. Midgley, Cambridge University Press, Cambridge, United Kingdom and New York, NY, USA.

Neu, V., C. Neill, and A. V. Krusche (2011), Gaseous and fluvial carbon export from an Amazon forest watershed, *Biogeochemistry*, *105*, 133-147, doi:10.1007/s10533-011-9581-3.

Pacheco, F. (2015), Regional groundwater flow in hard rocks, *Sci. Total Environ.*, *506–507*, 182-195, doi:10.1016/j.scitotenv.2014.11.008.

Park, J., R. A. Sanford, and C. M. Bethke (2009), Microbial activity and chemical weathering in the Middendorf aquifer, South Carolina, *Chem. Geol.*, *258*, 232-241, doi:10.1016/j.chemgeo.2008.10.011.

Rantakari, M., T. Mattsson, P. Kortelainen, S. Piirainen, L. Finér, and M. Ahtiainen (2010), Organic and inorganic carbon concentrations and fluxes from managed and unmanaged boreal first-order catchments, *Sci. Total Environ.*, *408*, 1649-1658, doi:10.1016/j.scitotenv.2009.12.025.

Rasera, F. M. d. F., M. V. R. Ballester, A. V. Krusche, C. Salimon, L. A. Montebelo, S. R. Alin, R. L. Victoria, and J. E. Richey (2008), Estimating the surface area of small rivers in the southwestern Amazon and their role in CO_2 outgassing, *Earth Interact.*, *12*, 1-16, doi:10.1175/2008EI257.1.

Raymond, P. A., C. J. Zappa, D. Butman, T. L. Bott, J. Potter, P. Mulholland, A. E. Laursen, W. H. McDowell, and D. Newbold (2012), Scaling the gas transfer velocity and hydraulic

geometry in streams and small rivers, *Limnol. Oceanogr.: Fluids and Environments*, *2*, 41-53, doi:10.1215/21573689-1597669.

Reid, S. E., P. A. Mackinnon, and T. Elliot (2007), Direct measurements of reaeration rates using noble gas tracers in the River Lagan, Northern Ireland, *Water Environ. J.*, *21*, 182-191, doi:10.1175/2008EI257.1.

Richey, J. E., J. M. Melack, A. K. Aufdenkampe, V. M. Ballester, and L. L. Hess (2002), Outgassing from Amazonian rivers and wetlands as a large tropical source of atmospheric CO_2, *Nature*, *416*, 617-620, doi:10.1038/nature12797.

Rivé, K., J. Gaillardet, P. Agrinier, and S. Rad (2013), Carbon isotopes in the rivers from the Lesser Antilles: origin of the carbonic acid consumed by weathering reactions in the Lesser Antilles, *Earth Surf. Process. Landf.*, *38*, 1020-1035, doi:10.1002/esp.3385.

Sawakuchi, H. O., D. Bastviken, A. O. Sawakuchi, A. V. Krusche, M. V. Ballester,and J. E. Richey, (2014), Methane emissions from Amazonian Rivers and their contribution to the global methane budget. *Glob. Change Biol*., *20*, 2829-2840, doi:10.1111/gcb.12646.

Schaller, M. F., and Y. Fan (2009), River basins as groundwater exporters and importers: Implications for water cycle and climate modeling, *J. Geophys. Res.*, *114*, D04103, doi:10.1029/2008JD010636.

Schlesinger, W. H., and E. S. Bernhardt (2013), *Biogeochemistry: an analysis of global change*, Academic press, Waltham, MA.

Smerdon, B. D., W. P. Gardner, G. A. Harrington, and S. J. Tickell (2012), Identifying the contribution of regional groundwater to the baseflow of a tropical river (Daly River, Australia), *J. Hydrol.*, *464–465*, 107‑115, doi:10.1016/j.jhydrol.2012.06.058.

Snyder, G., R. Poreda, U. Fehn, and A. Hunt (2003), Sources of nitrogen and methane in Central American geothermal settings: Noble gas and ^{129}I evidence for crustal and magmatic volatile components, *Geochem. Geophys.Geosyst.*, *4*, 1-28, doi:10.1029/2002GC000363.

Sollins, P., F. Sancho, R. Mata, and R. Sanford (1994), Soils and soil process research, in *La Selva: ecology and natural history of a neotropical rain forest.* , edited by L. A. McDade, et al., pp. 34-53, University of Chicago Press, Chicago, IL.

Solomon, D. K., D. P. Genereux, L. N. Plummer, and E. Busenberg (2010), Testing mixing models of old and young groundwater in a tropical lowland rain forest with environmental tracers, *Water Resour. Res.*, *46*, W04518,doi:10.1029/2009WR008341.

Striegl, R. G., M. Dornblaser, C. McDonald, J. Rover, and E. Stets (2012), Carbon dioxide and methane emissions from the Yukon River system, *Global Biogeochem. Cycles*, *26*, doi:10.1029/2012GB004306.

Schwendenmann, L., E. Veldkamp, T. Brenes, J. J.O'Brien, and J. Mackensen (2003), Spatial and temporal variation in soil CO_2 efflux in an old-growth neotropical rain forest, La Selva, Costa Rica, *Biogeochemistry*, *64*, 111-128, doi:10.1023/A:1024941614919.

Tamimi, A., E. B. Rinker, and O. C. Sandall (1994), Diffusion coefficients for hydrogen sulfide, carbon dioxide, and nitrous oxide in water over the temperature range 293-368 K, *J. Chem. Eng. Data*, *39*, 330-332, doi:10.1021/je00014a031.

Tanaka, M., G. Girard, R. Davis, A. Peuto, and N. Bignell (2001), Recommended table for the density of water between 0 °C and 40 °C based on recent experimental reports, *Metrologia*, *38*, 301, doi:10.1088/0026-1394/38/4/3.

Tóth, J. A. (2009*), Gravitational Systems of Groundwater Flow: Theory, Evaluation, Utilization*, Cambridge University Press, New York.

Thomas, W., and M. Adams (1965), Measurement of the diffusion coefficients of carbon dioxide and nitrous oxide in water and aqueous solutions of glycerol, *Trans. Faraday Soc*., 61, 668-673, doi:10.1039/TF9656100668.

Veldkamp, E., A. Becker, L. Schwendenmann, D. A. Clark, and H. Schulte-Bisping (2003), Substantial labile carbon stocks and microbial activity in deeply weathered soils below a tropical wet forest, *Global Change Biol., 9*, 1171-1184, doi:10.1046/j.1365-2486.2003.00656.x.

Wallin, M. B., M. G. Öquist, I. Buffam, M. F. Billett, J. Nisell, and K. H. Bishop (2011), Spatiotemporal variability of the gas transfer coefficient (KCO_2) in boreal streams: Implications for large scale estimates of CO_2 evasion, *Global Biogeochem. Cycles*, *25*, GB3025, doi:10.1029/2010GB003975.

Wilcock, R. J. (1988), Study of river reaeration at different flow rates, *J. Environ. Eng.*, *114*, 91-105.

Wilcock, R. J., and B. K. Sorrell (2008), Emissions of greenhouse gases CH_4 and N_2O from low-gradient streams in agriculturally developed catchments, *Water, Air, Soil Pollut.*, *188*, 155-170, doi:10.1007/s11270-007-9532-8.

Witherspoon, P., and D. Saraf (1965), Diffusion of methane, ethane, propane, and n-butane in water from 25 to 43°, *J. Phys. Chem.*, *69*, 3752-3755, doi:10.1021/j100895a017.

Witherspoon, P., and L. Bonoli (1969), Correlation of diffusion coefficients for paraffin, aromatic, and cycloparaffin hydrocarbons in water, *Ind. Eng. Chem. Fund.*, *8*, 589-591, doi:10.1021/i160031a038.

Yamada, M., S. Ohsawa, K. Kazahaya, M. Yasuhara, H. Takahashi, K. Amita, H. Mawatari, and S. Yoshikawa (2011), Mixing of magmatic CO_2 into volcano groundwater flow at Aso volcano assessed combining carbon and water stable isotopes, *J. Geochem. Explor.*, *108*, 81-87, doi:10.1016/j.gexplo.2010.10.007.

Yotsukura, N., D. Stedfast, R. Draper, and W. Brutsaert (1983), *An Assessment of Steady-state Propane-gas Tracer Method for Reaeration Coefficients, Cowaselon Creek, New York*, U.S. Geological Survey Water Resources Investigations Report 83-4183, 95 pages.

Zanon, C. (2011), Watershed Hydrologic Modeling to Assess Interbasin Groundwater Flow in a Tropical Rainforest, M.S. thesis, North Carolina State University, Raleigh, NC, 225 pages, http://repository.lib.ncsu.edu/ir/handle/1840.16/6738.

Zanon, C., D. P. Genereux, and S. F. Oberbauer (2014), Use of a watershed hydrologic model to estimate interbasin groundwater flow in a Costa Rican rainforest, *Hydrol. Process.*, *28*, 3670-3680, doi:10.1002/hyp.9917.

Zeebe, R. E. (2011), On the molecular diffusion coefficients of dissolved, and and their dependence on isotopic mass, *Geochim. Cosmochim. Acta, 75*, 2483-2498, doi:10.1016/j.gca.2011.02.010

Chapter 3: Chamber measurements of high CO_2 emissions from a rainforest stream receiving old C-rich regional groundwater

Diana Oviedo-Vargas[1], Diego Dierick[2], David P. Genereux[1], Steven F. Oberbauer[2]
[1] Marine Earth and Atmospheric Sciences, North Carolina State University, Raleigh, NC
[2] Biological Sciences, Florida International University, Miami, FL

Abstract

Carbon emissions from fluvial systems are a key component of local and regional carbon cycles. We used floating chambers to investigate the CO_2 flux from stream water to air (f_{CO2}) in the Arboleda, a stream in the lowland rainforest of Costa Rica, fed partly by old regional groundwater high in dissolved inorganic carbon (DIC). Drifting and static chambers showed f_{CO2} averaging 35.5 and 72.7 μmol C m^{-2} s^{-1}, respectively, bracketing the previously-published f_{CO2} value of 56 μmol C m^{-2} s^{-1} obtained using tracer methods in this stream. These values are much higher than most f_{CO2} data in the literature and reflect a large flux of deep crustal (non-biogenic) CO_2 out of the Arboleda, a flux that does not represent a component of ecosystem respiration. Static chambers appeared to overestimate f_{CO2} by creating artificial turbulence, while drifting chambers may have underestimated f_{CO2} by under-sampling areas of potentially high gas exchange (e.g., riffles around coarse woody debris obstructions). Both static and drifting chambers revealed high spatial heterogeneity in f_{CO2} at the scale of 5-30 m reaches. Some observed temporal trends were localized, e.g., among three reaches with repeated measurements through the wet and dry seasons, (1) only the reach located between the other two showed significantly lower f_{CO2} during the dry season, and (2) the highest and lowest f_{CO2} were consistently observed in the reaches farthest upstream and downstream, respectively. Streams like the Arboleda receiving significant inputs of high-DIC regional groundwater merit additional study as hotspots for C emissions from terrestrial ecosystems.

Keywords: stream, carbon dioxide, chamber, emissions, flux, regional groundwater, gas exchange

1. Introduction

In light of current climate change challenges, the quantification of Earth's global carbon (C) cycle is critical for a sustainable future. There is a growing consensus that inland waters may represent a significant carbon dioxide (CO_2) source to the atmosphere (Cole et al. 2007; Raymond et al. 2013), and degassing of CO_2 from streams and rivers has received significant attention in recent years (e.g., Billett and Moore 2008; Butman and Raymond 2011; Campeau et al. 2014; Hope et al. 2001; Hotchkiss et al. 2015; Jonsson et al. 2007; Richey et al. 2002; Striegl et al. 2012; Teodoru et al. 2015). Despite the increased interest in understanding biogeochemical mechanisms driving fluvial emissions of CO_2, the role of old regional groundwater, including its interaction with surface water, has been largely overlooked. Regional groundwater flow is a hydrogeological process by which groundwater moves long distances through deep subsurface pathways beneath surface topographic divides, possibly recharging in one watershed and discharging in another many kilometers away (Tóth, 2009; Schaller and Fan, 2009; Smerdon et al., 2012; Pacheco, 2015), thus creating the potential for long-distance subsurface transport of C between watersheds and ecosystems. However, little is known about CO_2 emissions from streams and rivers affected by regional groundwater discharge and the potential effects on C balances of the aquatic and surrounding terrestrial ecosystems.

At La Selva Biological Station in the lowland rainforest of Costa Rica, several streams and wetlands receive significant inputs of old regional groundwater that has high concentrations of major ions and dissolved inorganic carbon (DIC) (Genereux and Jordan 2006; Genereux et al. 2009, 2013). This regional groundwater is recharged outside La Selva at higher elevations in the volcanic Cordillera Central, and enters watersheds at La Selva through the process of interbasin groundwater flow (IGF) (Genereux and Jordan 2006; Genereux et al. 2005, 2009; Solomon et al. 2010). Quantifying CO_2 emissions from tropical streams with this kind of input may be especially important as they can act as hotspots of CO_2 degassing (Genereux et al. 2013; Oviedo Vargas et al. 2015) and because tropical streams and rivers are emerging as a key component of the global C cycle (Alin et al. 2011; Rasera et al. 2013; Richey et al. 2002).

Evasion of CO_2 from flowing waters can be estimated from the gradient in CO_2 concentration across the air-water interface and the gas exchange piston velocity (k, units of length time^{-1}) of CO_2 (k_{CO2}). Whole-stream tracer additions (e.g., Genereux and Hemond 1992; Kilpatrick et al. 1989; Wallin et al. 2011) are generally considered the most robust and reliable approach for field determination of k in streams and rivers. The method is well-suited for stream reaches on the order of 100 m to a few kilometers, but not for showing dynamics at a small spatial scale (e.g., reaches of ~10 m) or for repeated measurements (e.g., frequent monitoring).

A number of recent studies investigating CO_2 emissions from streams and rivers have used floating chambers to measure CO_2 fluxes (e.g., Billett et al. 2007; Crawford et al. 2013; Dinsmore et al. 2010; Neu et al. 2011; Rasera et al. 2013; Sand-Jensen and Staehr 2012; Striegl et al. 2012; Teodoru et al. 2015; Wu et al. 2007). In this technique, the CO_2 flux across the water surface is measured by monitoring the buildup of CO_2 emitted into the chamber. Potential benefits of this technique include the relatively low financial cost and simplified logistics in comparison with tracer injections (which facilitates repeated measurements for monitoring), and the small spatial scale of the measurements, which may allow insights into relationships between gas exchange and potential controlling variables (insights that may not be possible at the scale of whole-stream tracer additions). Also, chambers offer direct measurements of CO_2 fluxes, eliminating the need to determine k_{CO2}. However, the floating chamber technique has been

criticized for introducing artifacts that affect the estimation of gas exchange rate (e.g., Belanger and Korzum 1991; Broecker and Peng 1984; Hartman and Hammond 1984; Matthews et al. 2003; Vachon et al. 2010), by means such as sheltering the water surface beneath the chamber from wind, not sampling riffles or similar high-turbulence areas, inducing turbulence by flow against the bottom edge of chamber, or warming of chambers exposed too long to direct sunlight, with potentially different effects depending on whether the chamber is allowed to travel with the water current (drifting) or is placed in a fixed position (static) (Lorke et al. 2015).

The primary objective of this study was to quantify the magnitude and temporal and spatial variability of CO_2 emissions from the Arboleda stream at La Selva Biological Station, a stream receiving significant inputs of DIC-rich regional groundwater. We used both drifting and static floating chambers. A second objective was to assess the feasibility of chamber work on this relatively small rainforest stream (most chamber work has been done in larger rivers). Our third objective was to examine the differences in results between drifting and static chambers, and between chambers and previously-published work that used whole-stream tracer methods to quantify CO_2 emissions from the same stream (Oviedo-Vargas et al. 2015).

2. Study site

La Selva Biological Station is a 16 km^2 tropical rainforest reserve located at the transition between the Caribbean lowland plains and the foothills of the Cordillera Central of Costa Rica (Fig. 1). La Selva ranges in elevation from 35 to 130 m. Average annual rainfall at La Selva from 1963 to 2013 was 4.3 m, with February, March, and April as the driest months and July, November, and December as the wettest (La Selva Biological Station website. Online meteorological data. http://www.ots.ac.cr/meteoro/default.php?pestacion=2). From 1982 to 2013, the mean air temperature was 25.0 °C and diurnal changes averaged 9.5 °C (La Selva Biological Station website. Online meteorological data. http://www.ots.ac.cr/meteoro/default.php?pestacion=2). Annual evapotranspiration is about 2.1 m in a year of typical annual rainfall (Loescher et al. 2005).

The Arboleda stream at La Selva Biological Station (Fig. 1) drains a surface area of 46.1 ha and has an average annual streamflow of approximately 13 m (annual water discharge normalized by watershed area; Zanon et al. 2014), of which about 34% comes from regional groundwater (Genereux et al. 2005). Based on ^{14}C age dating, the regional groundwater is estimated to be much older (2400-4000 years) than the local groundwater recharged in the lowland watersheds (10 years or less), and this is consistent with other geochemical and hydrogeological observations (Genereux et al. 2005, 2009; Solomon et al. 2010). Concentrations of DIC and dissolved aqueous CO_2 in the Arboleda stream, [DIC] and $[CO_2]_{aq}$ respectively, averaged 4.1 and 2.0 mM in 2010, 4.3 and 2.1 mM in 2011, 4.1 and 2.0 mM in 2013, and 4.2 and 2.0 mM in 2014 (Table 1, Appendix 1).

The regional groundwater input to the Arboleda made it an ideal location for the chamber work; the CO_2 degassing flux from the Arboleda was large enough that the deployment time of the chamber could be reduced to a fraction of what is often needed: 90 seconds rather than 5-60 min (e.g., Matthews et al. 2003; Striegl et al. 2012). This helped limit artifacts from changes in air temperature, pressure, and air-water concentration gradient inside the chamber. Also, the Arboleda has few riffles and few emergent natural debris dams of branches and leaves, likely due in part to the higher stream discharge and depth (about 0.8 m) associated with the large input of regional groundwater. These physical characteristics, together with a short deployment time,

facilitated the use of the chamber, particularly for the drifting mode which requires the chamber to float freely along a stream section.

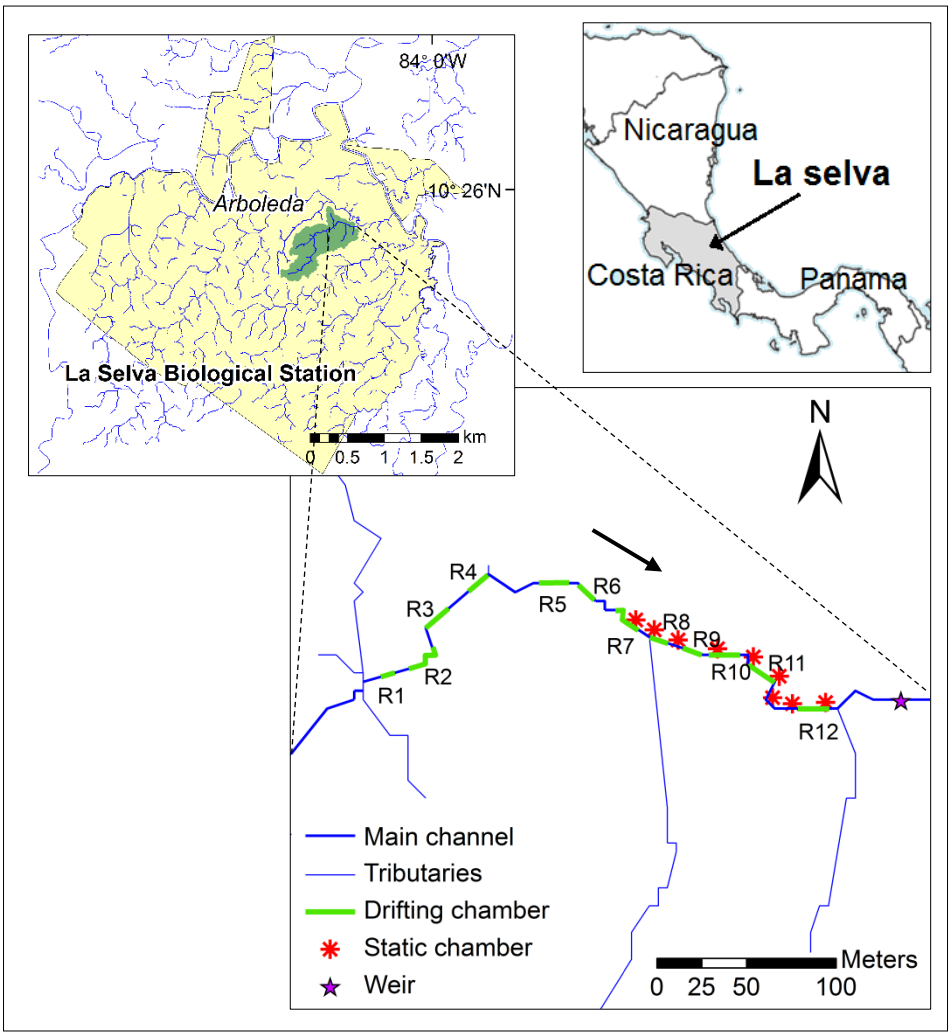

Figure 1. Arboleda stream at La Selva Biological Station in Costa Rica. The black arrow in the map showing chamber measurement locations indicates the direction of stream flow. The drifting chamber measurements were conducted in reaches R1 to R12 (in green). Static chamber measurements were conducted at three points in each of nine cross-sectional transects of the stream at the locations marked with red asterisks. Repeated measurements during the wet and dry seasons were conducted with drifting chambers in reaches R6, R8, and R9.

3. Materials and Methods

3.1. Discharge and dissolved CO_2 concentration.

During the chamber experiments, volumetric discharge (Q) of the Arboleda stream was monitored at high frequency (15 min) at a V-notch weir downstream of the chamber measurement sites (Fig. 1). Just upstream of the weir, pH was measured weekly using an Oakton 11 pH meter and weekly water samples collected at the same time as the pH measurements were

analyzed for alkalinity (Alk) using a digital titrator (Hach, Inc.) and 1.6 N sulfuric acid (Hach Company 2013). $[CO_2]_{aq}$ was calculated from Alk and pH following Stumm and Morgan (1996):

$$[CO_2]_{aq} = \frac{\alpha_0(\text{Alk} + [OH^-] - [H^+])}{\alpha_1 + 2\alpha_2} \quad (1)$$

where α_0, α_1, and α_2 are the ionization fractions for CO_2 (or carbonic acid H_2CO_3), bicarbonate, and carbonate, respectively. The ionization fractions were calculated as:

$$\alpha_0 = \left(1 + \frac{K_1}{[H^+]} + \frac{K_1K_2}{[H^+]^2}\right)^{-1} \quad (2)$$

$$\alpha_1 = \left(1 + \frac{[H^+]}{K_1} + \frac{K_2}{[H^+]}\right)^{-1} \quad (3)$$

$$\alpha_2 = \left(1 + \frac{[H^+]}{K_2} + \frac{[H^+]^2}{K_1K_2}\right)^{-1} \quad (4)$$

where K_1 and K_2 correspond to the first and second acid dissociation constants of the carbonate system (Stumm and Morgan 1996). CO_2 concentrations derived from alkalinity can be problematic for systems where pH is very low and/or organic acid concentrations are high (Hunt et al. 2011; Abril et al. 2015), however this does not represent a major concern for the Arboleda stream where pH is close to neutral (the mean of weekly measurements from 2010 to 2014 was 6.4), and DOC concentrations are low (averaging 93 μM; Genereux et al. 2013).

3.2. Chamber measurements

Degassing fluxes of CO_2 (f_{CO2}) from the Arboleda stream were measured using floating cylindrical chambers that penetrated about one cm below the stream surface. An infrared CO_2 sensor (GMP343, Vaisala, Inc.), a temperature/humidity sensor (ChipCap2™, GE Measurement & Control), and a mixing fan were built inside the chamber. A microcontroller board (Arduino, LLC) with SD storage, a display, and a 12 V battery (1300 mAh) were housed in an enclosure secured on top of the chamber. Two chambers used in this work had different water coverage area and floatation devices. One chamber had an area (A) of 0.126 m^2, headspace volume (V) of 10.9 L, and two rectangular Styrofoam pieces for floatation. The Styrofoam pieces were placed ~10 cm from the outer wall of the chamber on opposite sides of it (Fig. 1, Appendix 1). A smaller chamber (A = 0.041 m^2, V = 5.6 L) remained afloat by means of a Styrofoam ring fixed ~5 cm from the outer wall of the chamber (Fig. 2, Appendix 1). The floating devices were not installed directly adjacent to the chambers to ensure that the stream surface area contributing to the measured flux was limited to the footprint of the chamber (Figs. 1 and 2, Appendix 1).

During static deployment the chamber was held in place for 90 s, and during drifting deployment the chamber was allowed to be carried downstream by the water current for 90 s. For each measurement, the drifting chamber was released from the same location three times (or a sufficient number of times to capture three complete replicate runs). If the drifting chamber got caught at the stream edge or on any obstruction, data were discarded and the measurement was repeated. Before static or drifting measurements a 30-s air flush was conducted holding the chamber upside down to remove the chamber air from the previous run with the help of the fan. Observed increases of chamber CO_2 concentrations during the last 30 seconds of chamber deployment were used to calculate values of f_{CO2}, the rate of CO_2 flux out of the stream water following equation (5):

$$f_{co2} = \frac{10VP}{ART} \cdot \frac{dC}{dt} \quad (5)$$

where f_{CO2} has units of μmol CO_2 m^{-2} s^{-1}, V corresponds to the chamber volume (cm^3), P is the air pressure in the chamber (assumed equal to 1 atm, or 101.3 kPa), A represents the chamber area (cm^2), R is the universal gas constant (8.314 cm^3 MPa K^{-1} mol^{-1}), T is the chamber air temperature (K), dC/dt is the rate of change of gas phase CO_2 concentration in the chamber (ppm s^{-1}, i.e., μmol of CO_2 per mol of bulk gas, per second), and 10 is a factor that accounts for unit conversions. All chamber measurements had linear increases of CO_2 with $R^2 > 0.95$ (88% had $R^2 > 0.99$).

The spatial variability of f_{CO2} in the Arboleda stream was examined using both static and drifting chamber measurements. Drifting chamber measurements with the smaller chamber (Fig. 2, Appendix 1) were conducted on 17-18 August 2014 in 12 reaches (R1 through R12) spaced along a 348-m section of the Arboleda stream (Fig. 1). The length of the reaches varied between 4 and 32 m (the approximate length of reaches R1 through R12 was 10, 13, 8, 32, 9, 20, 12, 7, 10, 12, 4, and 9 m, respectively). Water velocity was measured at three or four locations within the path followed by the drifting chamber in each deployment, using a Flowtracker hand-held acoustic Doppler velocimeter. Measurements with the static chamber were conducted on 31 July 2014 at nine different cross-sections of the stream (three points per cross-section) in the lower part of the 348-m stream section (Fig. 1), using the larger chamber (Fig. 1, Appendix 1). Water velocity was measured at the chamber locations in these nine cross-sections using a Flowtracker. In addition, five static and seven drifting measurements were made within a single small reach of the Arboleda stream near reach R9 within a 35-minute period on the morning of 16 August 2014, using the small chamber (Table 2, Appendix 1).

To examine temporal variability of f_{CO2}, we used the smaller chamber in drifting mode to measure f_{CO2} values in three of the 12 reaches used in the spatial survey (R6, R8, and R9, Fig. 1) on 11 days from October 2014 to November 2014 (during the wet season) and six days from March 2015 to April 2015 (during the dry season). In each reach, deployments were conducted five to 15 times on each measuring day.

3.3. Statistical analysis

We used t-tests to determine if (1) average f_{CO2} measured with the smaller chamber in drifting mode was different from that measured with the same chamber in static mode (16 August 2014); (2) average f_{CO2} measured with the static chamber on 31 July 2014 was significantly different from that measured with the drifting chamber on 17 August 2014 (in the stream section in which both sets of measurements were conducted). A two-way analysis of variance (ANOVA) was used to determine significant differences in f_{CO2} among reaches and seasons (n = 11 per reach during the wet season and n = 6 per reach during the dry season). Significant ANOVAs were followed by Tukey's honest significant difference (HSD) for multiple comparisons. Pearson correlation coefficient (r) was used to examine the linear correlation between f_{CO2} and water velocity during the spatial variation measurements on 31 July and 17-18 August 2014. Statistical analyses were performed in Sigma Plot 11. Significance was tested at the 95% confidence (*P*-value, $P < 0.05$).

4. Results

4.1. Spatial survey (static and drifting chambers, wet season)

Average stream discharge was 10.4 m^3 min^{-1} during the period of the static chamber measurements on 31 July 2014, and 11.0 and 11.5 m^3 min^{-1} during the drifting chamber measurements on 17 and 18 August 2014, respectively (Table 1). $[CO_2]_{aq}$ measured weekly at the weir during this part of the study period (27 July 2014 to 24 August 2014) was 1.4±0.2 mM (mean ± standard deviation, SD). Results for f_{CO2} from the static chamber averaged 72.7 µmol C m^{-2} s^{-1} and ranged from 9.9 to 157.6 µmol C m^{-2} s^{-1} (n = 27, Table 1, Fig. 2a). Results from the drifting chamber in reaches overlapping with locations of the static chamber (R7 to R12 sampled on 17 August 2016) averaged 24.4 µmol C m^{-2} s^{-1} and ranged from 14.2 to 43.1 µmol C m^{-2} s^{-1} (n = 18, Table 1, Fig. 2a). Mean f_{CO2} from static chambers was 3.0 times higher than that from drifting chambers and this difference was statistically significant (t-test, $t_{43} = 4.55$, $P < 0.001$). Average f_{CO2} from the drifting chamber in all 12 reaches was 35.5 µmol C m^{-2} s^{-1} (range: 14.2-104.2 µmol C m^{-2} s^{-1}).

Table 1 Carbon dioxide degassing flux (f_{CO2}) from the Arboleda stream estimated using static and drifting chambers. NA = not applicable.

Chamber	Date	Stream discharge[a] m^3 min^{-1}	Reach (length)	Mean f_{CO2} (min-max) µmol C m^{-2} s^{-1}	n	CV %
Wet season spatial survey						
Static	31 Jul 2014	10.4	NA	72.7[b] (9.9–157.6)	27	52
Drifting	17 Aug 2014	11.0	R7–R12[c] (4–12 m)	24.4 (14.2–43.1)	18	44
	17 & 18 Aug 2014	11.0 & 11.5	R1–R12 (4–32 m)	35.5 (14.2–104.2)	36	68
Repeated measurements, wet and dry season, three reaches						
Drifting	Wet season (11 days, 15 Oct 2014 to 10 Dec 2014)	9.4–19.0	R6 (20 m)	38.1 (28.7–49.2)	90	18
			R8 (7 m)	26.3 (21.2–32.3)	90	13
			R9 (10 m)	19.1 (12.2–28.4)	90	26
	Dry season (6 days, 25 Mar 2015 to 29 April 2015)	8.8–9.9	R6 (20 m)	34.3 (31.1–37.8)	83	7
			R8 (7 m)	17.8 (11.3–24.9)	84	31
			R9 (10 m)	16.1 (12.6–20.5)	84	6
	Overall	8.8–19.0	R6, R8, & R9 (7-20 m)	26.0 (11.3–49.2)	522	37

[a]Average of discharge values recorded at the weir (15-min frequency) during the f_{CO2} measurements.
[b]Average of all 27 measurements at 9 different stream cross-sections.
[c]The six drifting chamber reaches that overlapped with the sites of the static chamber measurements.

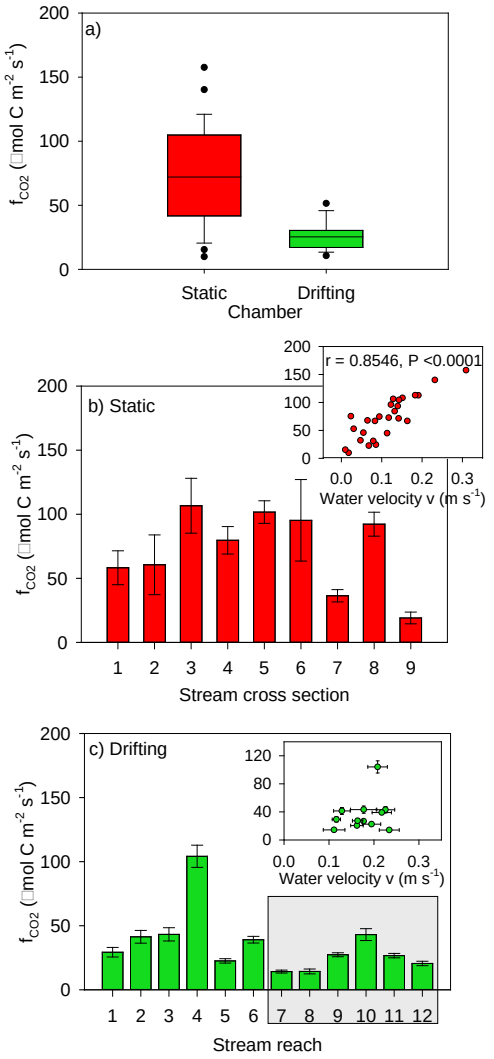

Figure 2. (a) Box plot for all 27 static chamber measurements of f_{CO2} conducted at 9 different cross sections of the stream on 31 July 2014, and 18 drifting chamber measurements made on 17 August 2014 in reaches that overlap spatially with the static measurements (R7 through R12 in Fig. 1, and gray box in Fig. 2.c.). (b) f_{CO2} measured with a static chamber in 9 transects on 31 July 2014. Error bars represent the standard error of the three repetitions made in the same transect. Inset shows stream water velocity versus static chamber f_{CO2}. (c) f_{CO2} measured with a drifting chamber in reaches 1 through 12 on 17-18 August 2014. Error bars represent the standard error of the three repetitions made in the same reach. Reaches within the gray box (7 through 12) overlapped spatially with static chamber measurements (Fig 2.b.). Inset shows stream water velocity versus drifting chamber f_{CO2} for all 12 reaches; horizontal and vertical error bars are the standard error of the three drifting repetitions made in each reach, and the three or four measurements of stream velocity made along the path of the chamber, respectively.

The coefficient of variation (CV) for f_{CO2} measured with the static chamber was 53% (Table 1). For the drifting chamber, the CV was 44% for reaches R7 through R12 (overlapping with static chamber measurements) and 68% for reaches R1 through R12 (Table 1). Static

chamber f_{CO2} values were positively correlated with stream velocity measured at the location of the chamber deployment (Pearson r = 0.85, P < 0.0001, Fig. 2b inset). No correlation was observed between f_{CO2} measured with the drifting chamber and water velocity (r = 0.27, P = 0.391, Fig.2c inset).

Five static and seven drifting measurements were made with the smaller chamber near reach R9 within a 35-minute period on 16 August 2014; the ratio of static to drifting CO_2 degassing flux was 3.3 (Table 2, Appendix 1), similar to the ratio of 3.0 from more numerous measurements at more sampling locations when static chamber measurements were done on 31 July 2014 and drifting chamber measurements were done on 17 August 2014.

4.2. Repeated measurements (drifting chamber, wet and dry seasons)

Stream discharge at the Arboleda during the study periods included frequent high flow events throughout the wet season (October 2014 - December 2014), in particular during December (Fig. 3a), and a steadier baseflow discharge during the dry season (Fig. 3b). $[CO_2]_{aq}$ measured at the Arboleda weir during the wet and dry season study periods averaged 2.4±0.3 mM and 2.4±0.4 mM (Fig. 3a and 3b), respectively.

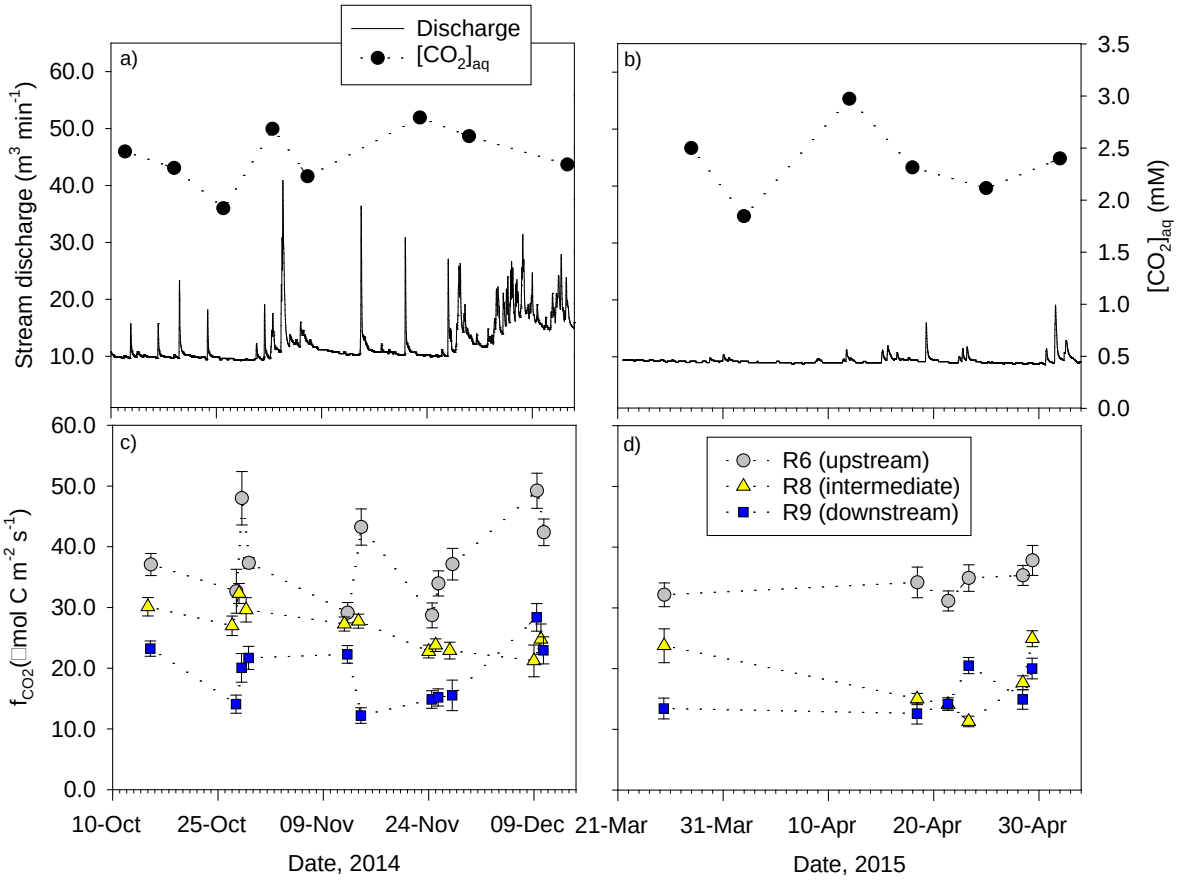

Figure 3. Wet season (a) and dry season (b) continuous stream discharge (every 15 min) and weekly dissolved CO_2 concentration at the Arboleda weir, and wet season (c) and dry season (d) repeated measurements of f_{CO2} using the drifting chamber in reaches R6, R8, and R9. Error bars represent standard error (SE) of the 5-15 repetitions made each day at each reach.

Among the reaches repeatedly sampled to assess temporal variability, f_{CO2} generally decreased from upstream to downstream (R6>R8>R9, Fig. 3c and 3d): during both wet and dry seasons, mean f_{CO2} in R6 was significantly higher than the mean values in R8 (Tukey's HSD, $P < 0.001$; dry and wet season) and R9 (Tukey's HSD, $P < 0.001$; dry and wet season), and mean f_{CO2} in R8 was significantly higher than that of R9 but only during the wet season (Tukey's HSD, $P < 0.001$ and $P=0.78$ for the wet and dry seasons, respectively). Through the wet season, f_{CO2} averaged 38.1, 26.3, and 19.1 µmol C m^{-2} s^{-1} in reaches R6, R8 and R9, respectively (Fig. 3c, Table 1). In the dry season, f_{CO2} averaged 34.3, 17.8, and 16.1 µmol C m^{-2} s^{-1} in reaches R6, R8, and R9 respectively (Fig. 3d, Table 1). Although mean f_{CO2} in all three reaches was lower during the dry season, this difference was only significant in R8 (Tukey's HSD for R6, R8, and R9 had P values of 0.139, < 0.002, and 0.273, respectively). In general, decreased variability in f_{CO2} measurements was observed during the dry season relative to the wet season (Fig. 3, Table 1). A significant relationship was observed between f_{CO2} and discharge in reaches R6 and R9, but that was not the case for R8 (Fig. 4). In reaches R6 and R9, discharge explained about 35% of the variation in f_{CO2}, however these relationships are sensitive to data from two high discharge events in December 2014 (Fig. 4).

5. Discussion

5.1. Magnitude of CO_2 emissions from the Arboleda

Regardless of the season or chamber mode (static or drifting), f_{CO2} values measured in the Arboleda were at least 10 times higher than most average values reported for other streams and rivers in studies using floating chambers, whether tropical, temperate, or polar (Table 2). Emissions reaching magnitudes similar to those from the Arboleda (average f_{CO2} = 35.5 µmol C m^{-2} s^{-1} for drifting chambers) were reported by Neu et al. (2011) from a tropical headwater stream in Brazil (Table 2), apparently linked to stream inputs of groundwater carrying CO_2 from microbial respiration of deep soil organic matter (Johnson et al. 2008). Teodoru et al. (2015) measured emissions comparable to those in the Arboleda stream in some locations of the Zambezi River in Africa (Table 2), downstream of wetlands or floodplains. Unlike the systems investigated by Neu et al. (2011) and Teodoru et al. (2015), in which high CO_2 emissions were associated with local enrichment of surface water or young groundwater with biogenic CO_2, high f_{CO2} from the Arboleda stream results from a large input of CO_2 of deep crustal origin (Genereux et al. 2009) by discharge of old regional groundwater to the stream (Genereux et al. 2009; Oviedo-Vargas et al. 2015). The distinction is important because the processes fueling fluvial CO_2 emissions influence how this flux should be accounted for in the C budgets of ecosystems.

In recent years, it has become apparent that terrestrial respiration can be underestimated if CO_2 export by streamflow or stream degassing is ignored, thereby overstating the land as a C sink (Aufdenkampe et al. 2011; Cole et al. 2007). However, that is only true if the exported or degassed CO_2 is biogenic. If this CO_2 is instead of geological origin, as in the Arboleda stream, then it does not represent ecosystem respiration, and counting it as part of ecosystem respiration in an ecosystem C budget may lead to overestimation of ecosystem respiration and underestimation of the true C sink strength of the ecosystem. Thus, understanding the origin of stream CO_2 (which may be connected to regional as well as local hydrogeology) is critical for using field data to address the fundamental question of whether the ecosystem is a net source or sink for CO_2. This has recently been stressed for peatlands where there is evidence of CO_2 emission of geological origin (Billett et al. 2015), but remains largely overlooked. Results from

the Arboleda are among the few that shed light on how old regional groundwater (as opposed to much younger shallower local groundwater) influences understanding of the C source/sink status of ecosystems. However, the Arboleda is very unlikely to be a unique case, given that the hydrogeological factors resulting in high f_{CO2} at the Arboleda have been documented not only for the Central American isthmus (e.g., Pringle et al. 1993) but globally (e.g., Genereux et al. 2013 and references therein). Streams like the Arboleda may represent relatively common hotspots for CO_2 emission and thus merit a closer look regarding their degassing fluxes.

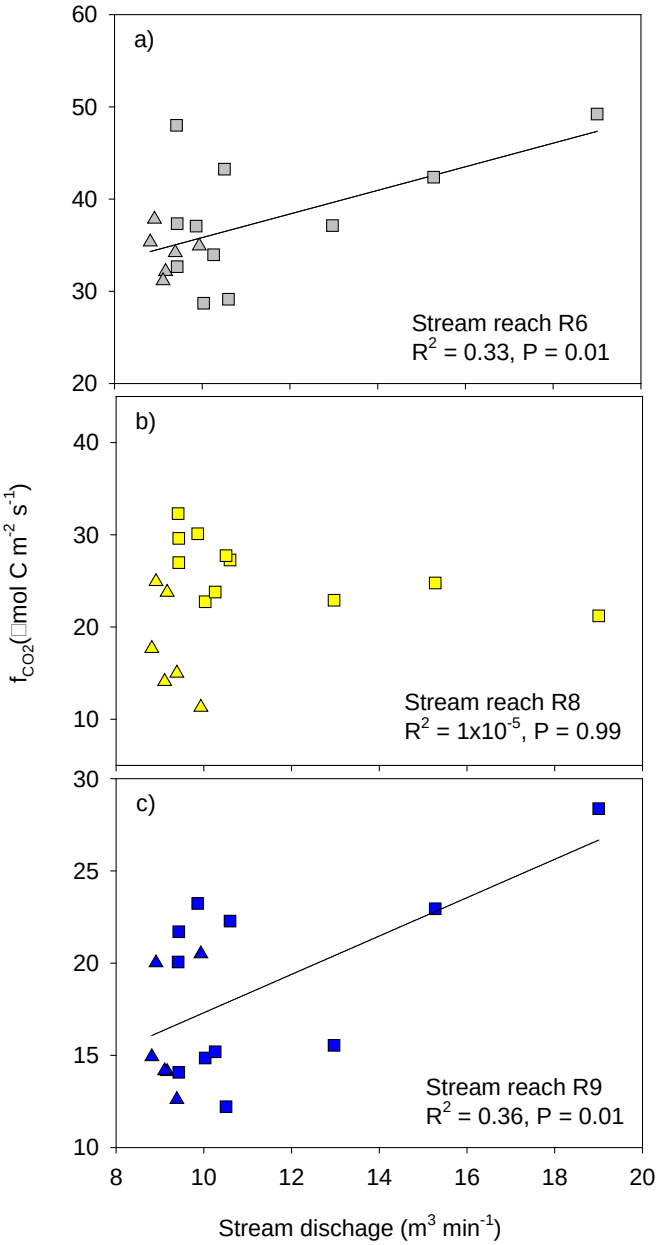

Figure 4. Relationship between f_{CO2} in stream reaches R6, R8, and R9 and stream discharge measured downstream of the reaches at the Arboleda V-notch weir. Triangles represent dry season f_{CO2} and squares represent wet season f_{CO2}.

Table 2 Summary of studies using chambers to measure CO_2 fluxes (f_{CO2}) from streams and rivers. NS = not specified. SD = standard deviation.

Reference	Zone/Site	Chamber specifications	Drifting or static chamber (wall depth)[a]	Deployment time	Mean f_{CO2} (min-max) µmol m^{-2} s^{-1}	n
This study	Tropical/Arboleda stream, Costa Rica	Polypropylene chamber with built-in fan and IR CO_2 sensor. A = 0.126 m^2, V = 10.9 L	Static (1 cm)	90 s	72.7 (9.9–157.6)	27
		Polypropylene chamber with built-in fan and IR CO_2 sensor. A = 0.041 m^2, V = 5.6 L	Drifting (1 cm)	90 s	35.5 (14.2–104.2)	68
Billett et al. (2007)	Temperate/Peatland catchments, UK	Polypropylene chamber with circulation system to IR CO_2 sensor. A = 0.073 m^2, V = 9.0 L (Billett et al. 2006)	NS (2-3 cm)	10 min	3.9 (1.5–9.5)	27
Billett and Moore (2008)	Temperate/Streams draining the Mer Bleue bog/Canada	Polypropylene chamber with circulation system to IR CO_2 sensor. A =0.1450 m^2, V = 19.1 L	Static (NS)	15 min	4.0 (0.8-11.5)[b]	24
Wu et al. (2007)	Subtropical/Danshuei and Gaoping Rivers, Taiwan	Acrylic chamber with electronic fan, thermometer and sampling ports. A =0.064 m^2, V = 18 L	Static (NS)	60 min	NS (-2.0–8.1)[c]	54
Dinsmore et al. (2010)	Temperate/Black Burn stream, Scottland	Polypropylene chamber with circulation system to IR CO_2 sensor. A = 0.1450 m^2, V = 19.1 L (Billett and Moore 2008)	Static[d] (NS)	NS	NS (0.8–7.5)[e]	20
Neu et al. (2011)	Tropical/Tanguro River 1st order tributary, Brazil	Plexiglass chamber with circulation system to IR CO_2 sensor. A = 0.125 m^2, V = 13.5 L	Drifting[d] (NS)	6 min	17.7[f] (15.0–25.4)[g]	>40
Sand-Jensen and Staehr	Temperate/Pøle and Havelse streams, Denmark	Elongated tubular chamber with circulation system into IR CO_2 sensor.	Static (1 cm)	150 s	5.15[h] (0.29–13.89)[h]	600

(2012)		A = 0.117 m^2, V = 19.1 L				
Striegl et al. (2012)	Temperate-Polar/Yukon River system, North America	Chamber with circulation system IR CO_2 sensor. A = 0.07 m^2 V = 20.5 L	Static in small streams, drifting in rivers (2.5 cm)	5 min	3.60[i]	365
Crawford et al. (2013)	Temperate/Alaskan headwater stream network, U.S.	Clear polycarbonate chamber (similar to a canoe to limit disruptions to near-surface turbulence) with circulation system into IR CO_2 sensor	Static (2 cm)	5 min	5.10 (0.5–18.5)[j]	94
Huotari et al. (2013)	Temperate/Kymijoki River, Finland	Opaque cylinder with a built-in fan and IR CO_2 sensor. A = 0.028 m^2, V = 6.8 L	Drifting and static (2 cm)	NS	0.98±0.76(SD)	8
Rasera et al. (2013)	Tropical/Amazon tributaries	Plexiglas chamber with circulation system into IR CO_2 sensor. A = 0.125 m^2, V = 10.6 L	Drifting (2-3 cm)	5 min	NS (-0.2–12.2)	>300[k]
Panneer Selvam et al. (2014)	Tropical/Rivers in Southern India	Plastic chamber with circulation system into IR CO_2 sensor. V = 6.5 L	Drifting (3 cm)	18 min	0.23±0.44(SD) (0.11-1.51)	24
Campeau et al. (2014)	Temperate/Streams and rivers in the Abitibi and James Bay regions, Canada	Plastic chamber thermometer and circulation system into IR CO_2 sensor. A = 0.09 m^2, V = 16 L	Drifting (NS)	10 min	0.85 (0.02–5.66)[l]	110
Crawford et al. (2014)	Temperate/Streams in Wisconsin and Michigan, U.S.	Clear polycarbonate chamber (similar to a canoe to limit disruptions to near-surface turbulence) with circulation system into IR CO_2 sensor (Crawford et al. 2013)	Static (2 cm)	5 min	5.9 (-0.6–23.5)[m]	93
Teodoru et al. (2015)	Tropical/Zambezi River, Africa	PVC chamber with thermometer and circulation system into IR CO_2 sensor. A = 0.11 m^2, V = 17 L	Drifting[n] (7 cm)	30 min	1.4 (-0.3–30.8)[p]	36

Lorke et al. (2015)	Temperate/Five streams in Germany and Poland	Circular chamber with off-axis integrated cavity output spectroscopy gas analyzer. A = 0.126 m^2, V = 16.8 L	Static (1.8 cm)	NS	8.3±3.3(SD)[q]	18
			Drifting (1.8 cm)		4.2±1.6(SD)[q]	18
	Temperate/Bode River in Germany	Rectangular chamber with circulation system into IR CO_2 sensor. A = 0.098 m^2, V = 14.7 L	Static (2.3 cm)	Up to 5 min	3.5±1.7(SD)[q]	27
			Drifting (2.3 cm)		0.6±0.3(SD)[q]	27
	Temperate/Three streams in Upper Rhine Valley, Germany	Circular chamber with built-in low-cost CO_2 logger A = 0.066 m^2, V = 6.8 L	Static (2.5)	NS	1.2±0.5(SD)[q]	24
			Drifting (2.5 cm)		0.6±0.4(SD)[q]	24

[a] Length of the chamber wall below the water surface.
[b]Calculated from average of 47.9 and range of 2.41–137.83 µg C m^{-2} s^{-1}, reported by Billett and Moore (2008) in Table II for flowing waters.
[c]Estimated from Figs. 1 and 2 in Wu et al. (2007).
[d]Personal communication
[e]Estimated from Fig. 2 in Dinsmore et al. (2010): 8–90 µg C m^{-2} s^{-1}. Measurements of floating chambers were used to upscale evasion rates determined from reaeration flux equations (Dinsmore et al. 2010).
[f]Calculated from average of 766 mg C m^{-2} h^{-1} reported by Neu et al. (2011) in Table 4.
[g]Estimated from Fig. 4 in Neu et al. (2011).
[h]Calculated from values reported in mmol C m^{-2} d^{-1} by Sand-Jensen and Staehr (2012) in Table 3.
[i]Calculated from 311 mmol C m^{-2} of water surface d^{-1} as reported in Table 1 by Striegl et al. (2012).
[j]Estimated from Fig. 2 in Crawford et al. (2013).
[k]Estimated as the number of campaigns in which chamber were deployed times an average of 4 deployments per campaign as indicated by Rasera et al. (2013).
[l]Calculated from Table 2 in Campeau et al. (2014). Overall mean and range: 888 and 19.70–5,879 mg C m^{-2} d^{-1}.
[m]Calculated from mean (range) = 0.51 (-0.05–2.03 mol m^{-2} d^{-1}) reported by Crawford et al. (2014).
[n]Whenever possible, flux chamber measurements were performed in both static and drift mode, but these data represent results from drift mode (Teodoru et al. 2015).
[p]Estimated from Fig. 9a in Teodoru et al. (2015).
[q] Calculated from values reported in mmol m^{-2} d^{-1} in Table 2 of Lorke et al. (2015).

5.2. Spatiotemporal dynamics of CO_2 emissions

Floating chambers proved to be both practical and informative in investigating CO_2 fluxes from the Arboleda stream at a small spatial scale (at the fixed locations of static chambers and the small reaches defined by chamber drift paths of 5-30 m), and repeatedly through time. Both drifting and static chambers showed high spatial variability in f_{CO2} within the 348 meters of stream length studied (Fig. 2). Spatial differences appear to be maintained though time, as shown by the repeated measurements at reaches R6, R8, and R9 (Fig. 3); with few exceptions, f_{CO2} generally decreased from upstream to downstream (from R6 to R8 to R9). These results suggest that small-scale geomorphic characteristics of the stream locations play a significant role in the magnitude of the CO_2 fluxes, consistent with results from the spatial survey. For example, in reach R4 where the highest f_{CO2} was measured (Fig. 2), water spilled over a tree log partially submerged perpendicular to the stream flow, and the log also directed a large part of the water flow into a small cross-section of the stream. Comparing among reaches R6, R8, and R9, R6 (20 m) was straight with relatively shallow and fast-flowing stream water, R8 (7 m) included a bend in the channel and slow flow, and R9 (10 m) was straight with slow flow impounded by a large log near the end (all flow went underneath the log). To obtain representative CO_2 fluxes from fluvial systems, it appears critical to deploy chambers at numerous locations of varying hydraulic/geomorphic character throughout the reach of interest.

Temporal variation in f_{CO2} was lower than spatial variation. The coefficient of variation (CV) in f_{CO2} was about 10-30% for each individual reach (R6, R8, or R9) within an individual season, wet or dry (Table 1), which is lower than the CV of 50-70% obtained from the wet season spatial surveys (Table 1). Repeated drifting chamber measurements showed that overall, differences in CO_2 fluxes between seasons were small and that higher variability in f_{CO2} occurred during the wet season (Fig. 3). Also, in reaches R6 and R9, f_{CO2} and stream discharge at the weir were positively related (Fig. 4) and f_{CO2} was not significantly different between the wet and dry seasons, while reach R8, located between R6 and R9, had the opposite behavior: no statistically significant relationship between f_{CO2} and stream discharge (Fig. 4), and significantly different f_{CO2} between seasons. These differences between reach R8 and reaches just upstream (R6) and downstream (R9) may lie in some as-yet unrecognized connection between CO_2 emissions and small geomorphic or hydraulic variations along the channel such as those mentioned for R6, R8, and R9 in the previous paragraph. The variation we have observed in CO_2 fluxes and their linkages to season and to stream discharge suggests the usefulness of chambers in revealing new insights regarding stream CO_2 emissions, but also highlights the underlying complexity of those emissions, with possible biological, hydrological, hydraulic, and other controls.

5.3. Static and drifting chambers

Measurements made within a 35-minute period on the morning of 16 August 2014 showed the ratio of static to drifting f_{CO2} was 3.3 (Table 2 APPENDIX 1), similar to the ratio of 3.0 found with more numerous measurements at more sampling locations when static chamber measurements were done on 31 July 2014 and drifting chamber measurements were done on 17 August 2014. This is within the range of static to drifting f_{CO2} ratios (2.0 to 5.5) found recently by Lorke et al. (2015) for three data sets representing eight different streams and one river in Germany and Poland (Table 2). Of course, it is possible that the static/drifting ratio of 3.0 from

our Arboleda data was determined in part by an actual difference in f_{CO2} from 31 July to 17 August (i.e., not solely the difference between static and drifting chambers).

CO_2 degassing flux from a stream can be expressed as: $f_{CO2} = k_{CO2}(C - C_{sat}) = \lambda_{CO2}D(C - C_{sat})$, where k_{CO2} is the gas exchange piston velocity for CO_2 (length time^{-1}), C is the aqueous CO_2 concentration in the stream water, C_{sat} is the aqueous CO_2 concentration that would be in equilibrium with atmospheric CO_2, λ_{CO2} is the first-order gas exchange rate constant for CO_2 (time^{-1}), and D is the stream depth (Rathbun and Tai 1982; Duran and Hemond 1984; Parker and Gay 1987). Given an atmospheric CO_2 concentration, there are three stream controls on f_{CO2}: λ_{CO2}, D, and C. The first-order gas exchange rate constant has been observed to be relatively steady over at least an order of magnitude range in stream discharge (Genereux et al. 1992), supporting the idea that it is unlikely there was significant change in λ_{CO2} from 31 July to 17 August (stream discharge increased by only about 6%; Table 1). Measurements at the Arboleda weir indicate that from 27 July to 24 August 2014, C increased by about 26% (Table 1, Appendix 1) while D increased by about 3% (from 35 to 36 cm), suggesting a potential increase in f_{CO2} of about 29% during this time, corresponding to a hypothetical static (31 July) to drifting (17 August) ratio of 0.78. The observed ratio of 3.0 is much closer to the estimate of 3.3 from the 16 August 2014 measurements. Thus, while some change in f_{CO2} from 31 July to 17 August cannot be ruled out, the ratio of f_{CO2} between those dates seems to be controlled more by differences between the static and drifting chambers, and the ratio of 3.3 from 16 August (when static and drifting measurements were made within 35 minutes) indicates that static chambers yielded f_{CO2} values about 3 times those from drifting chambers on the Arboleda.

We found that stream water velocity in the Arboleda was highly correlated to f_{CO2} measured with the static chamber but not the drifting chamber (Fig. 2). Teodoru et al. (2015) also report a strong linear correlation between f_{CO2} and stream water velocity beneath static chambers. In Danish lowland streams, Sand-Jensen and Staehr (2012) found logk_{CO2} determined using static chambers strongly correlated to the logarithm of stream velocity (their Table 2), and discussed the potential benefits of such a relationship for scaling up (i.e., estimating values of k_{CO2} for a stream system based on measured or modeled stream velocity). However, Teodoru et al. (2015) viewed their correlation as an artifact of induced turbulence from the disturbance of stream flow by the lower part of the chamber walls, and f_{CO2} values measured with static chambers were excluded from their results because of this. Lorke et al. (2015) attributed elevated gas fluxes beneath static chambers (relative to drifting chambers) to the increased turbulence found beneath, and caused by, static chambers. In our results from the Arboleda stream, the positive correlation of f_{CO2} with stream velocity for static chambers and lack of correlation for drifting chambers are consistent with the static chamber introducing artificial turbulence as stream water flowed past the lower edge of the chamber, enhancing stream degassing and resulting in overestimation of f_{CO2}.

The mean f_{CO2} values from the static and drifting chambers (73 and 36 µmol C m^{-2} s^{-1}, respectively) overestimate and underestimate, respectively, what is likely the best estimate of overall CO_2 emissions: the mean f_{CO2} of 56 µmol C m^{-2} s^{-1} determined using tracer injections of propane and chloride to estimate k_{CO2} (Oviedo-Vargas et al. 2015) in the same section of the Arboleda where the chamber measurements were conducted (R1 to R12 in Fig. 1). The tracer injections were conducted on August 4 and 6, 2014, in between the measurements with static chambers (31 July) and drifting chambers (17-18 August). To our knowledge, only one other

direct comparison between chamber and tracer methods at approximately the same time and place has been published for a stream (Crawford 2012; Crawford et al. 2013). In an Alaskan stream reach, Crawford (2012) measured k_{CO2} five times using propane injections (reach length ≤ 400 m), followed immediately by the deployment of static chambers at the downstream end of the reach; k_{CO2} based on the propane work was 1.9x higher than that from the static chambers. Crawford's results contrast with our results that showed higher f_{CO2} values from static chambers than from injected tracer work. It is possible that in the study by Crawford (2012), the CO_2 fluxes at the downstream end of the reach were not representative of the reach used for the tracer injections.

Assuming the tracer-based value of f_{CO2} is the best estimate, our results suggest that the drifting chamber underestimated f_{CO2}. The paths of the drifting chamber may have been biased in favor of obstacle-free areas in the thalweg where the chamber was generally released. If there was higher CO_2 flux near natural debris dams of logs, branches, and leaves and/or near the stream edge where water was shallower, then the under-sampling of these areas by the drifting chamber may explain the lower f_{CO2} from the drifting chamber. Assessment of lateral variation in f_{CO2} across the channel should be a focus in future work with drifting chambers.

Doyle and Ensign (2009) suggest different potential benefits for environmental measurement reference frames that are fixed in place (Eulerian) or following individual water parcels (Lagrangian). In the case of estimating stream water degassing with floating flux chambers, our results and those of Lorke et al. (2015) suggest a systematic bias (overestimation of reach-scale degassing flux) from fixed (static) chambers in streams, and our results further caution that even drifting chambers may contain bias (in our case, underestimation of reach-scale degassing flux), perhaps arising from the drifting chamber preferentially following paths that are not fully representative of gas exchange within the reach.

Models of stream gas exchange based on correlations with stream hydraulic parameters have been and remain problematic as predictive tools (Genereux and Hemond 1992; Raymond et al. 2012; Wallin et al. 2011). For instance, using hydraulic parameters from the Arboleda in empirical equations presented by Raymond et al. (2012) to determine *k*, we estimated that f_{CO2} at the Arboleda spanned almost a factor of 3 (58-155 μmol C m^{-2} s^{-1},Table 3, Appendix 1), and the equations presented by Raymond et al. as having the highest predictive power (equations 1 and 7 in their Table 2) gave the poorest agreement with Arboleda f_{CO2} results from the chamber and tracer injection techniques. With the complexity and incomplete understanding of the dynamics of CO_2 sources and sinks in streams, reliable prediction of stream CO_2 emissions remains an elusive goal. Creative and sound application of chamber, tracer, and other methods is critical, given the emerging climatic and biogeochemical importance of CO_2 emissions from streams and rivers and the little-explored role of old regional groundwater in driving high emissions. Drifting chambers can be an important tool, especially if they can be released in adequate numbers and from different points across the width of the channel (not all in the center or thalweg) to allow some to drift near the shoreline where gas fluxes might differ from those in the thalweg.

Table 1. Dissolved inorganic carbon (DIC) and carbon dioxide (CO_2) weekly concentrations (mM) in stream water just above the 120-degree V-notch weir on the Arboleda stream at La Selva Biological Station, from January 2010 to December 2014.

	2010			2011			2012			2013			2014		
	Date	**DIC**	**CO_2**	**Date**	**DIC**	**CO_2**	**Date**	**DIC**	**CO_2**	**Date**	**DIC**	**CO_2**	**Date**	**DIC**	**CO_2**
	1/2/2010	4.58	2.10	1/3/2011	4.00	1.87	01/14/12	4.61	2.23	01/05/13	4.12	2.06	01/02/14	4.23	2.03
	1/6/2010	3.97	2.41	1/8/2011	3.75	1.61	01/20/12	4.46	2.12	01/14/13	4.35	2.05	01/07/14	4.18	1.90
	1/16/2010	4.09	1.79	1/17/2011	3.30	1.58	01/30/12	4.58	2.16	01/20/13	4.50	2.12	01/13/14	4.30	1.97
	1/22/2010	3.89	1.47	1/22/2011	4.00	2.02	02/03/12	5.00	2.44	01/25/13	1.70	0.81	01/20/14	4.72	2.54
	1/30/2010	4.03	1.52	1/29/2011	4.18	1.90	02/12/12	4.63	2.16	02/03/13	4.47	2.05	01/27/14	4.17	1.86
	2/6/2010	3.72	1.26	2/6/2011	4.04	1.72	02/19/12	4.84	2.32	02/10/13	4.69	2.17	02/01/14	4.69	2.21
	2/12/2010	3.94	1.44	2/12/2011	3.76	1.42	02/25/12	4.75	2.30	02/17/13	4.78	2.25	02/08/14	4.27	1.87
	2/20/2010	3.18	1.50	2/19/2011	4.80	2.50	03/04/12	4.45	2.06	02/24/13	4.48	2.00	02/16/14	4.10	1.76
	2/26/2010	3.73	1.51	2/25/2011	4.99	2.60	03/11/12	4.39	2.03	03/02/13	4.71	2.12	02/22/14	4.58	2.14
	3/5/2010	3.72	1.94	3/6/11	4.26	2.06	03/18/12	4.15	1.87	03/10/13	4.08	1.94	03/02/14	4.35	1.87
	3/12/2010	3.85	1.61	3/13/11	4.32	2.00	03/25/12	4.45	2.06	03/17/13	4.44	1.98	03/08/14	4.42	1.88
	3/19/2010	3.92	1.67	3/18/11	4.37	2.13	03/30/12	4.73	2.29	03/27/13	5.22	2.72	03/16/14	4.45	1.95
	3/26/2010	3.65	1.57	3/27/11	4.64	2.32	04/14/12	4.44	1.98	03/31/13	4.54	2.10	03/23/14	4.73	2.29
	4/4/2010	3.70	1.24	4/2/2011	4.57	2.25	04/21/12	4.50	2.10	04/06/13	5.18	2.68	03/30/14	4.92	2.32
	4/9/2010	4.16	1.64	4/10/2011	4.56	2.30	04/28/12	4.26	1.92	04/14/13	5.10	2.32	04/06/14	4.64	2.09
	4/16/2010	3.76	1.33	4/15/2011	4.53	2.19	05/05/12	4.36	2.00	04/22/13	4.65	2.19	04/13/14	4.60	2.11
	4/25/2010	3.63	1.47	4/24/2011	4.54	2.16	05/13/12	4.40	2.00	04/28/13	4.54	2.01	04/19/14	4.39	1.85
	5/1/2010	3.89	1.75	4/30/2011	4.69	2.25	05/19/12	4.50	2.14	05/04/13	4.77	2.23	04/27/14	4.93	2.51
	5/8/2010	3.98	1.84	5/8/2011	4.15	2.11	05/27/12	4.08	1.84	05/12/13	3.99	2.03	05/03/14	4.30	1.97
	5/16/2010	4.45	2.21	5/15/2011	4.85	2.59	06/01/12	3.98	2.04	05/19/13	4.37	2.13	05/11/14	3.54	2.02
	5/21/2010	5.36	3.08	5/22/2011	4.40	2.13	06/09/12	4.05	1.91	05/26/13	4.21	1.95	05/19/14	4.51	2.09
	5/30/2010	4.80	2.50	5/29/2011	4.41	2.15	06/16/12	3.84	1.76	06/01/13	4.30	1.90	05/26/14	4.08	1.64
	6/5/2010	4.89	2.53	6/5/2011	4.37	2.17	06/23/12	4.05	1.91	06/09/13	4.54	2.10	06/01/14	4.30	2.10
	6/13/2010	2.24	1.43	6/12/2011	4.37	2.15	07/01/12	4.45	2.21	06/16/13	4.14	2.07	06/07/14	5.06	2.66
	6/18/2010	3.69	1.60	6/17/2011	4.12	2.08	07/08/12	4.07	1.97	06/20/13	3.69	2.03	06/15/14	3.85	1.59
	6/26/2010	4.98	2.80	6/26/2011	3.98	2.04	07/14/12	4.08	1.92	06/27/13	4.03	2.16	06/22/14	3.40	1.76
	7/3/2010	4.42	2.14	7/1/2011	3.99	2.03	07/22/12	2.72	1.53	07/06/13	4.33	2.22	06/29/14	3.87	1.89
	7/8/2010	5.38	3.05	7/11/2011	3.87	1.89	08/04/12	3.63	1.71	07/13/13	5.09	2.25	07/07/14	2.68	1.44
	7/17/2010	4.39	2.16	7/14/2011	3.89	2.01	08/11/12	3.10	1.51	07/21/13	3.99	1.75	07/13/14	3.59	2.21

	7/30/2010	4.89	2.77	7/24/2011	4.23	2.15	08/18/12	3.50	1.59	07/28/13	3.69	1.91	07/27/14	2.56	1.24
	8/7/2010	4.67	2.53	7/31/2011	4.29	2.13	08/26/12	4.08	2.01	08/03/13	3.66	1.86	08/03/14	2.71	1.30
	8/13/2010	4.72	2.44	8/7/2011	4.49	2.19	08/31/12	4.11	1.99	08/10/13	3.88	1.86	08/10/14	3.61	1.55
	8/20/2010	4.85	2.63	8/13/2011	4.61	2.25	09/09/12	3.69	1.63	08/18/13	4.03	1.83	08/24/14	3.74	1.56
	8/28/2010	3.79	1.93	8/19/2011	4.80	2.34	09/17/12	4.10	2.00	08/25/13	4.32	2.00	08/31/14	4.46	2.10
	9/5/2010	4.39	2.38	8/26/2011	4.65	2.23	09/22/12	4.00	1.90	09/01/13	3.70	1.37	09/07/14	4.72	2.52
	9/11/2010	4.63	2.51	9/4/2011	4.61	2.23	09/29/12	3.96	1.90	09/08/13	3.13	0.77	09/16/14	4.10	1.83
	9/17/2010	4.72	2.36	9/11/2011	4.53	2.17	10/06/12	3.60	1.68	09/16/13	4.12	1.84	09/21/14	4.57	2.25
	9/25/2010	4.19	2.20	9/17/2011	4.35	2.05	10/13/12	4.13	1.98	09/22/13	3.84	1.48	09/28/14	3.96	1.72
	10/3/2010	4.06	1.98	9/25/2011	4.66	2.14	10/20/12	5.28	2.73	09/29/13	4.21	1.81	10/07/14	4.33	1.88
	10/9/2010	4.39	2.18				10/27/12	4.72	2.36	10/05/13	4.08	1.82	10/12/14	4.80	2.46
	10/16/2010	4.41	2.15				11/03/12	4.50	2.12	10/14/13	4.05	1.71	10/19/14	4.73	2.31
	10/24/2010	4.38	2.19				11/10/12	3.24	1.93	10/20/13	4.15	1.65	10/26/14	4.30	1.92
	11/7/2010	4.33	2.22				11/18/12	2.16	1.32	10/27/13	4.49	2.32	11/02/14	4.80	2.68
	11/14/2010	4.64	2.36				11/24/12	3.64	1.88	11/03/13	4.38	2.12	11/07/14	4.49	2.23
	11/20/2010	4.27	2.17				11/30/12	3.47	1.88	11/11/13	4.16	1.98	11/23/14	5.07	2.79
	11/26/2010	2.65	0.51				12/08/12	4.03	1.85	11/17/13	4.29	1.97	11/30/14	4.54	2.61
	12/5/2010	3.55	1.73				12/17/12	4.05	1.91	11/24/13	4.24	1.91	12/14/14	3.62	2.34
	12/12/2010	3.73	1.74				12/24/12	2.83	1.51	11/30/13	3.46	1.32	12/23/14	3.40	1.97
	12/22/2010	3.83	1.68				12/30/12	3.75	1.97	12/07/13	4.46	2.12			
	12/27/2010	3.73	1.79							12/12/13	4.33	2.13			
										12/21/13	4.25	1.93			
										12/25/13	3.88	1.62			
n		**50**	**50**		**39**	**39**		**49**	**49**		**52**	**52**		**48**	**48**
Mean		**4.14**	**1.98**		**4.33**	**2.11**		**4.09**	**1.97**		**4.23**	**1.96**		**4.21**	**2.04**
Max		**5.38**	**3.08**		**4.99**	**2.60**		**5.28**	**2.73**		**5.22**	**2.72**		**5.07**	**2.79**
Min		**2.24**	**0.51**		**3.30**	**1.42**		**2.16**	**1.32**		**1.70**	**0.77**		**2.56**	**1.24**
St Dev		**0.60**	**0.51**		**0.36**	**0.24**		**0.59**	**0.26**		**0.55**	**0.35**		**0.59**	**0.36**
CV (%)		**14%**	**26%**		**8%**	**11%**		**15%**	**13%**		**13%**	**18%**		**14%**	**17%**

Table 2. CO_2 degassing flux (f_{CO2}) measured in a reach of the Arboleda stream on 16 August 2014 (near R9, Figure 1) using the same chamber (Fig. 2) in drifting (n = 5) and static (n = 7) modes. The two modes of chamber deployment gave significantly different f_{CO2} (t-test, t_{10} = 8.76, P < 0.0001), with a ratio of the means (static/drifting) of 3.3.

Measurement	**CO_2 flux (f_{CO2}) μmol C m^{-2} s^{-1}**	
	Drifting Chamber	**Static Chamber**
1	15	51
2	20	68
3	17	40
4	12	63
5	20	61
6	-	50
7	-	58
Mean	**17**	**56**
SD	**3**	**9**
Ratio of static to drifting means	**3.3**	

Table 3. CO_2 degassing flux (f_{CO2}) estimated using aqueous CO_2 concentration $[CO_2]_{aq}$ at the Arboleda weir around the time of the chamber deployment (1.4 mM, see manuscript for details) and k_{CO2} derived from k_{600} using a Schmidt number for CO_2 of 457.63 at 25°C. k_{600} was calculated from model equations empirically derived by Raymond et al. (2012) as a function of all, or some of the following variables: stream discharge (Q), water velocity (v), depth (D) and slope (S). The calculations were made using values for Q, v, D and S measured at the time of the chamber deployments: Q = 0.183 m^3 s^{-1} (average of Q measured at the weir on the days of the chamber deployments, Table 1 of the manuscript), v = 0.157 m s^{-1} (average of all the values of water velocity taken within the studied stream section at the time of chamber deployment, insets in Figure 2b and 2c of the manuscript), D = 0.820 m (average of all values measured at the chamber deployment locations), and S = 0.004 (determined using topographic maps of the studied stream section). r^2 values correspond to those reported in Table 2 of Raymond et al. 2012.

Equation number in Table 2 of Raymond et al. (2012)	r^2	k_{600} (m d^{-1})	k_{CO2} (m d^{-1})	f_{CO2} (μmol m^{-2} s^{-1})
1	0.72	5.8	6.6	106
3	0.54	3.2	3.6	58
4	0.53	3.2	3.7	59
5	0.55	3.6	4.1	66
6	0.53	4.3	4.9	79
7	0.76	8.4	9.7	155

Figure 1. Floating chamber used for measurements in static mode. The area of stream coverage by the chamber alone was 0.126 m^2, and the chamber volume was 10.9 L. The gray plates are Styrofoam pieces installed ~10 cm from the outer wall of the chamber for floatation.

Figure 2. Floating chamber deployed in the Arboleda stream for all drifting measurements and for the comparison between static and drifting modes conducted on 16 August 2014. The area of stream coverage by the chamber alone was 0.041 m^2, and the chamber volume = 5.6 L. The gray ring around the chamber is a Styrofoam piece installed ~5 cm from the outer wall of the chamber for floatation.

Acknowledgments

The authors thank Emily Barnett, Ruben Vargas, Danilo Villegas, and William Ureña for their help with the field and laboratory tasks. Financial support from the US Department of Energy (award DE-SC0006703) is gratefully acknowledged. Logistical support at the field site was provided by the Organization for Tropical Studies. Statements and opinions in this report are those of the authors and do not necessarily reflect the views of the sponsoring agency.

References

Abril G, Bouillon S, Darchambeau F, Teodoru CR, Marwick TR, Tamooh F, Ochieng Omengo F, Geeraert N, Deirmendjian L, Polsenaere P, Borges AV (2015) Technical Note: Large overestimation of pCO_2 calculated from pH and alkalinity in acidic, organic-rich freshwaters. Biogeosciences 12: 67-78.

Alin SR, Rasera M-d-F FL, Salimon CI, Richey JE, Holtgrieve GW, Krusche AV, Snidvongs A (2011) Physical controls on carbon dioxide transfer velocity and flux in low-gradient river systems and implications for regional carbon budgets. J Geophys Res-Biogeo 116:G01009. doi:10.1029/2010jg001398

Aufdenkampe AK, Mayorga E, Raymond PA, Melack JM, Doney SC, Alin SR, Aalto RE, Yoo K (2011) Riverine coupling of biogeochemical cycles between land, oceans, and atmosphere. Front Ecol Environ 9:53-60. doi:10.1890/100014

Belanger TV, Korzum EA (1991) Critique of floating-dome technique for estimating reaeration rates. J Environ Eng 117:144-150.

Billett MF, Garnett MH, Dinsmore K (2015) Should aquatic CO_2 evasion be included in contemporary carbon budgets for peatland ecosystems? Ecosystems 18:471-480. doi:10.1007/s10021-014-9838-5

Billett, MF, Garnett, MH, Hardie SL (2006) A direct method to measure $^{14}CO_2$ lost by evasion from surface waters. Radiocarbon 48: 61– 68.

Billett MF, Garnett MH, Harvey F (2007) UK peatland streams release old carbon dioxide to the atmosphere and young dissolved organic carbon to rivers. Geophys Res Lett 34:L23401. doi:10.1029/2007GL031797

Billett MF, Moore T (2008) Supersaturation and evasion of CO_2 and CH_4 in surface waters at Mer Bleue peatland, Canada. Hydrol Process 22:2044-2054.

Broecker WS, Peng T-H (1984) Gas exchange measurements in natural systems. In: Gas transfer at water surfaces. Springer, pp 479-493

Butman D, Raymond PA (2011) Significant efflux of carbon dioxide from streams and rivers in the United States. Nature Geoscience 4:839-842. doi:10.1038/ngeo1294

Campeau A, Lapierre J-F, Vachon D, Giorgio PA (2014) Regional contribution of CO_2 and CH_4 fluxes from the fluvial network in a lowland boreal landscape of Québec. Global Biogeochem Cy 28:57-69.

Cole JJ, Prairie YT, Caraco NF, McDowell WH, Tranvik LJ, Striegl RG, Duarte CM, Kortelainen P, Downing JA, Middelburg JJ (2007) Plumbing the global carbon cycle: integrating inland waters into the terrestrial carbon budget. Ecosystems 10:172-185. doi:10.1007/s10021-006-9013-8

Crawford JT (2012) Hydrologic and geomorphologic controls on carbon dioxide and methane emissions from a headwater stream network of interior Alaska. Masters Thesis, University of Wisconsin

Crawford JT, Lottig NR, Stanley EH, Walker JF, Hanson PC, Finlay JC, Striegl RG (2014) CO_2 and CH_4 emissions from streams in a lake-rich landscape: Patterns, controls, and regional significance. Global Biogeochem Cy 28:197-210. doi:10.1002/2013GB004661

Crawford JT, Striegl RG, Wickland KP, Dornblaser MM, Stanley EH (2013) Emissions of carbon dioxide and methane from a headwater stream network of interior Alaska. J Geophys Res-Biogeosci 118:482-494.

Dinsmore KJ, Billett MF, Skiba UM, Rees RM, Drewer J, Helfter C (2010) Role of the aquatic pathway in the carbon and greenhouse gas budgets of a peatland catchment. Glob Change Biol 16:2750-2762. doi:10.1111/j.1365-2486.2009.02119.x

Doyle MW, Ensign SH (2009) Alternative reference frames in river system science. BioScience 59:499-510.

Duran AP, Hemond HF (1984) Dichlorodifluoromethane (Freon-12) as a tracer for nitrous oxide release from a nitrogen-enriched river. Pages 421-429 in: Gas Transfer at Water Surfaces, W. Brutsaert and G.H. Jirka (eds.), D. Reidel Publishing Co., Hingham, MA.

Genereux DP, Hemond HF (1992) Determination of gas exchange rate constants for a small stream on Walker Branch Watershed, Tennessee. Water Resour Res 28:2365-2374.

Genereux DP, Jordan MT (2006) Interbasin groundwater flow and groundwater interaction with surface water in a lowland rainforest, Costa Rica: a review. J Hydrol 320:385-399. doi:10.1016/j.jhydrol.2005.07.023

Genereux DP, Jordan MT, Carbonell D (2005) A paired-watershed budget study to quantify interbasin groundwater flow in a lowland rain forest, Costa Rica. Water Resour Res 41:W04011. doi:10.1029/2004WR003635

Genereux DP, Nagy LA, Osburn CL, Oberbauer SF (2013) A connection to deep groundwater alters ecosystem carbon fluxes and budgets: Example from a Costa Rican rainforest. Geophys Res Lett 40:2066-2070. doi:10.1002/grl.50423

Genereux DP, Webb M, Solomon DK (2009) Chemical and isotopic signature of old groundwater and magmatic solutes in a Costa Rican rain forest: Evidence from carbon, helium, and chlorine. Water Resour Res 45:W08413. doi:10.1029/2008WR007630

Hach Company (2013) Digital titration manual: Model 16900. 25th edn

Hartman B, Hammond DE (1984) Gas exchange rates across the sediment-water and air-water interfaces in south San Francisco Bay. J Geophys Res-Oceans (1978-2012) 89:3593-3603.

Hope D, Palmer SM, Billett MF, Dawson JJ (2001) Carbon dioxide and methane evasion from a temperate peatland stream. Limnol Oceanogr 46:847-857.

Hotchkiss ER, Hall Jr RO, Sponseller RA, Butman D, Klaminder J, Laudon H, Rosvall M, Karlsson J (2015) Sources of and processes controlling CO_2 emissions change with the size of streams and rivers. Nat Geosci. doi:10.1038/ngeo2507

Huotari J, Haapanala S, Pumpanen J, Vesala T, Ojala A (2013) Efficient gas exchange between a boreal river and the atmosphere. Geophys Res Lett 40:5683-5686.

Hunt CW, Salisbury JE, Vandemark D (2011) Contribution of non-carbonate anions to total alkalinity and overestimation of pCO_2 in New England and New Brunswick rivers. Biogeosciences 8: 3069-3076.

Johnson MS, Lehmann J, Riha SJ, Krusche AV, Richey JE, Ometto JPH, Couto EG (2008) CO_2 efflux from Amazonian headwater streams represents a significant fate for deep soil respiration. Geophys Res Lett 35:L17401. doi:10.1029/2008GL034619

Jonsson A, Algesten G, Bergström A-K, Bishop K, Sobek S, Tranvik LJ, Jansson M (2007) Integrating aquatic carbon fluxes in a boreal catchment carbon budget. J Hydrol 334:141-150.

Kilpatrick FA, Rathbun R, Yotsukura N, Parker G, DeLong L (1989) Determination of stream reaeration coefficients by use of tracers. Department of the Interior, US Geological Survey.

Loescher HW, Gholz H, Jacobs JM, Oberbauer SF (2005) Energy dynamics and modeled evapotranspiration from a wet tropical forest in Costa Rica. J Hydrol 315:274-294. doi:10.1016/j.jhydrol.2005.03.040

Lorke A, Bodmer P, Noss C, Alshboul Z, Koschorreck M, Somlai-Haase C, Bastviken D, Flury S, McGinnis DF, Maeck A, Müller D (2015) Technical note: drifting versus anchored flux chambers for measuring greenhouse gas emissions from running waters. Biogeosciences 12:7013-7024. doi:10.5194/bg-12-7013-2015

Matthews CJ, St. Louis VL, Hesslein RH (2003) Comparison of three techniques used to measure diffusive gas exchange from sheltered aquatic surfaces. Environ Sci Tech 37:772-780.

Neu V, Neill C, Krusche AV (2011) Gaseous and fluvial carbon export from an Amazon forest watershed. Biogeochemistry 105:133-147. doi:10.1007/s10533-011-9581-3

Oviedo-Vargas D, Genereux DP, Dierick D, Oberbauer SF (2015) The effect of regional groundwater on carbon dioxide and methane emissions from a lowland rainforest stream in Costa Rica. J Geophys Res-Biogeosci 120. doi:10.1002/2015JG003009

Pacheco FA (2015) Regional groundwater flow in hard rocks. Sci Total Environ 506:182-195.

Parker GW, Gay FB (1987) A procedure for estimating reaeration coefficients for Massachusetts streams. U.S. Geological Survey Water Resources Investigations Report 86-4111, Boston, MA, 34 pages.

Panneer Selvam B, Natchimuthu S, Arunachalam L, Bastviken D (2014) Methane and carbon dioxide emissions from inland waters in India-implications for large scale greenhouse gas balances. Glob Change Biol 20:3397-3407. doi:10.1111/gcb.12575

Pringle CM, Rowe GL, Triska FJ, Fernandez JF, West J (1993) Landscape linkages between geothermal activity and solute composition and ecological response in surface waters draining the Atlantic slope of Costa Rica. Limnol and Oceanogr 38:753-74. doi: 10.4319/lo.1993.38.4.0753

Rasera M-d-FF, Krusche AV, Richey JE, Ballester MV, Victória RL (2013) Spatial and temporal variability of pCO_2 and CO_2 efflux in seven Amazonian Rivers. Biogeochemistry 116:241-259.

Rathbun RE, Tai DY (1982) Volatilization of organic compounds from streams. Journal of the Environmental Engineering Division, Proceedings of the ASCE 108(EE5):973-989.

Raymond PA, Hartmann J, Lauerwald R, Sobek S, McDonald C, Hoover M, Butman D, Striegl R, Mayorga E, Humborg C (2013) Global carbon dioxide emissions from inland waters. Nature 503:355-359. doi:10.1038/nature12760

Raymond PA, Zappa CJ, Butman D, Bott TL, Potter J, Mulholland P, Laursen AE, McDowell WH, Newbold D (2012) Scaling the gas transfer velocity and hydraulic geometry in streams and small rivers. Limnol Oceanogr-Fluids and Environments 2:41-53.

Richey JE, Melack JM, Aufdenkampe AK, Ballester VM, Hess LL (2002) Outgassing from Amazonian rivers and wetlands as a large tropical source of atmospheric CO_2. Nature 416:617-620.

Sand-Jensen K, Staehr PA (2012) CO_2 dynamics along Danish lowland streams: water-air gradients, piston velocities and evasion rates. Biogeochemistry 111:615-628.

Schaller MF, Fan Y (2009) River basins as groundwater exporters and importers: Implications for water cycle and climate modeling. J Geophys Res-Atmos (1984-2012) 114 doi:10.1029/2008JD010636

Smerdon BD, Gardner WP, Harrington GA, Tickell SJ (2012) Identifying the contribution of regional groundwater to the baseflow of a tropical river (Daly River, Australia). J Hydrol 464:107-115.

Solomon DK, Genereux DP, Plummer LN, Busenberg E (2010) Testing mixing models of old and young groundwater in a tropical lowland rain forest with environmental tracers. Water Resour Res 46:W04518. doi:10.1029/2009WR008341

Striegl RG, Dornblaser M, McDonald C, Rover J, Stets E (2012) Carbon dioxide and methane emissions from the Yukon River system. Global Biogeochem Cy 26: GB0E05. doi:10.1029/2012GB004306

Stumm W, Morgan J (1996) Aquatic chemistry, chemical equilibra and rates in natural waters. Environmental Science and Technology Series, 3rd edn. Wiley-Interscience, New York

Teodoru CR, Nyoni F, Borges A, Darchambeau F, Nyambe I, Bouillon S (2015) Dynamics of greenhouse gases (CO_2, CH_4, N_2O) along the Zambezi River and major tributaries, and their importance in the riverine carbon budget. Biogeosciences 12:2431-2453.

Tóth J (2009) Gravitational systems of groundwater flow: theory, evaluation, utilization. Cambridge University Press

Vachon D, Prairie YT, Cole JJ (2010) The relationship between near-surface turbulence and gas transfer velocity in freshwater systems and its implications for floating chamber measurements of gas exchange. Limnol Oceanogr 55:1723-1732. doi:10.4319/lo.2010.55.4.1723

Wallin MB, Öquist MG, Buffam I, Billett MF, Nisell J, Bishop KH (2011) Spatiotemporal variability of the gas transfer coefficient (K_{CO2}) in boreal streams: Implications for large scale estimates of CO_2 evasion. Global Biogeochem Cy 25:GB3025. doi:10.1029/2010GB003975

Wu L-C, Wei C-B, Yang S-S, Chang T-H, Pan H-W, Chung Y-C (2007) Relationship between Carbon Dioxide/Methane Emissions and the Water Quality/Sediment Characteristics of Taiwan's Main Rivers. J Air Waste Ma 57:319-327.

Zanon C, Genereux DP, Oberbauer SF (2014) Use of a watershed hydrologic model to estimate interbasin groundwater flow in a Costa Rican rainforest. Hydrol Process 28:3670-3680. doi:10.1002/hyp.9917

Chapter 4: Extreme effects of regional groundwater and storms on the quality and export of DOM in tropical streams

Christopher L. Osburn[1*], Emily Barnett[1], Diana Oviedo-Vargas[1#], Diego Dierck[2], Stephen F. Oberbauer[2], and David P. Genereux[1]

1 Department of Marine, Earth, and Atmospheric Sciences, North Carolina State University, Raleigh, North Carolina

2 Department of Biology, Florida International University, Miami, Florida,

* corresponding author, closburn@ncsu.edu; +1-919-515-0382

present address, Stroud Water Research Center, Avondale, Pennsylvania

Abstract

A paired-watershed approach was used to compare the quality and fluxes of dissolved organic matter (DOM) in two tropical rainforest streams located in northeastern Costa Rica. The Arboleda stream received regional groundwater (RGW) discharge via interbasin groundwater flow whereas the Taconazo stream did not. DOM in both streams was compared during baseflow and stormflow and compared to DOM sources from regional groundwater, precipitation, throughfall, and soil leachate. DOM quality was assessed with chromophoric dissolved organic matter (CDOM) absorbance and fluorescence and stable carbon isotope values (δ^{13}C-DOC). Parallel factor analysis (PARAFAC) of excitation-emission matrices from stream samples resulted in six distinct components: four were humic-like and representative of terrestrial DOM sources and two were protein-like, also attributable to phenolics or tannins from land plants and was enriched in throughfall. RGW DOM appeared as degraded as surface ocean DOM, lacking fluorescence, and having specific ultraviolet absorption ($SUVA_{254}$) values <1.0 L mg C^{-1} m^{-1} and CDOM slope ratio (S_R) values >7. $SUVA_{254}$ values were lower, and S_R values higher, in the Arboleda during baseflow compared to the Taconazo, presumably due to dilution by RGW. However, no significance difference in $SUVA_{254}$ or S_R occurred between the streams during stormflow. Moreover, $SUVA_{254}$ was correlated to δ^{13}C-DOC (r^2=0.61, p<0.001) demonstrating a strong linkage between stream DOM characteristics and the relative amounts of RGW, soil, and throughfall impacting stream organic matter cycles. Export of DOC computed for the Taconazo was 3.06 g C m^{-2} yr^{-1}, consistent with other tropical streams. However, DOC export from the Arboleda was 23.96 g C m^{-2} yr^{-1}, one of the highest exports reported and reflective of the substantial impact that groundwater can have on surface water carbon cycling.

1. Introduction

Dissolved organic matter (DOM) plays a key role in aquatic food webs, influences the availability of dissolved nutrients and metals, and affects the optical properties and overall biogeochemistry of aquatic ecosystems [*Findlay and Sinsabaugh*, 2003]. Rivers and streams transport or store about 2 Pg of terrestrial organic carbon (C) annually and at least half of the C inputs to fluvial systems are outgassed to the atmosphere before reaching the oceans [*Cole et al.*, 2007*; Aufdenkampe et al.*, 2011]. About 50% of the total organic carbon exported from watersheds by rivers to the oceans is in the form of dissolved organic carbon, DOC [*Raymond and Bauer*, 2001]. With a major active role in the global inland carbon cycle, the quality of DOM is as important to study as its quantity [*Cole et al.*, 2007; *Spencer et al.*, 2012].

DOM quality in streams often is studied via bulk properties such as chromophoric DOM (CDOM) content and its stable isotopic composition, both of which provide information on its sources and biogeochemical cycling [*Findlay and Sinsabaugh*, 2003]. CDOM specific ultraviolet (UV) absorbance at 254 nm ($SUVA_{254}$) is related to its aromaticity [*Weishaar et al.*, 2003], while CDOM spectral slope ratio (S_R) is related to molecular weight [*Helms et al.*, 2008]. CDOM quality derived from excitation-emission matrices of its fluorescence (EEMs) include biological and humification indices (BIX and HIX, respectively), which correspond to DOM produced recently by planktonic organisms (BIX) and DOM that contains recalcitrant humic substances (HIX). Chemometric techniques have been used to analyze EEM fluorescence and provide distinct signatures ("components") that provide information on the chemical composition of DOM [*Fellman et al.*, 2010]. Stable carbon isotope values of DOM (δ^{13}C-DOC) indicate its sources and often distinguish between C3 and C4 plant sources as well as between fresher plant leachate and humic substances [*Lloret et al.*, 2016].

There are multiple sources of DOM to fluvial systems: soil organic matter, in-situ primary production, atmospheric precipitation, throughfall, stemflow, and groundwater [*Mulholland*, 2003*; Inamdar et al.*, 2011*; Lloret et al.*, 2011]. Previous studies have shown that precipitation events lead to greater DOC concentration and flux during stormflow compared to baseflow conditions and DOC sources to fluvial systems shift from groundwater to surface water during such events and as different components of the watershed are activated [*McGlynn and McDonnell*, 2003; *Raymond and Saiers*, 2010*; Inamdar et al.*, 2011]. This shift in from groundwater to surface water also changes DOM sources to streams. Rain events tend to flush more terrestrial DOM from the land surface into the stream, changing the quality of the DOM due to water movement overland during storms [*McGlynn and McDonnell*, 2003; *Raymond and Saiers*, 2010]. The resulting exported DOM is of a more terrestrial origin than is observed during baseflow which is dominated by groundwater inputs [*Hood et al.*, 2006; *Lloret et al.*, 2011; 2016]. DOC concentrations tend to increase on the rising limb of a hydrograph and decrease on the falling limb; this likely represents that water-soluble soil organic matter is depleted after a certain amount of flushing from rain via hydrologic throughflow [*Hornberger et al.*, 1994]. Recent work indicates that sources of this terrestrial material originate from fresh plant litter as well as labile substrates washed from plant surfaces via throughfall and stemflow [*Inamdar et al.* 2011; *Lloret et al.* 2016]. By contrast, groundwater inputs tend to be lower in DOM concentration and exhibit much less terrestrial quality [*Chen et al.* 2010; *Inamdar et al.* 2011; *Inamdar et al.* 2012]. The residence time of DOM in groundwater may contribute to these characteristics [*Genereux et al.* 2013]. Considering the importance of storms in exporting large amounts of DOC from watersheds, it is important also to

understand how the quality of the DOC export from watersheds differs between stormflow and baseflow [*Raymond et al.* 2016].

Uncertainties in DOM quality and quantity in tropical ecosystems than in temperate or boreal ecosystems, despite having a disproportionately greater role in downstream transport of C; in general, tropical ecosystems are understudied in the inland carbon cycle [*Aufdenkampe et al.*, 2011; *Raymond et al.,* 2013]. DOC and CDOM concentrations in tropical streams tend to increase during storm events and during wet seasons [*Newbold et al.*, 1995*; Johnson et al.*, 2006*; Spencer et al.*, 2010*; Bass et al.*, 2011]. However, only a few studies have examined DOM quality in addition to quantity in tropical streams and rivers under these contrasting conditions and fewer still have considered the influence of groundwater on DOM quality [*Spencer et al.*, 2010*; Genereux et al.,* 2013; *Ganong et al.*, 2015]. Closing this knowledge gap is an essential task as hydrology, vegetation, and biological activity are expected to change with the increasing climate variability, particularly in the tropics, where rainfall is substantial, yet the frequency and duration of droughts and storms are changing [*O'Gorman et al.*, 2012].

The aim of this study was to determine differences in DOM quality between baseflow and stormflow in tropical streams and to consider the influence of groundwater, throughfall, and soil leachate sources of DOM under these conditions. We used a paired-watershed approach to study the temporal variability of DOM quantity and quality of two headwater streams, the Arboleda and the Taconazo, draining adjacent watersheds located at the La Selva Biological Station in Costa Rica. The streams share similar soils and vegetation but differ in their water sources. Only young, shallow, local groundwater discharges into the Taconazo, whereas both local groundwater and much older regional groundwater discharge into the Arboleda [*Genereux et al.*, 2009, 2002, 1997]. DOM was evaluated on samples collected approximately weekly over a 2-year period (2012-2013), with higher resolution during three specific rain events in June 2013. Our objectives were to analyze DOC concentration, CDOM absorption and fluorescence, and δ^{13}C-DOC values along with stream discharge to determine: 1) the influence of regional groundwater on stream DOM; 2) the spatial variability of DOM quality and quantity between stormflow and baseflow in two adjacent watersheds; and 3) sources of DOM to the tropical streams. Results were placed in context of prior work on stream DOM quality and export in temperate and tropical ecosystems.

2. Study Site

This study was conducted at La Selva Biological Station (LSBS), a field research station of the Organization for Tropical Studies (OTS). LSBS is a 1536 ha research preserve in the Heredia province of Costa Rica near the town of Puerto Viejo de Sarapiquí (Fig. 1). The geology of the site is mainly volcanic rocks of Quaternary age and intermediate composition [*Genereux et al.*, 2009]. Average annual rainfall at La Selva from 1963 to 2013 was 4328 mm, with February, March, and April as the driest months and July, November, and December as the wettest (online meteorological data at http://www.ots.ac.cr/meteoro/default.php?pestacion=2). From 1982 to 2013, the mean air temperature was 25.0°C.

The two streams studied at LSBS were the Arboleda and the Taconazo (Fig. 1), adjacent streams whose watersheds are identical or nearly so with regard to many characteristics, including vegetation, relief, soil type, rainfall, temperature, and evapotranspiration [*Genereux et al.*, 2005]. However, the Arboleda has much higher inorganic solute concentrations than the Taconazo, a product of a high influx of interbasin groundwater flow which contributes older regional

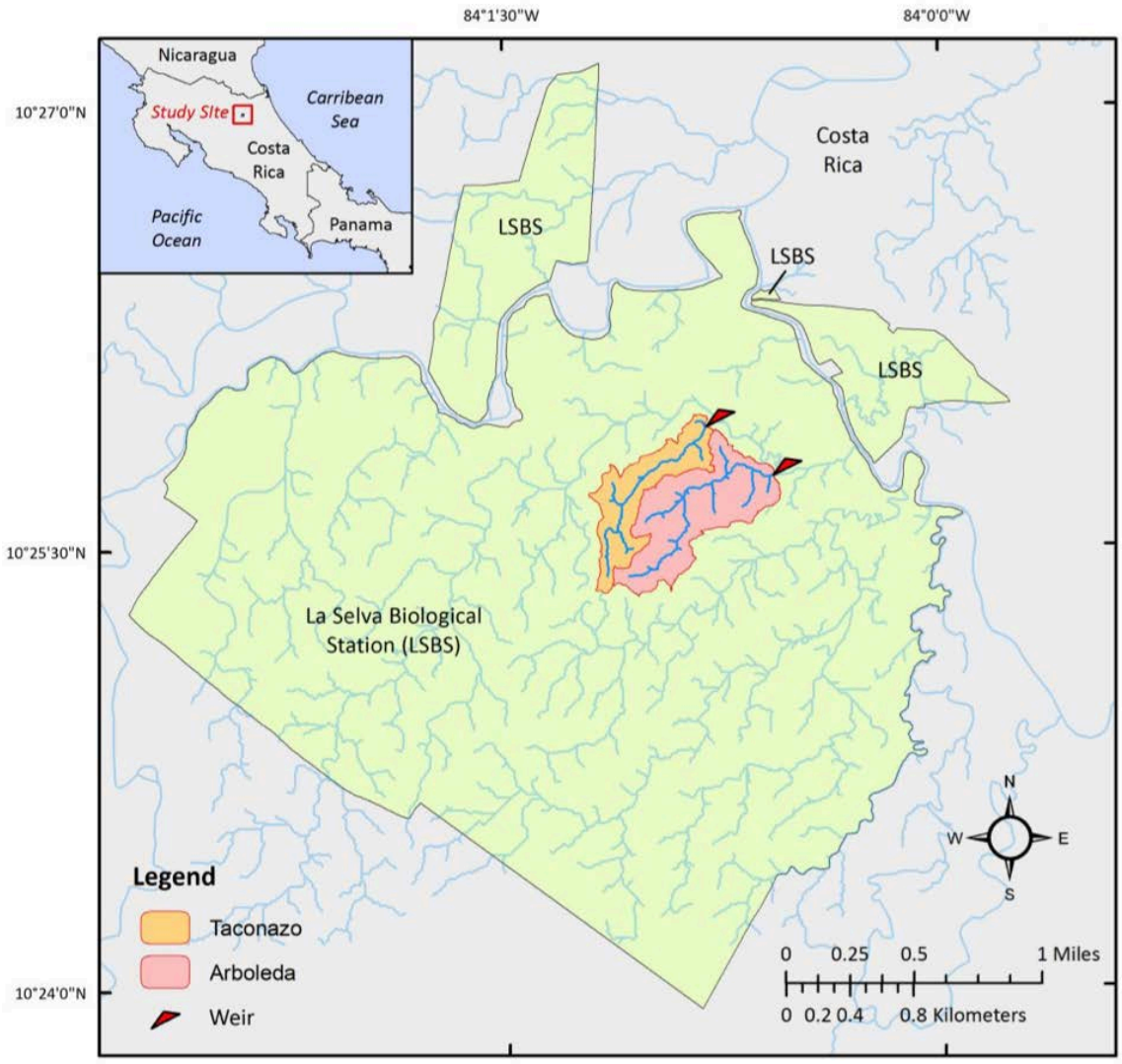

Figure 1. Map of study site at La Selva Biological Station showing location of the Taconazo and the Arboleda watersheds (from Nagy, 2012). Guacimo Spring is located south of La Selva Biological Station.

groundwater to the Arboleda but not to the Taconazo [*Genereux et al.*, 2002; 2005; 2009]. Regional groundwater accounts for about 34% of the annual discharge of the Arboleda but 0% of the Taconazo discharge [*Genereux et al.*, 2005]. Stream discharge was measured at a sharp-crested V-notch weir on each watershed; watershed areas upstream of the weirs are 47.1 ha for the Arboleda and 27.9 ha for the Taconazo.

3. Methods

3.1. Water Sample Collection and Processing

Water samples for the analysis of DOC concentration and isotopic composition as well as optical properties of the DOM were collected approximately weekly from the Arboleda and

Taconazo streams from January 2012 through March 2014 (Table 1). Samples were also taken at Guácimo Spring, a spring located to the south of LSBS with water representative of old regional groundwater (RGW) at the site. For the weekly sampling stream water samples were collected in pre-cleaned 1-L high density polyethylene bottles.

Table 1. Summary of stream water sampling for the Arboleda and Taconazo streams at La Selva Biological Station, Costa Rica.

Activity	Frequency	Start date	End date
Routine sampling			
Automated stream discharge	15 minutes	1 Jan 2012	14 Mar 2014
Absorbance and fluorescence	Weekly	30 Jan 2012	14 Mar 2014
Dissolved organic carbon (DOC)	Weekly	30 Jan 2012	14 Mar 2014
Stable isotope data (δ^{13}C-DOC)	Weekly	30 Jan 2012	14 Mar 2014
Storm sampling (Absorbance, fluorescence, DOC, $\delta^{13}C$)			
Storm 1	Every hour for	13 Jun 2013	14 Jun 2013
Storm 2	12 hours	14 Jun 2013	15 Jun 2013
Storm 3		25 Jun 2013	25 Jun 2013

Using Teledyne ISCO 3700 samplers deployed near the weirs, we sampled storm events at high frequency in the Arboleda and the Taconazo in June 2013. Hourly stream samples were collected (before, during, and after rainfall) for 12 hours on three days: June 13, June 14, and June 25. Discharge data from V-notch weirs were taken every 15 minutes in both the Arboleda and the Taconazo [*Genereux et al.*, 2013]. Some dates do not have recorded data due to instrument malfunction; in this case the watershed hydrologic model TOPMODEL was used to estimate the discharge based on the regional precipitation measured at a tipping-bucket rain gauge that is within 1.5 km of both weirs [*Zanon et al.*, 2014].

Stream samples were classified as either baseflow or stormflow, based on visual examination of the plotted discharge and precipitation data. All discharge values below 9 m^3 min^{-1} in the Arboleda were classified as baseflow, while discharge values above 11 m^3 min^{-1} were classified as stormflow. For the Taconazo, discharge values <0.5 m^3 min^{-1} were classified as baseflow and discharges >1.5 m^3 min^{-1} were classified as stormflow. Samples collected at discharges in between these values were classified as stormflow if there had been measured precipitation within five hours of sample collection.

DOM source samples were collected in December 2015. Precipitation was collected in pre-cleaned, round and shallow 7-L plastic containers which in an open area with no trees in a 15-m radius and deployed for 24 hr, then returned to the laboratory at LSBS for processing. Throughfall was collected in similar 7-L containers which were deployed randomly under the canopy of forested areas in the Arboleda and Taconazo watersheds. After a 24-h period (accumulated precipitation ~ 11.7 mm), the volume of throughfall collected in the containers was measured using 1-L calibrated cylinders, transferred into HDPE dark 2-L bottles and transported immediately to the laboratory facilities at LSBS.

Soil samples from the top 4 cm were collected from the Arboleda and Taconazo watersheds (1 sample each) and from near the LSBS laboratory (N = 3) using cleaned 50-mL polypropylene centrifuge tubes to core and collect the sample. The samples were immediately transported to the

laboratory at LSBS, where 15 mg of soil was transferred into clean 50 mL polypropylene centrifuge tubes to which 40 mL of ultrapure water was added. The soils were agitated on a shaker table for 24 hours to disaggregate soil particles and facilitate extraction of OM into water and then centrifuged. The supernatant was decanted and filtered using 0.7 um GF/F filters, and the filtrate was considered soil leachate DOM. Precipitation, throughfall, and soil leachate samples were stored frozen and returned to NC State University for measurements of DOM optical and chemical properties.

3.2. Dissolved Organic Carbon, Stable Carbon Isotope, and Chromophoric Dissolved Organic Matter Analyses

After field collection, samples were transferred to 125-mL polycarbonate bottles, frozen and transported from Costa Rica to the United States and stored at -20 C upon arrival at North Carolina State University. Prior to analysis, samples were thawed to room temperature. A vacuum pump (Barnant Company) was used to filter the samples through pre-combusted 0.7-µm porosity glass fiber filter (Whatman GF/F) into a cleaned 500 mL glass Erlenmeyer flask within 24 hours of thawing. The volume filtered was recorded and then absorbance and fluorescence was measured on filtrates within one week. After optical measurements, the remaining filtrate was transferred to a pre-combusted glass vial and acidified with 85% phosphoric acid to a pH of 2 for DOC and stable carbon isotope (δ^{13}C-DOC) analysis.

DOC concentration ([DOC]) was measured using an OI Analytical Aurora Model 1030 Total Organic Carbon Analyzer while carbon stable isotopes were measured on a Delta V Isotope Ratio Mass Spectrometer [*Osburn and St-Jean*, 2007]. Reference carbon dioxide pulses were sent through the system before analysis until an acceptable standard deviation (<0.05) was observed. A standard curve for DOC concentration was created consisting of six solutions of IAEA-600 caffeine over DOC concentrations ranging from 0.25 mg L^{-1} to 25 mg L^{-1}. DOC measurement using this technique had a coefficient of variance <5%. Carbon stable isotope ratios from the IRMS were blank-corrected and then calibrated to the Vienna Pee Dee Belemnite (VPDB) scale ($\delta^{13}C_{VPDB}$) with caffeine solutions ($\delta^{13}C_{VPDB}$ = -27.77±0.04‰) and solutions of IAEA C6 sucrose ($\delta^{13}C_{VPDB}$ = -10.45±0.03‰). Samples and standards were blank-corrected and a linear regression of the area of the curve of the caffeine standards was created to relate area under the curve to DOC concentrations. Reproducibility of this method is ±0.4‰.

CDOM absorbance spectra of the samples were measured from 200 to 800 nm on a Varian Cary 300UV spectrophotometer in quartz cells that were either 1-cm or 10-cm in length, depending on the CDOM concentration in the sample. Samples were diluted if necessary to keep the absorbance <0.4 in 1-cm cells; samples in 10-cm cells did not require dilution. Blank-corrected absorbance values were converted to Napierian units using the following equation:

$$a(\lambda) = \frac{A_{(\lambda,\text{sample})} - A_{(\lambda,\text{blank})}}{L} \times 2.303 \quad (1)$$

where *a* is the absorption coefficient at wavelength λ, A is the absorbance, and L is the pathlength of the quartz cell, in meters. The value 2.303 converts the decadal absorption to Napieran absorption. CDOM was quantified as Napierian absorption at 254 nm (a_{254}). The ratio of decadal a_{254} to DOC concentration, *i.e.*, the *specific UV absorption* ($SUVA_{254}$), was computed and used to estimate the relative amount of the aromatic groups in DOM [*Weishaar et al.,* 2003]. Spectral slopes (*S*) were computed over 275-295 nm and 350-400 nm via linear regression of natural-log transformed absorption spectra. Slope ratio (S_R) values were calculated as $S_{275\text{-}295}$ divided by $S_{350\text{-}400}$. S_R values were used as proxies for the molecular weight of DOM, with high values

corresponding to low molecular weight (LMW) DOM and low values corresponding to high molecular weight (HMW) DOM [*Helms et al.*, 2008].

Fluorescence excitation-emission spectra were measured on a Varian Eclipse spectrofluorometer, sampled from 240 to 450 nm in the excitation mode (Ex) and 300 to 600 nm in the emission mode (Em). These samples were corrected by subtracting an ultrapure lab water blank. Samples were also corrected for the inner filtering effect and to the spectrofluorometer's water Raman signal before a final normalization to quinine sulfate units (QSU). Corrections of absorbance and fluorescence spectra were done with in-house processing scripts using MATLAB 2014a (Mathworks). The intensity and shape of the excitation-emission matrix (EEM) coupled with the multivariate technique, parallel factor analysis (PARAFAC) was used quantify and characterize DOM in this study. Fluorescence emission spectra for each sample were processed into an EEM, and matrices were then compiled into an array and processed with the DOMFluor toolbox [*Stedmon and Bro*, 2008; *Murphy et al.*, 2013] in MATLAB. PARAFAC models containing three to six components were fit to the data array and validated using split-half analysis, random starts, and inspection of any residuals. Maximum fluorescence values (FMax) for each component are reported in QSU and percentages of each component (e.g. %C1-%C6) express the abundance of each component in a sample relative to the total abundance of all six components.

3.3. Calculation of DOC export fluxes

Export fluxes of DOC were calculated by comparing two methods: Runkel's Load Estimator (LOADEST) [*Runkel et al.*, 2004] and method M5 from *Birgand et al.*, [2010]. LOADEST estimates constituent export fluxes based on a time series of stream flow and constituent concentration by developing a regression model. Calibration and estimation procedures are based on three statistical methods (adjusted maximum likelihood estimation, maximum likelihood estimation, and least absolute deviation), depending on whether calibration errors are normally distributed, and diagnostic tests are provided to evaluate the appropriateness of the chosen method. M5 is an averaging method in which the export flux is calculated as the annual flow volume by an estimator of the flow (at the time of sampling) weighted average of the constituent concentration [*Littlewood*, 1992].

3.4. Statistical tests

Assumptions for parametric statics were not met by most of the results, thus non-parametric tests were used. For univariate data, ANOVA on ranks (Kruskal-Wallis test) with Dunn's post-hoc test were undertaken to determine differences between streams and between storm- and baseflow. Fluorescence excitation-emission matrix (EEM) spectra were decomposed into components representing the most variation in the data using parallel factor analysis (PARAFAC). PARAFAC results are multivariate data that often are intercorrelated and require non-parametric techniques for making comparisons [*Murphy et al.*, 2014]. Thus, permutation MANOVA (PERMANOVA) tests were conducted on PARAFAC results based on Euclidean distances.

4. Results

4.1. Stream DOM concentrations compared between the two watersheds and between baseflow and stormflow

Minimum and maximum baseflow values of 8.7 m^3 min^{-1} and 10.6 m3 min-1, respectively, were measured in the Arboleda. In the Taconazo, minimum baseflow was 0.05 m^3 min^{-1} and maximum baseflow was 1.3 m^3 min^{-1}. Maximum observed stormflow was 93.7 m^3 min^{-1} in the

Arboleda and 35.4 m^3 min^{-1} in the Taconazo.

There were clear differences in DOC and CDOM concentrations between the streams, and between baseflow and stormflow (Table 2 and Fig. 2). DOM data were generally not normally distributed, hence median, minimum, and maximum values are reported (Table 3). Median DOC concentration, [DOC], in the Arboleda at baseflow (0.83 mg L^{-1}) was roughly half that in the Taconazo (1.26 mg L^{-1}), and [DOC] was significantly higher ($P<0.01$) in the Taconazo. However, during stormflow, [DOC] was not significantly different between the two streams ($P>0.05$). Within each stream, median [DOC] was significantly higher at stormflow than at baseflow ($P<0.001$ for the Arboleda, $P<0.05$ for the Taconazo), and stormflow median in the Arboleda (2.04 mg L^{-1}) approached that in the Taconazo (2.25 mg L^{-1}).

In general, CDOM concentrations (quantified as a_{254}) followed similar trends to DOC concentrations. Median a_{254} values during stormflow in the Arboleda and the Taconazo streams were higher (9.71 m^{-1} and 9.39 m^{-1}, respectively) than at baseflow (2.23 m^{-1} in the Arboleda and 6.25 m^{-1} in the Taconazo) (Table 2). However, median stormflow CDOM concentrations in the Arboleda increased by 4-fold from baseflow to stormflow, compared to 1.5-fold increase in CDOM for the Taconazo (Table 2). Differences between flow conditions were significant for a_{254} as for [DOC] (Table 3).

Table 2. Summary statistics for stream DOM under the following categories: Arboleda at baseflow, Arboleda at stormflow, Taconazo at baseflow, and Taconazo at stormflow. Med = median; Min = minimum; Max = maximum; N = number of observations.

Parameter	Statistic	Arboleda baseflow	Arboleda stormflow	Taconazo baseflow	Taconazo stormflow
DOC (mg L^{-1})	Med	0.83	2.04	1.26	2.25
	Min	0.22	0.45	0.52	0.65
	Max	2.73	11.52	8.25	5.81
	N	62	46	47	63
a_{254} (m^{-1})	Med	2.23	9.39	6.25	9.71
	Min	1.65	1.86	4.17	2.27
	Max	9.93	25.95	14.25	23.06
	N	80	54	80	75
$SUVA_{254}$ (L mg C^{-1} m^{-1})	Med	1.36	2.03	2.12	2.45
	Min	0.46	0.47	0.44	0.31
	Max	3.56	4.04	4.74	5.36
	N	62	46	44	63
S_R	Med	1.05	0.91	0.77	0.78
	Min	0.85	0.81	0.73	0.73
	Max	1.56	1.49	2.08	3.92
	N	80	54	80	75
δ^{13}C-DOC (‰)	Med	-27.58	-26.69	-27.72	-27.15
	Min	-36.98	-32.81	-34.51	-34.39

	Max	-21.04	-21.78	-21.65	-21.20
	N	75	46	47	64
FMax C1 (QSU)	Med	1.46	6.07	3.89	6.81
	Min	0.60	0.54	1.79	1.92
	Max	6.49	13.81	7.93	12.15
	N	65	46	43	61
FMax C2 (QSU)	Med	1.34	5.20	3.12	5.76
	Min	0.59	0.57	1.43	1.54
	Max	5.77	11.16	6.94	9.70
	N	65	46	43	61
FMax C3 (QSU)	Med	0.80	3.18	1.45	2.65
	Min	0.31	0.34	0.66	0.76
	Max	3.06	7.30	3.20	4.84
	N	65	46	43	61
FMax C4 (QSU)	Med	1.34	4.01	1.80	3.97
	Min	0.54	0.73	0.88	1.08
	Max	4.23	8.79	6.98	6.73
	N	65	46	43	61
FMax C5 (QSU)	Med	0.53	2.21	0.65	1.75
	Min	0.20	0.26	0.32	0.27
	Max	3.34	3.84	2.66	3.28
	N	65	46	43	61
FMax C6 (QSU)	Med	0.21	0.78	0.56	0.92
	Min	0	0	0.14	0
	Max	4.02	2.39	6.91	8.27
	N	65	46	43	61

δ^{13}C-DOC can be used to elucidate sources of organic matter to natural waters and infer in-stream processing. Measured δ^{13}C-DOC values in the Taconazo and Arboleda streams spanned nearly the entire range of values observed for most freshwater ecosystems: -22 to -36‰ [*Raymond and Bauer*, 2001]. Median values for both streams at baseflow were about -27‰, indicative of C3 terrestrial vegetation (Table 2). The median value at stormflow was slightly enriched in the Arboleda (δ^{13}C-DOC = -26.69‰) and but not in the Taconazo (δ^{13}C-DOC = -27.15‰). No significant differences were observed between baseflow and stormflow for either stream, likely due in part to the relatively large range of values measured, that perhaps were due to similar DOM sources in regional and local groundwater though the longer residence of RGW likely subjects it to substantial degradation [*Genereux et al.*, 2013].

CDOM quality however did vary significantly between the streams (Fig. 2). $SUVA_{254}$ increase with a greater aromatic content of DOM and typically range from 1-4 L mg C^{-1} m^{-1} in stream and rivers [*Spencer et al.*, 2012]. For the Arboleda, the median $SUVA_{254}$ value during

baseflow was on the lower end of this range (1.36 L mg C^{-1} m^{-1}) yet increased significantly during stormflow to 2.03 L mg C^{-1} m^{-1} (Tables 2 and 3).

Table 3. Summary of non-parametric ANOVA on ranks (Kruskal-Wallis) with Dunn's test conducted on DOM measurements to determine significant differences between the two sets compared. 'ns' indicates no significant difference (P>0.05).

Parameter	Arboleda Baseflow vs. Arboleda Stormflow	Taconazo Baseflow vs. Taconazo Stormflow	Arboleda Baseflow vs. Taconazo Baseflow	Arboleda Stormflow vs. Taconazo Stormflow
DOC	P<0.001	P<0.05	P<0.001	ns
a_{254}	P<0.001	P<0.001	ns	ns
$SUVA_{254}$	P<0.05	ns	P<0.01	ns
S_R	P<0.05	ns	P<0.001	P<0.001
δ^{13}C-DOC	ns	ns	ns	ns

In the Taconazo, median $SUVA_{254}$ values were 2.12 and 2.45 L mg C^{-1} m^{-1} at baseflow and stormflow, respectively. There was no significant difference in $SUVA_{254}$ values between the Taconazo at baseflow and stormflow. Median $SUVA_{254}$ was significantly different between the Arboleda and the Taconazo at baseflow but not at stormflow (Table 3).

Slope ratios (S_R) <1 indicate CDOM of high molecular weight and aromaticity [e.g., *Spencer et al.*, 2012]. S_R was generally higher in the Arboleda than the Taconazo [*Genereux et al.*, 2013]. In the Arboleda, median S_R was slightly higher at baseflow (1.05) than stormflow (0.91); in the Taconazo, median S_R was virtually identical between baseflow and stormflow (Table 4 and Fig. 2) and significantly lower than S_R in the Arboleda (Table 3).

Table 4. P-values matrix from non-parametric MANOVA on ranks conducted on FMax values between the Arboleda and Taconazo streams at stormflow and baseflow. Significant differences where P <0.05. 'NA' means not applicable.

	Arboleda stormflow	Arboleda baseflow	Taconazo stormflow	Taconazo baseflow
Arboleda stormflow	NA	0.001	0.1727	0.0537
Arboleda baseflow	0.001	NA	0.0001	0.0006
Taconazo stormflow	0.1727	0.0001	NA	0.7818
Taconazo baseflow	0.0537	0.0006	0.7818	NA

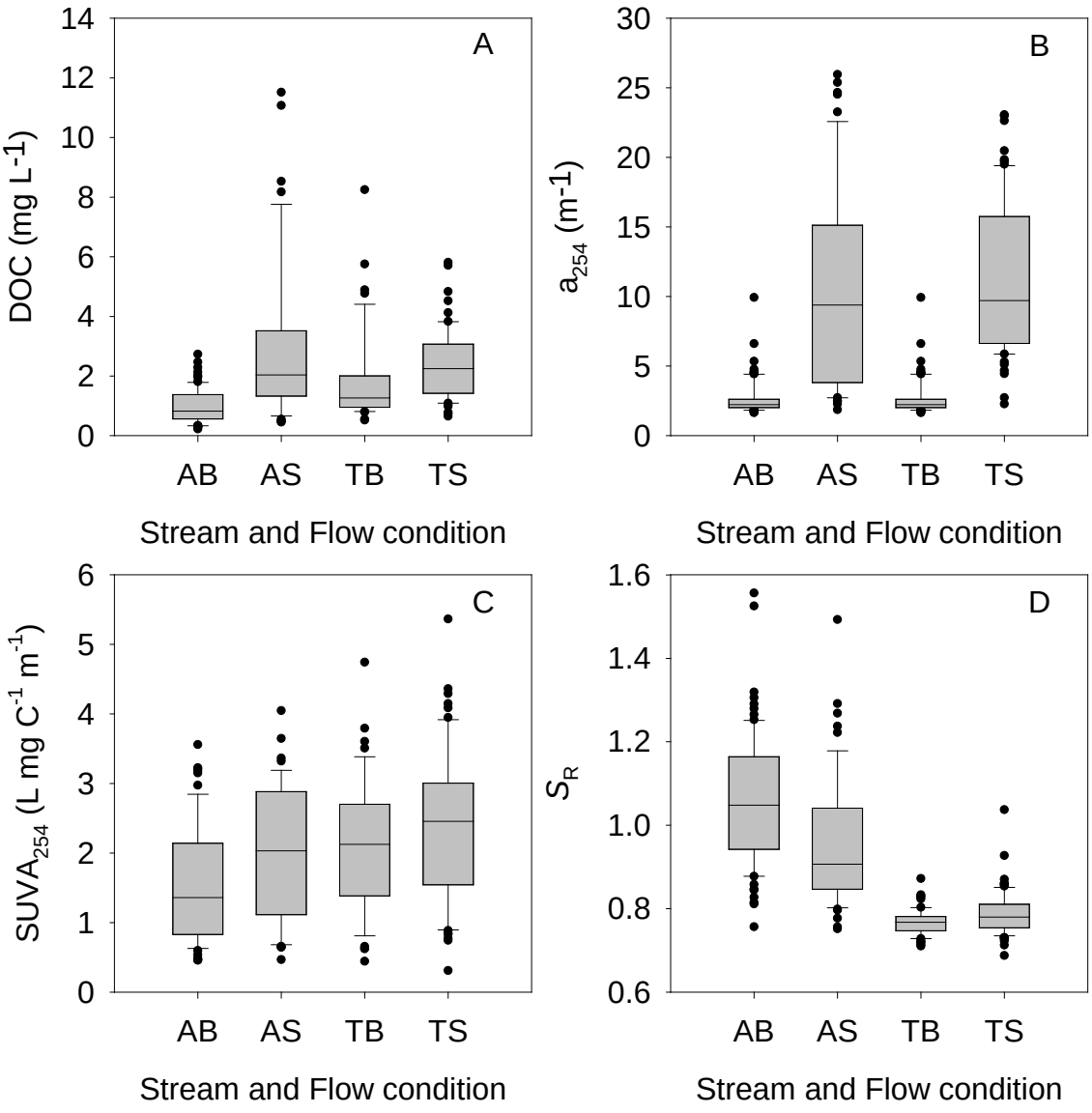

Figure 2. Boxplots of (A) DOC, (B) a_{254}, (C) $SUVA_{254}$, and (D) spectral slope ratio S_R for the Arboleda at base flow (AB) and stormflow (AS) and the Taconazo at baseflow (TB) and stormflow (TS). Horizontal lines in boxes indicated median values while horizontal edges indicate 25th and 75th percentiles. Error bars indicate 10th and 90th percentiles and black filled circles indicate outliers.

A six-component PARAFAC model was fit to the stormflow and baseflow DOM fluorescence measurements from the Arboleda and the Taconazo (Fig. 3). Each component (C) exhibited key fluorescence properties that partition DOM into four allochthonous (external to stream) sources (C1-C4) and two autochthonous (internal to stream) sources (C5-C6), based on comparison to previously published models in the OpenFluor database (Table 5). In general, C1-C4 exhibited excitation and emission spectra consistent with humic substances from soils and

freshwaters [*Senesi*, 1990]. Component 1 (C1) matched with 10 models and exhibited a terrestrial, humic-like signal consistent with photoreactive material found in lakes, rivers, and coastal waters. C2 matched with 13 models from productive ecosystems such as estuaries but also European lakes and streams and tropical rivers, and it shared spectral properties common to microbial humic-like substances [*Kothawala et al.*, 2014; *Osburn et al.*, 2016; *Lambert et al.*, 2016]. C3 exhibited the longest excitation and emission spectral features, often associated with fulvic acids extracted from soils and matched with 17 models, including a wide variety of humic-rich freshwaters, estuaries, and coastal waters, including tropical rivers [*Yamashita et al.*, 2010; *Chen et al.*, 2010; *Osburn et al.*, 2016].

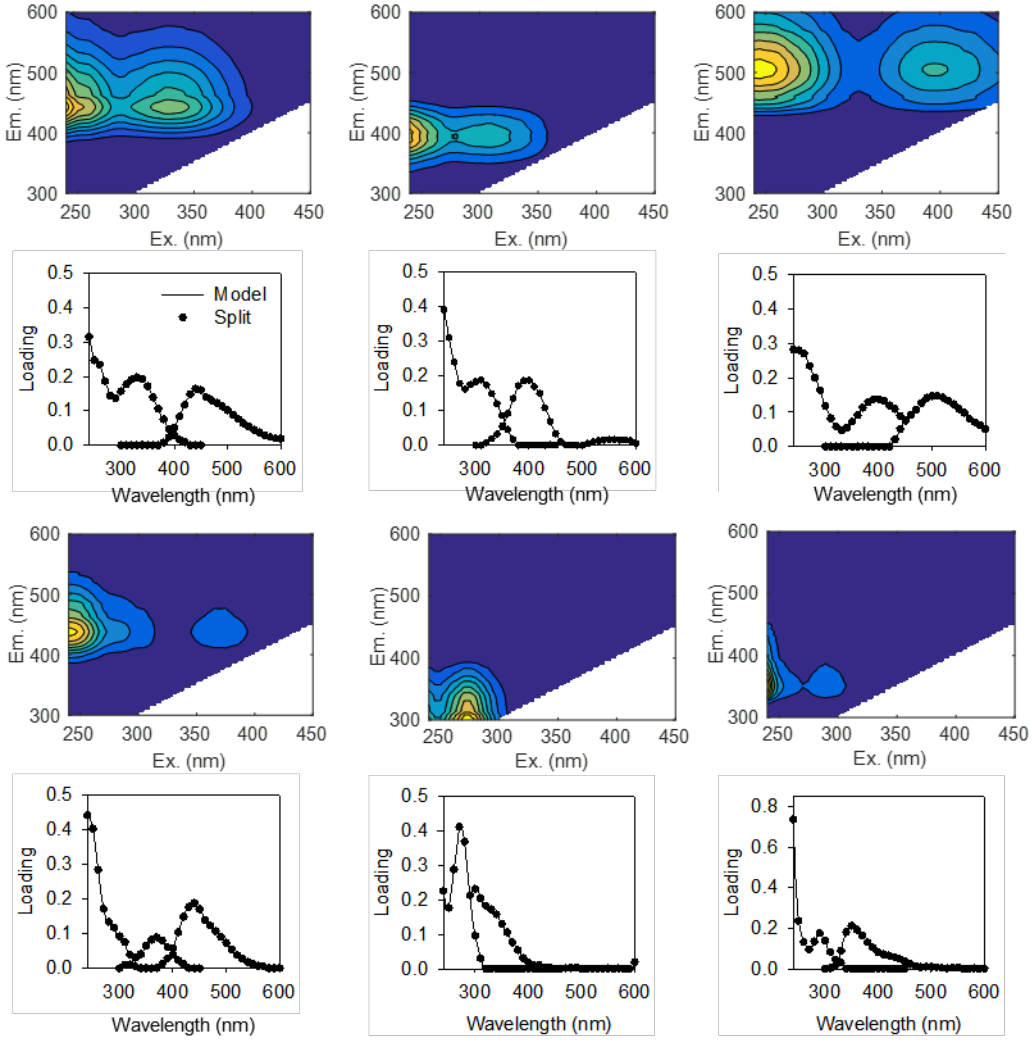

Figure 3. Excitation (Ex) – emission (Em) contour plots ("EEMs") of six fluorescent components modeled using PARAFAC on DOM from the Arboleda and Taconazo streams, with corresponding Ex and Em spectra loadings from the PARAFAC model for each component, below, the product of which produced the EEM. Solid line is the model for the whole data set and filled circles are the model fit to a randomly selected half of the whole data set. This procedure is used to validate the PARAFAC model.

Component 4 (C4) had primary excitation <240 nm, secondary excitation at 360 nm, and emission at 440 nm. While no statistical match was found in OpenFluor, its primary Ex/Em corresponds to a degradation component that has been produced photochemically [*Stedmon et al.*, 2007]. Components 5 and 6 exhibited fluorescence that often is attributed to protein-like substances but also shares characteristics with phenolic material from lignin and tannin [*Hernes et al.*, 2009; *Stubbins et al*., 2014; *Wünsch et al*., 2016]. C5 matched with 14 models ranging from the open ocean to lakes, rivers, and estuaries. The spectral features of C6 matched with two models of mostly coastal waters [e.g., *Kowalczuk et al.*, 2009].

Fluorescence intensity of components (FMax values) for the Arboleda and Taconazo streams at baseflow and stormflow exhibited similar fluorescent patterns (Table 2). Compared to the baseflow samples, the stormflow samples in both streams tended to have greater fluorescence intensity. Median intensities for Arboleda were ranked C1>C2=C4>C3>C5>C6 for baseflow and C1>C2>C4>C3>C5>C6 for stormflow. Median Taconazo FMax values were ranked C1>C2>C4>C3>C5>C6 both at baseflow and stormflow. These patterns indicated similar sources of CDOM in the streams, dominated by humic substances but subtly influenced by perhaps fresh plant material.

Table 5. Maximum excitation (Ex) and emission (Em) wavelengths of PARAFAC components along with number of models matched on OpenFluor (criterion of 95% similarity), source of fluorescence, and other environments where the component has been found. Values in parentheses are secondary maxima.

Component	Ex/Em Maxima	Number of matches	Probable source	Representative ecosystems
C1	240/442	10	Terrestrial, humic-like	North American lakes[1], European lakes[2], North American estuaries[3], South Atlantic Bight[4]
C2	240 (300)/400	13	Microbial, humic-like	European lakes[2], North American estuaries[3], Coastal and shelf seas[5], Zambezi River basin[6]
C3	245/504	17	Terrestrial, soil fulvic-like	Coastal and shelf seas[5], Tropical rivers[7], Florida Everglades[8]
C4	240 (365)/438	0	Terrestrial degradation product	no matches
C5	270/302	14	Protein-like, amino-acid	European lakes[2]; Florida Everglades[8], Florida Keys[9]; European estuary[10]
C6	240/350	2	Protein-like; possible plant phenolic (lignin/tannin)	South Atlantic Bight[4]

[1]*Osburn et al.*, [2011], [2]*Kothawala et al.*, [2013], [3]*Osburn et al.*, [2016], [4]*Kowalczuk et al.*, [2009], [5]*Murphy et al.*, [2014], [6] *Lambert, et al.*, [2016], [7] *Yamashita et al.*, [2010a], [8] *Yamashita et al.*, [2010b]. [9] *Yamashita et al.*, [2013], [10]*Osburn and Stedmon*, [2011]

4.2. Trends in stream DOM properties with discharge

Non-parametric correlations between discharge and DOC and CDOM concentrations and qualitative properties were not significant, except for a positive correlation with FMaxC5 (Kendall's τ = 0.12; P = 0.01). However, separating results by each stream revealed some significant correlations and indicating that within each watershed, DOM increased with discharge, especially during storms (Table 6). The only significant correlation with discharge during baseflow was with a_{254} in the Arboleda. Correlations between DOC and discharge were weak for the Arboleda (τ = 0.324) and not significant for the Taconazo, which differed from CDOM absorbance and fluorescence concentrations, which generally were significant during stormflow for both streams (range of 0.25 to 0.58 for Arboleda and 0.11 to 0.38 for Taconazo). Correlations between DOM quantity and quality and discharge were stronger in the Arboleda compared to the Taconazo. Discharge appeared to have less of clear influence on DOM properties (Table 6). $SUVA_{254}$ was significantly correlated with increasing discharge, only for the Taconazo during stormflow, yet the τ value was <0.3, indicating little influence of discharge on $SUVA_{254}$. S_R values were significant with discharge during stormflow but interestingly showed opposite trends, in which S_R decreased in the Arboleda yet increased in the Taconazo. Carbon isotopic composition of DOC was not influenced by discharge.

Table 6. Coefficient matrix of rank correlation values, using Kendall's tau statistic (τ), between discharge and DOM quantity and quality parameters. C1-C6 are FMax values for each PARAFAC component. '***' indicates P>0.001, '**' indicates P<0.01, '*', indicates P<0.05.

	Kendall's τ			
Parameter	Arboleda baseflow	Arboleda stormflow	Taconazo baseflow	Taconazo stormflow
DOC	0.040	0.324**	-0.008	0.157
C1	0.154	0.472***	0.012	0.303***
C2	0.151	0.490***	0.021	0.288***
C3	0.144	0.503***	0.026	0.325***
C4	0.064	0.569***	-0.010	0.186***
C5	0.025	0.347***	-0.030	0.306*
C6	-0.041	0.331**	0.128	0.019
a_{254}	0.254**	0.453***	-0.074	0.428***
S_R	-0.058	-0.347***	-0.092	0.223**
δ^{13}C-DOC	0.011	0.140	-0.194	-0.141
$SUVA_{254}$	0.057	0.101	0.063	0.284**

4.3. Properties of Probable DOM Sources

RGW, local groundwater, and storm events constituted the effects on DOM quality influencing the streams in this study (Table 7). During storm events, major sources of DOM to these streams were considered to be soils, throughfall, and precipitation. We included Guacimo Spring as representative of the regional groundwater (RGW) discharging into the Arboleda as a result of IGF [*Genereux et al.*, 2009]. Though not specifically a source of DOM, RGW was expected to transport degraded soil DOM into the Arboleda due to the several thousand year

residence time [*Genereux et al.*, 2009]. The mean (±SD) DOC value for RGW was 0.48±0.20 mg L^{-1} (N=6) and mean a_{254} value was 0.48±0.05 m^{-1}, much lower than in either stream. Regional groundwater $SUVA_{254}$ values were extremely low (mean = 0.49±0.20 L mg C^{-1} m^{-1}) indicating very low amounts of aromatic C in the regional groundwater discharging into the Arboleda. Mean S_R in regional groundwater was 7.29±2.89, 4-6 fold higher than in the streams.

Table 7. Summary statistics for regional groundwater (RGW) sampled at Guacimo Spring; precipitation; throughfall, and soil leachate. Standard deviations (±S.D.) of mean values are given in the text.

Parameter	Statistic	RGW	Precipitation	Throughfall	Soil leachate
DOC (mg L^{-1})	Mean	0.48	2.04	7.19	17.97
	Min	0.29	0.45	1.84	7.42
	Max	0.84	11.52	22.04	28.39
	N	6	2	10	3
a_{254} (m^{-1})	Mean	0.48	9.39	51.60	69.55
	Min	0.40	1.86	10.78	20.06
	Max	0.55	25.95	129.98	99.00
	N	6	2	10	3
$SUVA_{254}$ (L mg C^{-1} m^{-1})	Mean	0.49	2.03	3.03	1.64
	Min	0.28	0.47	1.84	1.17
	Max	0.76	4.04	4.08	2.37
	N	6	2	10	3
S_R	Mean	7.29	0.93	0.92	0.76
	Min	3.89	0.81	0.70	0.69
	Max	11.31	1.49	1.25	0.85
	N	6	2	10	3
δ^{13}C-DOC (‰)	Mean	-27.53	-26.69	-29.14	-27.21
	Min	-28.96	-32.81	-30.24	-27.51
	Max	-26.21	-21.78	-27.91	-26.81
	N	6	2	9	3

We were primarily interested in the quality of the soil leachate DOM to use as a comparison with stream, RGW, precipitation, and throughfall DOM properties. $SUVA_{254}$ values of the three soil leachates averaged 1.64±0.64 L mg C^{-1} m^{-1} and S_R values averaged 0.76±0.08. Mean δ^{13}C-DOC value of soil DOM was -27.20±0.36‰.

Throughfall samples exhibited a wide range in concentration and narrower range in quality (N=10). The mean [DOC] in throughfall was 7.19±6.03 mg C L^{-1} and mean a_{254} was 51.60±41.24 m^{-1}. Despite large ranges in [DOC] and a_{254} values, throughfall $SUVA_{254}$ values averaged 3.03±0.72 L mg C^{-1} m^{-1} while throughfall S_R values averaged 0.92±0.19. Mean δ^{13}C-DOC value of the throughfall samples was -29.14±0.79‰.

During throughfall collection, two samples of precipitation were also collected. Mean [DOC] of precipitation at La Selva was 1.07±0.08 mg C L^{-1} and mean a_{254} value was 0.61±0.10 m^{-1}. The $SUVA_{254}$ value of precipitation was much lower than any other source, 0.25±0.06 L mg C^{-1} m^{-1}, while mean S_R was high 3.99±2.20, but not as high as in regional groundwater. Mean precipitation δ^{13}C-DOC was -26.46±1.25‰. Overall, DOM in precipitation was of the same magnitude and of similar quality as the regional groundwater DOM.

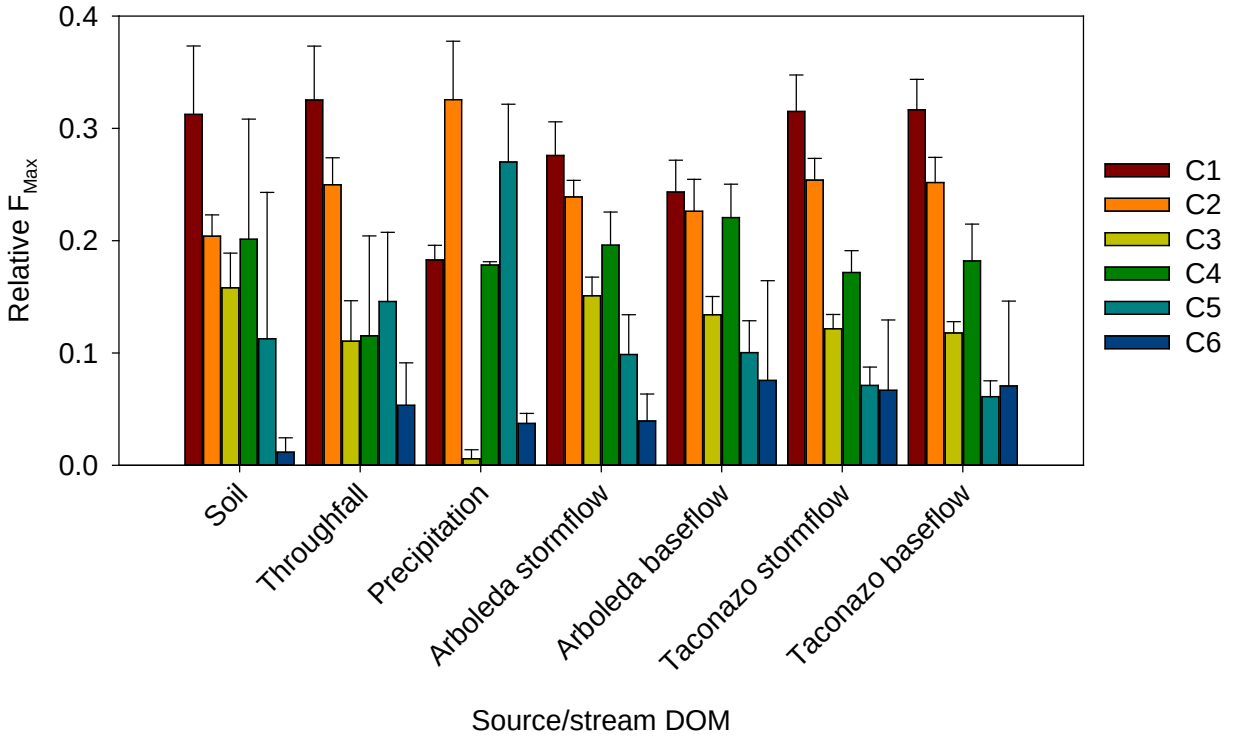

Figure 4. Relative F_{Max} values, expressed as a fraction of the sum of F_{max} values, for the six components identified in the PARAFAC model applied to DOM sources to the Arboleda and Taconazo stream: Soil leachate, throughfall, and precipitation. Mean values at stormflow and at baseflow are shown for the streams. Error bars indicate the standard deviation.

Because of the low number of observations for each DOM source, the PARAFAC model fit to Arboleda and Taconazo samples was applied to the soil leachate, precipitation, and throughfall samples. Regional groundwater generally had no detectable fluorescence. Much like the stream samples, FMax values of soil leachate and throughfall were ranked C1>C2>C4>C3>C5>C6 (Fig. 4). Precipitation deviated from this pattern, with a distribution of C2>C5>C1>C4>C6>C3 and nearly entirely lacking in the fluorescent marker for soil fulvic acid, C3. Notably, abundance of C6 was <5% for soil DOM, which also had the greatest abundance of C3 (ca. 15%). Throughfall was a mix of soil and precipitation signals.

PARAFAC model results demonstrate the similarity of DOM between the streams during stormflow was reflected in their similarity to soil and throughfall DOM fluorescence compared to

the precipitation DOM which was distinctly different (Fig. 4). Median FMax values for the each of the six components suggested that throughfall was enriched in C2, C5 and C6 relative to soil DOM which was enriched in C1 and C2 and C4. The spectral properties of C5 fluorescence were attributed to protein-like sources when matched to other PARAFAC models in the OpenFluor database, but these features also overlap with hydroxylated aromatic compounds such as tannins, which might indicate recent plant material rather than autochthonous production [*Hernes et al.*, 2009; *Stubbins et al.*, 2014]. C6 provided no matches in OpenFluor which presently lacks models of throughfall. The spectral properties of C6 are however quite similar to other plant-like aromatic compounds such as lignin phenols [*Hernes et al.*, 2009; *Wünsch et al.*, 2016].

4.4. Dissolved Organic Carbon Fluxes

The LOADEST, or Load Estimator program, was used to calculate stream export of DOC from the Arboleda and Taconazo watersheds, based on discharge and DOC concentrations [*Runkel et al.*, 2004]. DOC yield (DOC export divided by watershed area) was 17.5 g C m^{-2} yr^{-1} for the Arboleda and 2.79 g C m^{-2} yr^{-1} for the Taconazo (Table 8). Also, method M5 from *Birgand et al.*, [2010] was used to compute fluxes for the Arboleda and Taconazo as a comparison to LOADEST:

$$Flux = KV\frac{\sum_{i=1}^{n} CiQi}{\sum_{i=1}^{n} Qi} \quad (2)$$

where V is the annual cumulative stream water discharge (in m^3), C*i* and Q*i* are instantaneous [DOC] and stream discharge values (mg L^{-1} and m^3 min^{-1}, respectively), and K is a conversion factor to correct for different units. The M5 method resulted in DOC yields of 23.96 g C m^{-2} yr^{-1} for the Arboleda and 3.06 g C m^{-2} yr^{-1} for the Taconazo. The DOC yield values based on either methods were consistent with those calculated for the Arboleda and Taconazo by *Genereux et al.*, [2013] and *Ganong et al.*, [2015].

Table 8. Annual DOC export values (g C m^{-2} yr^{-1}) in 2012 and 2013 for the Arboleda and Taconazo streams computed using LOADEST and the M5 method, along with the mean export of the two methods.

Stream	LOADEST	Mean of M5 for 2012 and 2013	Mean of LOADEST and M5 methods
Arboleda	17.53	27.18	23.96
Taconazo	2.79	3.2	3.06

5. Discussion

5.1. Regional Groundwater Influences on Stream DOM

RGW exerted an extreme effect on DOM in the Arboleda via dilution with seemingly heavily degraded, lower molecular weight DOM. Median S_R values in Arboleda at baseflow (1.07 ± 0.1) were greater than median S_R values of the Taconazo during baseflow or stormflow (0.77 and 0.78). S_R values <1 typically are interpreted to indicate high molecular weight DOM, which likely is allochthonous [*Helms et al.*, 2008]. Our results are consistent with this interpretation and are clarified by the distinctiveness of the Arboleda S_R values which at base flow were greater than 1, owing to larger contribution by RGW at baseflow to this stream. *Genereux et al.*, [2002] estimate that IGF contributes roughly 35% of the flow to the Arboleda. Median S_R values for the Arboleda were 36% higher than for the Taconazo and appear to reflect the qualitative effect of dilution by

IGF as much as median DOC values reflect a quantitative effect.

Scant data exist in the literature for optical properties of DOM in groundwaters, especially for RGW. In our study, RGW $SUVA_{254}$ values (0.49±0.20 L mg C^{-1} m^{-1}) were much lower than values from other shallow and deep groundwaters [range: 0.8 to 3 L mg C^{-1} m^{-1}; *Chen et al.*, 2010; *Chapelle et al.*, 2011; *Shen et al.*, 2015]. Median S_R (7.29) likewise is much higher than the surface stream waters we sampled as well as reported values for local groundwaters (0.7 to 0.9) [*Chen et al.*, 2012; *Shen et al.*, 2015]. Also, RGW samples exhibited no measurable fluorescence, indicating any soil-derived DOM in RGW was heavily degraded. This result was remarkable in the sense that RGW fluorescence was essentially similar to our laboratory water used as a blank, water that has been extensively purified to remove DOM. A PARAFAC fluorescence model of deep groundwater (>600 m) compared to near-surface groundwater taken from a borehole in the Canadian Shield showed substantially reduced intensity, especially in humic-like components matching C1 and C4 from the La Selva model in this study [*Caron et al.*, 2010]. While the residence time in that study was not reported, the presence of fluorescent DOM, albeit at low intensities, suggests RGW impacting streams at La Selva was far more degraded than other bedrock groundwater. Altogether, these results strongly suggest that residence time of several thousand years [ca. 3000 yr; *Solomon et al.*, 2010] in bedrock groundwater during RGF affords ample time to remove DOM's fluorescence properties as well as produce DOM exhibiting $SUVA_{254}$ values <1 L mg C^{-1} m^{-1} and S_R values >5.

DOM quality parameters for RGW further suggest the long residence time was conducive to substantial DOM degradation. $SUVA_{254}$ and S_R values of RGW approximate heavily photobleached oligotrophic ocean seawater (0.82 to 0.41 L mg C^{-1} m^{-1} and 2.1to 8.9, respectively; *Helms et al.*, [2013]). Residence time of DOM in the ocean is on the order of 4000 years a timescale similar to regional groundwater in our study site. Extensive degradation of CDOM in the oceans via photochemistry and microbial degradation operate to produce weakly fluorescing DOM having $SUVA_{254}$ and S_R values similar in magnitude to the RGW in our study. The similarity in DOM quality between markedly different aquatic ecosystems is fascinating, and suggests that DOM converges to a common state in aquatic ecosystems and underscores the "recalcitrant" nature of oceanic and groundwater DOM in such dilute concentrations [*Arrieta et al., 2014*].

5.2. Stream DOM Quality Variations between Adjacent Watersheds

The major distinction between stream DOM quantity and quality in these paired, adjacent watersheds occurred at baseflow, which supported our assertion above about the effects of RGW on stream water DOM properties (Table 3 and Fig. 2). However, during stormflow we observed that the DOM quality in the streams became nearly indistinguishable (Table 3). This result at high stream discharge suggested the influence of terrestrial DOM pulses from the landscape to streams of both watersheds during storms.

We found a stronger effect of discharge on the Arboleda DOM than on the Taconazo DOM (Table 6). For example, Taconazo median DOC and CDOM concentrations increased by 78% and 53% respectively during stormflow, whereas in the Arboleda, DOC and CDOM concentrations increased nearly 200% (Table 3). Storm-induced increases in [DOC] have been widely reported in the literature for small, headwater catchments [e.g., *Qualls and Haines*, 1991; *Inamdar et al.*, 2006; *Raymond and Saiers*, 2010]. Recent work on a well-studied forested catchment in Maryland, eastern United States, showed roughly 6-fold increase in a_{254} values during stormflow compared

to baseflow, results consistent with our observed increases in a_{254} values during stormflow in the Costa Rican streams [*Singh et al.*, 2014] (Table 3). However, rank correlation values between [DOC] or CDOM concentration and discharge were generally low (<0.5) and this was consistent with the hysteresis often observed with [DOC] and other solute concentrations during storms, which has been described as a "flushing" of solutes from the watershed [*McDowell and Likens*, 1988; *Boyer et al.*, 1997; *Hinton et al.*, 1998]. The hysteresis appears attributable to the relative activation of different regions of the watershed and to the relative leaching of DOC from riparian or hillslope water sources to runoff in the catchment [*McGlynn et al.*, 2003].

Distribution of FMax values amongst sources from the PARAFAC model fit to EEM fluorescence provided distinct qualitative markers for the terrestrial DOM sources to the streams as a result of stormflow (Fig. 4). Soil and throughfall shared similar distributions though throughfall was enriched in C2, C5, and C6 relative to soil leachate. These latter components represent "protein-like" fluorescence as well as fluorescence signals from tannins such as gallic acid and soluble lignin degradation products [*Hernes et al.*, 2009; *Stubbins et al.*, 2014]. C5 and C6 fluorescence likely originated in DOM leaching of fresh land plant material washed off plant surfaces in throughfall but also material leached from leaf litter accumulating on the land surface during stormflow, as well as accumulating in these small streams during baseflow. This would explain the similar proportions of C6 during baseflow and stormflow in the Taconazo. In the Arboleda the dominance of RGW likely diluted this signal during baseflow. However, at stormflow, the similarity in relative FMax distributions between the Arboleda and the Taconazo is clear (Fig. 4). While FMax values were overall greater during stormflow than at baseflow for both streams, nonparametric MANOVA on all 6 PARAFAC components showed that there was a statistically significant difference ($P<0.05$) between stormflow and baseflow only in the Arboleda (Table 4). Further, there was not a significant difference between the Taconazo at stormflow and the Arboleda at stormflow. These results were consistent with $SUVA_{254}$ and S_R results and showed that DOM in the Arboleda and the Taconazo became more homogenous during stormflow, reflecting sources common to both streams, despite significant differences between the Arboleda and Taconazo during baseflow.

Our results were consistent with the assessment of groundwater-surface water mixing in the Arboleda and show the strength of the RGW effect on the Arboleda [*Genereux et al.*, 2013]. During stormflow the median S_R value for the Arboleda (0.93) was still much larger than the median S_R value of the Taconazo (0.78) and suggested an offset of the watershed addition of higher molecular weight material, which also was consistently higher in aromaticity. In fact, this observation suggests that RGW provided DOM inputs of similar quality and quantity to the Arboleda during both wet and dry seasons in Costa Rica [*Genereux et al.*, 2009; *Ganong et al.*, 2015]. RGW a_{254} values and [DOC] were far more similar to the Arboleda than to the Taconazo (Figs. 4 and 5). [DOC] in the RGW was roughly 50% and 30% of that in Arboleda and Taconazo at baseflow, respectively, and consistent with DOC concentrations reported in *Ganong et al.*, [2015]. These results support the prior observation that RGW discharging into the Arboleda dilutes CDOM and DOC from other sources such as local groundwater, precipitation, and overland flow [*Genereux et al.*, 2013]. By contrast, the Taconazo is fed by local groundwater (LGW) through surface organic horizons [*Solomon et al.*, 2010]. This resulted in less distinct differences in DOM quality between stormflow and baseflow in the Taconazo despite significant increases in DOC and CDOM concentrations (Tables 2 and 3).

5.3. Soil and Throughfall Influences on Stream DOM during Stormflow

We suspect the similarity in DOM properties between the streams during stormflow was due to overland runoff to the streams which was dominated both by DOM leached from soils and DOM in throughfall leached from canopy vegetation in the watersheds of each stream. Both soil leachate and throughfall have been shown previously to be present in streams at higher quantities during stormflow and exert a strong influence on DOM quality in those streams [*Inamdar et al.*, 2011; *Inamdar et al.*, 2013; *Singh et al*., 2014]. However, we did not have observations of stemflow which can also contribute large amounts of DOM to streams during rain events and could influence EEM spectra [*Hinton et al.*, 1998; *Levia et al.*, 2011; *Stubbins et al.*, 2017]. We used DOM fluorescence, $SUVA_{254}$, and $\delta^{13}C$ values to describe the relative contributions of these DOM sources to the Arboleda and Taconazo streams during stormflow.

We hypothesized that the ratio of the sum of throughfall components (C2+C5+C6) to the sum of soil components (C1+C3+C4) might be increased during a rain event (hereafter, the "TF/soil" ratio). Throughfall through the canopy accumulates DOM and should enrich streams at onset of significant precipitation and just prior to rising discharge. Figure 5 shows results from two storm events, one each from Arboleda and Taconazo, which confirm this supposition. The TF:soil ratio for DOM sampled in each stream over the 12-hour period of observation was highest as discharge was rising and then tapered off to a constant background during peak discharge and during the falling discharge (Figs. 4A,C).

This pattern is consistent with an influx of throughfall (and perhaps stemflow though we did not have observations of it) as precipitation fell through the canopy and contributed to the initial surface runoff into the stream. Then, as flood stage was reached and organic-rich surface soil regions of the watershed were activated, the stream DOM quality becomes more influenced by soil leachate. The ratio was linearly correlated with S_R values (Figs. 4B, D) which is consistent with the S_R values for throughfall (0.92±0.19) and soil DOM (0.76±0.08). Therefore, we hypothesize that the extensive canopy in the watersheds of these streams contributes substantial DOM to them during storm events.

$\delta^{13}C$-DOC values for both streams were highly variable (range: -21 to -37‰) but well within terrestrial DOM values from temperate and tropical streams and rivers [*Spencer et al. 2010*; *Bass et al. 2011; Lambert et al. 2016*]. However, neither the Arboleda nor the Taconazo exhibited a significant difference in $\delta^{13}C$-DOC value between baseflow and stormflow (Table 3). Sources of DOM from RGW, soil leachate, or throughfall exhibited a narrower range in $\delta^{13}C$-DOC values (-26.2 to -32.8‰) whereas precipitation $\delta^{13}C$-DOC values were as highly variable as the streams (Table 7). The wide range in $\delta^{13}C$-DOC values was surprising and suggested variability in $\delta^{13}C$-DOC values of the DOM sources themselves.

Fresh plant litter exhibits a range of $\delta^{13}C$ values (e.g., -25 to -30‰) in tropical ecosystems, based on differences among plant species [*Hammond et al.*, 2005]. Previous research on *Peperomia*, a common plant species in La Selva, found $\delta^{13}C$ values of -22.3 to -33.8‰, which overlaps the range of $\delta^{13}C$-DOC values we measured in the Arboleda and Taconazo [*Ting et al.*, 1985]. The variation in $\delta^{13}C$-DOC values within the same species could be due to seasonal changes [*Tieszen*, 1991]. Therefore, the heterogeneity of plant types and seasonal differences might partly explain the underlying variability in our $\delta^{13}C$-DOC values, and suggests that these $\delta^{13}C$ values reflect combinations of fresh plant-derived DOC in throughfall and soil DOM leached from the surrounding watershed.

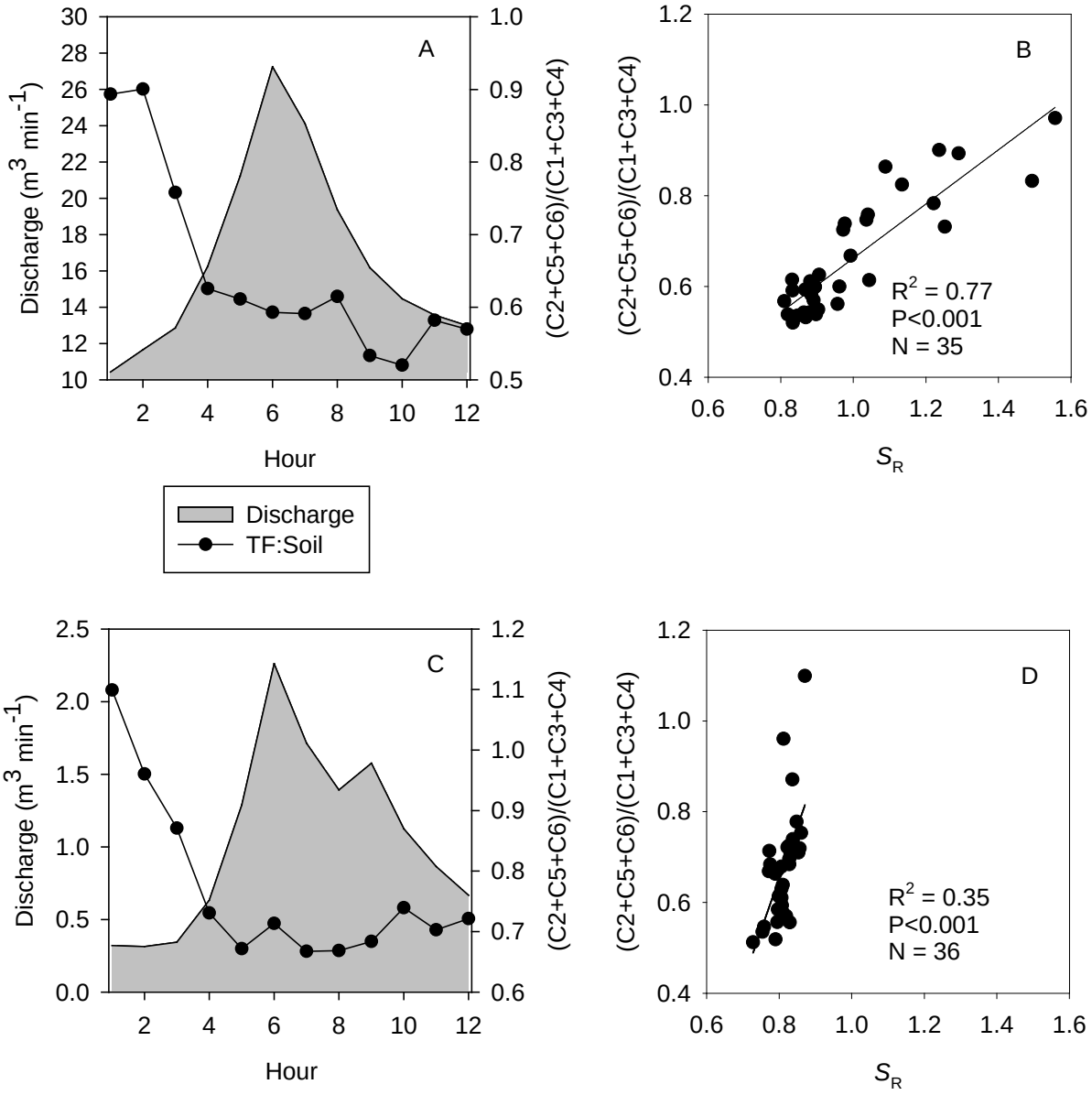

Figure 5. Changes in relative abundance of throughfall (TF) and soil sources of DOM to the Arboleda (A, B) and Taconazo (C, D) streams. A and C: ratio of TF to soil during a storm event plotted along with discharge. B and D: regression of ratio as a function of the spectral slope ratio value, S_R.

Lloret et al., [2016] have recently used $\delta^{13}C$ values to demonstrate the importance of plant litter to stream DOM pools in contrast to soil OM. Fresh plant litter consistently exhibited depleted $\delta^{13}C$ values (-29 to -30‰). However, these workers also discovered variability in isotope values between soil DOM extracted in water (-26 to -29‰) and to samples collected from lysimeters (wells; -30 to -34‰). The difference is attributed to an enrichment of soil OM of up to 4‰ relative

to plant material. Comparing wetland soils to hillslope soils during a storm event in the Kervidy-Naizin catchment (Brittany, France), a similar enrichment of δ^{13}C-DOC values was observed -28 to -23‰ [*Lambert et al.*, 2011]. The possible mechanism behind this enrichment is adsorption of ^{13}C-enriched carboxyl moieties onto soil inorganic particles. The resulting leached DOM is likewise enriched in ^{13}C.

$SUVA_{254}$ values and δ^{13}C values provided a framework to explain the variability of DOM sources to the Costa Rican streams, summarizing both effects of RGW and of soil and throughfall on stream DOM (Fig. 6). The DOM sources plotted along a gradient between enriched δ^{13}C-DOC value of low aromaticity (precipitation and RGW) and depleted δ^{13}C-DOC values of high aromaticity (throughfall). Notably, the high $SUVA_{254}$ values (>2.0 L mg C^{-1} m^{-1}) and δ^{13}C-DOC values <28‰ found in throughfall are consistent with a recent study of throughfall from trees in the coastal southeastern US, in which high resolution mass spectrometry was used to quantify aromaticity [*Stubbins et al.*, 2017]. Soil DOM plotted in between these end members likely for reasons previously discussed. Mean Arboleda and Taconazo values were plotted at baseflow and at stormflow with error bars representing standard deviations for both parameters. Mean stormflow values for each stream and mean Taconazo at baseflow plotted between the soil DOM and throughfall DOM values, implying the effect of both terrestrial sources on DOM quality.

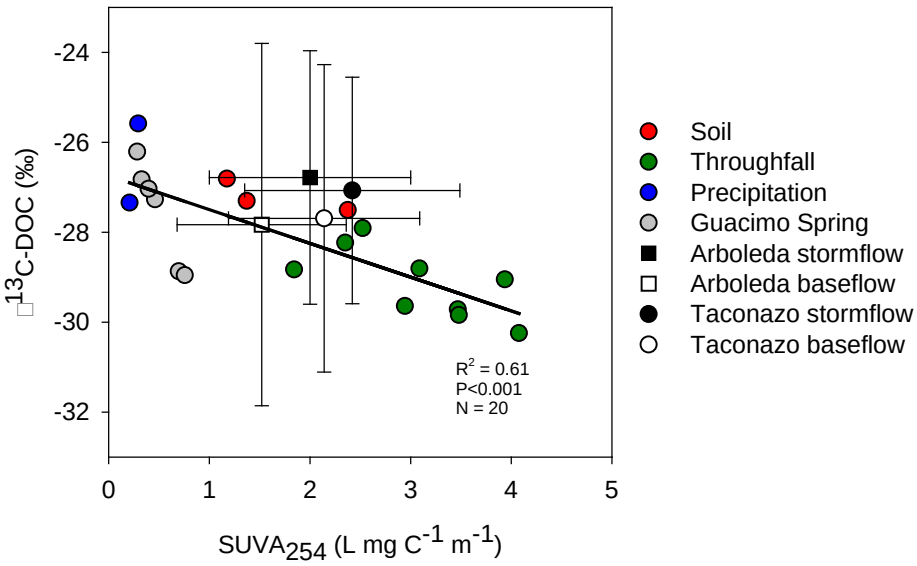

Figure 6. DOM stable carbon isotope composition (δ^{13}C-DOC) plotted as a function of DOC-specific absorption ($SUVA_{254}$) for probable DOM sources (regional groundwater at Guacimo Spring, soil DOM, precipitation, and throughfall) to the Arboleda and Taconazo streams. For the regression, only source sample data were used.

Heterogeneity in the results probably result from variable mixtures of these sources as well intense microbial recycling of organic matter in this warm tropical environment. It was also clear that the mean values of $SUVA_{254}$ and δ^{13}C-DOC for the Arboleda plotted closer to the Guacimo Spring values, which RGW. Interestingly, the stormflow mean δ^{13}C-DOC values for both streams was roughly 1‰ higher than baseflow mean values, a result which may be due to the difference in riparian wetland vs. hillslope soil sources of DOM as observed in the Kervidy-Naizin catchment. *Inmandar et al.* [2011] used a detailed study of stream and source DOM absorbance and fluorescence properties along with end-member mixing analysis (EMMA) to demonstrate that storm event DOM is enriched in aromatic and humic features, while baseflow DOM was less

aromatic and enriched in proteinaceous material. Their results are consistent with our findings for the Arboleda and Taconazo in that multiple sources – including throughfall, litter leachate and shallow soil water – produce DOM having high aromaticity (high $SUVA_{254}$ values). Although surface flowpaths exert a major control on DOM exports in streams, RGW appears to modulate this balance by creating a continuous export of water and solutes through the Arboleda during baseflow and stormflow [*Ganong et al.*, 2015]. The relationship of $SUVA_{254}$ to δ^{13}C-DOC is a clear linkage between the optics and chemistry of DOM in these streams and provided unique insight into the strong influence both of soil leachate and throughfall in shaping the DOM quality of these streams.

5.4. DOC Exports in Tropical Streams and the Role of RGW

DOC exports computed for the Taconazo were similar to DOC exports from other tropical and temperate watersheds, however the Arboleda exhibited much higher DOC exports than the Taconazo or many other streams. The Taconazo DOC export values fell within a range seen in other systems, ranging from small forested temperate and tropical streams to the Amazon River from 0.74 g C m^{-2} yr^{-1} to 9.40 g C m^{-2} yr^{-1} (Table 8). Estimates of Taconazo DOC export in this study also are similar to those calculated in 2006: 4.0 g C m^{-2} yr^{-1} [*Genereux et al., 2013*]. However, Arboleda DOC export calculated in this study was much higher than in 2006 [*Genereux et al. 2006*]. DOC export for the Arboleda was greater than many other studies, including comparatively large DOC exports from the tropical Q. Sonadora in Puerto Rico (6.59 g C m^{-2} yr^{-1}) and the Penobscot River in the northeastern US [*Aitkenhead and McDowell 2000*; *Spencer et al. 2013*]. However, the DOC export of the Arboleda was similar to Guadeloupe (French West Indies), particularly during the flood level exports. In Guadeloupe, the low water level exports ranged from 0.4 to 1.7 g C m^{-2} yr^{-1} and the flood level exports ranged from 11.3 to 42.2 g C m^{-2} yr^{-1} [*Lloret et al.*, 2011].

Storms exert an important control on DOC exports, representing about 30-70% of seasonal exports from catchments [*Hinton et al. 1998*; *Raymond and Saiers 2010*]. To assess the influence of storms on DOC flux from the Arboleda and Taconazo watersheds three storms were sampled every hour for 12 hours on three days in June 13, 2013, June 14, 2013, and June 25, 2013 (Table 9). The M5 method was used to compute storm fluxes (Equation 1). However, in this instance K represented the volume of water discharged per storm. In the Arboleda all three storms have a higher estimated flux (in only 12 hours) than the mean daily flux of 2.22×10^4 g C d^{-1}. The range of these storms was nearly 4-fold in DOC flux. In the Taconazo the mean daily flux was 2.13×10^3 g C d^{-1} and the range of DOC flux during storm events was nearly an order of magnitude larger. Similar to aforementioned studies of temperate watersheds, both the Taconazo and the Arboleda potentially export the majority of DOC during storms. However, the influence of IGF was apparent in that the magnitude of DOC flux contributed by a storm was proportionally less in the Arboleda than in the Taconazo. This result was consistent with the constant flow (and hence constant export) of DOC via the Arboleda due to the presence of regional groundwater.

Table 9. DOC exports for Arboleda and Taconazo streams compared to other tropical and temperate streams and large rivers.

Site	Export (g C m^{-2} yr^{-1})
Tropical streams	
Arboleda, Costa Rica[a]	23.96
Taconazo, Costa Rica[a]	3.06
Arboleda, Costa Rica[b]	14.10
Taconazo, Costa Rica[b]	4.00
R. Tempisquito, Costa Rica[c]	3.7
R. Tempisquito Sur, Costa Rica[c]	2.7
Q. Kathia, Costa Rica[c]	1.9
Q. Zompapa, Costa Rica[c]	4.3
Q. Sonadora, Puerto Rico[d]	7.43
Q. Toronja, Puerto Rico[d]	3.30
Rio Isocacos, Puerto Rico[d]	9.40
Juruena headwaters, Brazil[e]	3.15
Capesterra, French West Indies[f]	5.7
Deshaies, French West Indies[f]	1.60
Waikulu Stream, Hawaii – baseflow[g]	
Waikulu River, Hawaii – stormflow[g]	
Temperate streams	
Big Hollow Creek, Ohio[h]	4.40
Satellite Branch, North Carolina[h]	0.74
Batvia Kill, NY[i]	4.6
W. B. Neversink, NR Frost Valley, New York[i]	5.7
W. B. Neversink, NR Claryville, New York[i]	1.7
Big Elk Creek, Maryland[j]	1.8
Oberer Seebach, Austria[k]	4.01
Large rivers	
Amazon[l]	4.4
Congo[l]	3.4
Essequibo[l]	5.4
Mekong[l]	1.4
Fly[l]	8.6
Orinoco[l]	4.5
Parana[l]	2.1

[a]This study, [b] *Genereux et al.*, [2006], [c]*Newbold et al.*, [1995], [d]*Aitkenhead and McDowell*, [2000], [e]*Johnson et al.*, [2006], [f]*Lloret et al.*, [2011], [g]*Wiegner et al.*, [2009], [h]*Mulholland et al.*, [1997], [i]*Raymond and Saiers*, [2010], [j]*Dhillon and Inamdar*, [2013], [k]*Fasching et al.*, [2015], [l]*Raymond and Spencer*, [2014]

Table 10. Estimated DOC flux by each stream during three storm events in 2013.

Event	Arboleda Flux (g C storm^{-1})	Taconazo Flux (g C storm^{-1})
Storm 1	2.37 x 10^4	2.38 x 10^3
Storm 2	7.91 x 10^4	1.98 x 10^4
Storm 3	5.83 x 10^4	5.66 x 10^3

6. Conclusions

Emerging details on the variability of DOM dynamics in tropical ecosystems suggests that wet and dry periods result in different amounts of DOC being exported and, similar to temperate ecosystems, much of this export is event driven [*Raymond and Saiers*, 2010; *Bass et al.*, 2011; *Spencer et al.*, 2012]. Recent work at La Selva has shown that RGW adds complexity to this dynamic, driving higher export of DOC even with comparatively lower DOC concentrations that surface waters [*Genereux et al.*, 2013; *Ganong et al.*, 2015]. Here, we have demonstrated that stream DOM chemistry is similarly affected by RGW and strongly influences the quality of the DOM exported.

A major finding of this study is that the DOM properties in regional groundwater bears striking similarity to oligotrophic oceanic DOM: a lack of measureable fluorescence, yet CDOM absorption spectral features resembling photobleached surface seawater. This finding implies that substantial degradation – possibly by subsurface microbes – exerts a major control on DOM in groundwater systems. The possibilities for similar biogeochemical processing of DOM in deep groundwater systems and the ocean – which can operate on similar timescales of 1000s of years – demand further investigation.

A second major finding was that stormflow exerted clear changes on the quality of DOM in streams by mobilizing more aromatic DOM and increasing the concentration of CDOM in streams. The sources of DOM in the Arboleda and Taconazo at stormflow and baseflow was very similar, as indicated by a wide range of δ^{13}C-DOC values in both streams showing no statistically significant difference between flow regime or between streams. We believe this is evidence that the DOC in runoff to the streams during storms is comprised primarily of material leached from fresh plant litter which is mobilized in throughfall (and possibly stemflow) as well from organic-rich surface soils. Future work should investigate how storms in tropical watersheds influence the relative proportions of throughfall and stemflow to soil sources of DOM to streams, which could be an important dynamic in inland stream carbon cycling. Results from studies of lignin, an aromatic biopolymer of terrestrial vegetation considered to be recalcitrant to microbial degradation, in upstream waters of the Amazon River suggest a very rapid degradation of terrestrial DOM leading to a baseline stable state [*Ward et al.*, 2015]. This result is consistent with the baseline DOM properties of the Arboleda and Taconazo reflecting partially-degraded DOM and being markedly different from throughfall or soil-leached DOM. The transfer of canopy carbon into stream networks where it likely is rapidly metabolized is being realized as an important flux between terrestrial and aquatic ecosystems [*Stubbins et al.*, 2017]. Throughfall DOM in streams may therefore be converging flowpath “hot spots” during the “hot moments” of storm events,

representing poorly quantified C fluxes that warrant further study [*McClain et al.*, 2003*; Cole et al.*, 2007].

Exports of DOC from the Arboleda and the Taconazo showed that regional groundwater was very influential in the amount of carbon exported in surface water stream systems. In stream ecosystems with sufficient canopy in their watersheds, the connection of carbon biogeochemistry to forest dynamics and regional hydrogeology may be stronger than previously realized when considering the effect of DOM inputs from throughfall in addition to regional groundwater. Both clearly need consideration in future work because both exert strong controls on DOM quality as well as quantity.

7. Acknowledgments

We thank Daniel Rojas-Jiménez and William Ureña for assistance with field collection of samples. The La Selva Biological Station and Organization for Tropical Studies (OTS) are thanked for logistical support. This work was supported by the US Department of Energy award DE-SC0006703. Statements and opinions in this report are those of the authors and do not necessarily reflect the views of the sponsoring agency.

References

Aitkenhead, J. A., & McDowell, W. H. (2000). Soil C: N ratio as a predictor of annual riverine DOC flux at local and global scales. *Global Biogeochemical Cycles*, *14*(1), 127-138.

Arrieta, J. M., Mayol, E., Hansman, R. L., Herndl, G. J., Dittmar, T., & Duarte, C. M. (2015). Dilution limits dissolved organic carbon utilization in the deep ocean. *Science*, *348*(6232), 331-333.

Aufdenkampe, A. K., Mayorga, E., Raymond, P. A., Melack, J. M., Doney, S. C., Alin, S. R., Aalto, R. E., & Yoo, K. (2011). Riverine coupling of biogeochemical cycles between land, oceans, and atmosphere. *Frontiers in Ecology and the Environment*, *9*(1), 53-60.

Bass, A. M., Bird, M. I., Liddell, M. J., & Nelson, P. N. (2011). Fluvial dynamics of dissolved and particulate organic carbon during periodic discharge events in a steep tropical rainforest catchment. *Limnology and Oceanography*, *56*(6), 2282-2292.

Birgand, F., Faucheux, C., Gruau, G., Augeard, B., Moatar, F. and Bordenave, P. 2010. Uncertainties in assessing annual nitrate loads and concentration indicators: Part 1. Impact of sampling frequency and load estimation algorithms. *Trans. ASABE* 53(2): 437-446.

Caron, F., Sharp-King, K., Siemann, S., & Smith, D. S. (2010). Fluorescence characterization of the natural organic matter in deep ground waters from the Canadian Shield, Ontario, Canada. *Journal of radioanalytical and nuclear chemistry*, *286*(3), 699-705.

Catalá, T. S. et al., 2015. Turnover time of fluorescent dissolved organic matter in the dark global ocean. Nat. Commun. 6: 5986.

Chapelle, F. H., Shen, Y., Strom, E. W., & Benner, R. (2016). The removal kinetics of dissolved organic matter and the optical clarity of groundwater. *Hydrogeology Journal*, *24*(6), 1413-1422.

Chen, M., Price, R. M., Yamashita, Y., & Jaffé, R. (2010). Comparative study of dissolved organic matter from groundwater and surface water in the Florida coastal Everglades using multi-

dimensional spectrofluorometry combined with multivariate statistics. *Applied Geochemistry*, *25*(6), 872-880.

Cole, J. J., Prairie, Y. T., Caraco, N. F., McDowell, W. H., Tranvik, L. J., Striegl, R. G., Duarte, C. M., Kortelainen, P., Downing, J. A., Middelburg, J. J., & Melack, J. (2007). Plumbing the global carbon cycle: integrating inland waters into the terrestrial carbon budget. *Ecosystems*, *10*(1), 172-185.

Dhillon, G. S., & Inamdar, S. (2013). Extreme storms and changes in particulate and dissolved organic carbon in runoff: Entering uncharted waters?. *Geophysical Research Letters*, *40*(7), 1322-1327.

Fasching, C., Ulseth, A. J., Schelker, J., Steniczka, G., & Battin, T. J. (2015). Hydrology controls dissolved organic matter export and composition in an Alpine stream and its hyporheic zone. *Limnology and Oceanography*.

Fellman, J. B., Hood, E., & Spencer, R. G. (2010). Fluorescence spectroscopy opens new windows into dissolved organic matter dynamics in freshwater ecosystems: A review. *Limnology and Oceanography*, *55*(6), 2452-2462.

Findlay, S. E. G., & Sinsabaugh, R. L. (2003). *Aquatic ecosystems: interactivity of dissolved organic matter*. Academic Press.

Ganong, C. N., Small, G. E., Ardón, M., McDowell, W. H., Genereux, D., Duff, J. H., & Pringle, C. M. (2015). Interbasin transfers of geothermally modified ground water alter stream nutrient fluxes: an example from lowland Costa Rica in a global context. *Freshwater Science*, *34*, 276-286.

Genereux, D., & Pringle, C. (1997). Chemical mixing model of streamflow generation at La Selva biological station, Costa Rica. *Journal of hydrology*, *199*(3-4), 319-330.

Genereux, D. P., Wood, S. J., & Pringle, C. M. (2002). Chemical tracing of interbasin groundwater transfer in the lowland rainforest of Costa Rica. *Journal of Hydrology*, *258*(1), 163-178.

Genereux, D. P., Jordan, M. T., & Carbonell, D. (2005). A paired-watershed budget study to quantify interbasin groundwater flow in a lowland rain forest, Costa Rica. *Water Resources Research*, 41, W04011, doi:10.1029/2004WR003635.

Genereux, D. P., Webb, M., & Solomon, D. K. (2009). Chemical and isotopic signature of old groundwater and magmatic solutes in a Costa Rican rain forest: Evidence from carbon, helium, and chlorine. *Water Resources Research*, *45*, W08413, doi:10.1029/2008WR007630.

Genereux, D. P., Nagy, L. A., Osburn, C. L., & Oberbauer, S. F. (2013). A connection to deep groundwater alters ecosystem carbon fluxes and budgets: Example from a Costa Rican rainforest. *Geophysical Research Letters*, *40*(10), 2066-2070.

Helms, J. R., Stubbins, A., Ritchie, J. D., Minor, E. C., Kieber, D. J., & Mopper, K. (2008). Absorption spectral slopes and slope ratios as indicators of molecular weight, source, and photobleaching of chromophoric dissolved organic matter. *Limnology and Oceanography*, *53*(3), 955-969.

Helms, J. R., Stubbins, A., Perdue, E. M., Green, N. W., Chen, H., & Mopper, K. (2013). Photochemical bleaching of oceanic dissolved organic matter and its effect on absorption spectral slope and fluorescence. *Marine Chemistry, 155*, 81-91.

Hernes, P. J., Bergamaschi, B. A., Eckard, R. S., & Spencer, R. G. (2009). Fluorescence-based proxies for lignin in freshwater dissolved organic matter. *Journal of Geophysical Research: Biogeosciences, 114*, G00F03, doi:10.1029/2009JG000938.

Hinton, M. J., Schiff, S. L., & English, M. C. (1998). Sources and flowpaths of dissolved organic carbon during storms in two forested watersheds of the Precambrian Shield. *Biogeochemistry, 41*(2), 175-197.

Hammond, D.S. (Ed.), (2005), Tropical Forests of the Guiana Shield: Ancient Forests in a Modern World, CABI Publishing, Cambridge, MA.

Hood, E., Gooseff, M. N., & Johnson, S. L. (2006). Changes in the character of stream water dissolved organic carbon during flushing in three small watersheds, Oregon. *Journal of Geophysical Research: Biogeosciences, 111*, G01007, doi:10.1029/2005JG000082.

Hornberger, G. M., Bencala, K. E., & McKnight, D. M. (1994). Hydrological controls on dissolved organic carbon during snowmelt in the Snake River near Montezuma, Colorado. *Biogeochemistry, 25*(3), 147-165.

Inamdar, S., S. Singh, S. Dutta, D. Levia, M. Mitchell, D. Scott, H. Bais, and P. McHale (2011), Fluorescence characteristics and sources of dissolved organic matter for stream water during storm events in a forested mid‐Atlantic watershed, Journal of Geophysical Resesearch: Biogeosciences, 116, G03043, doi:10.1029/2011JG001735.

Inamdar, S., Finger, N., Singh, S., Mitchell, M., Levia, D., Bais, H., Scott, D., & McHale, P. (2012). Dissolved organic matter (DOM) concentration and quality in a forested mid-Atlantic watershed, USA. *Biogeochemistry, 108*(1-3), 55-76.

Johnson, M. S., Lehmann, J., Selva, E. C., Abdo, M., Riha, S., & Couto, E. G. (2006). Organic carbon fluxes within and streamwater exports from headwater catchments in the southern Amazon. *Hydrological Processes, 20*(12), 2599-2614.

Kothawala, D. N., C. A. Stedmon, R. A. Muller, G. A. Weyhenmeyer, S. J. Kohler, and L. J. Tranvik (2013), Controls of dissolved organic matter quality: Evidence from a large-scale boreal lake survey, Glob Chang Biol.

Kowalczuk, P., M. J. Durako, H. Young, A. E. Kahn, W. J. Cooper, M. Gonsior, 2009. Characterization of dissolved organic matter fluorescence in the South Atlantic Bight with use of PARAFAC model: Interannual variability. Marine Chemistry 113, 182-196.

Lambert, T., Pierson-Wickmann, A. C., Gruau, G., Thibault, J. N., & Jaffrezic, A. (2011). Carbon isotopes as tracers of dissolved organic carbon sources and water pathways in headwater catchments. *Journal of Hydrology, 402*(3), 228-238.

Lambert T., Teodoru C. R., Nyoni F., Bouillon S., Darchambeau F., Massicotte, P., and Borges A.V., 2016, Along-stream transport and transformation of dissolved organic matter in a large tropical river, Biogeosciences, 13, 2727-2741.

Levia, D. F., Van Stan, II, J. T., Inamdar, S. P., Jarvis, M. T., Mitchell, M. J., Mage, S. M., Scheik, C. E., & McHale, P. J. (2011). Stemflow and dissolved organic carbon cycling: temporal variability in concentration, flux, and UV-Vis spectral metrics in a temperate broadleaved deciduous forest in the eastern United States. *Canadian Journal of Forest Research, 42*(1), 207-216.

Littlewood, I. G. (1992). *Estimating contaminant loads in rivers: A review*. Report No. 117, Institute of Hydrology.

Lloret, E., Dessert, C., Gaillardet, J., Albéric, P., Crispi, O., Chaduteau, C., & Benedetti, M. F. (2011). Comparison of dissolved inorganic and organic carbon yields and fluxes in the watersheds of tropical volcanic islands, examples from Guadeloupe (French West Indies). *Chemical Geology, 280*(1), 65-78.

Lloret, E., Dessert, C., Buss, H. L., Chaduteau, C., Huon, S., Albéric, P., & Benedetti, M. F. (2016). Sources of dissolved organic carbon in small volcanic mountainous tropical rivers, examples from Guadeloupe (French West Indies). *Geoderma, 282*, 129-138.

McClain, M. E., Boyer, E. W., Dent, C. L., Gergel, S. E., Grimm, N. B., Groffman, P. M., Hart, S. C., Harvey, J. W., Johnston, C. A., Mayorga, E., McDowell, W. H., and Pinay G. (2003). Biogeochemical hot spots and hot moments at the interface of terrestrial and aquatic ecosystems. *Ecosystems, 6*(4), 301-312.

McGlynn, B. L., & McDonnell, J. J. (2003). Role of discrete landscape units in controlling catchment dissolved organic carbon dynamics. *Water Resources Research, 39*(4).

Mulholland, P. J. (1997). Dissolved organic matter concentration and flux in streams. *Journal of the North American Benthological Society, 16*(1), 131-141.

Mulholland, P. J. (2003). Large-scale patterns in dissolved organic carbon concentration, flux, and sources. *Aquatic ecosystems: interactivity of dissolved organic matter*, 139-159.

Murphy, K.R., Bro, R., Stedmon, C.A., 2014, Chemometric analysis of organic matter fluorescence. in: Coble, P., Baker, A., Lead, J., Reynolds, D., Spencer, R. (Eds.). Aquatic organic matter fluorescence. Cambridge University Press, New York. Osburn, C. L., Wigdahl, C. R., Fritz, S. C., & Saros, J. E. (2011). Dissolved organic matter composition and photoreactivity in prairie lakes of the US Great Plains. Limnology and Oceanography, 56(6), 2371-2390.

Newbold, J. D., Sweeney, B. W., Jackson, J. K., & Kaplan, L. A. (1995). Concentrations and export of solutes from six mountain streams in northwestern Costa Rica. *Journal of the North American Benthological Society, 14*(1), 21-37.

O'Gorman, P. A. (2012). Sensitivity of tropical precipitation extremes to climate change. *Nature Geoscience, 5*(10), 697-700.

Osburn, C. L., and St-Jean, G. (2007). The use of wet chemical oxidation with high-amplification isotope ratio mass spectrometry (WCO-IRMS) to measure stable isotope values of dissolved organic carbon in seawater. Limnology and Oceanography: Methods, 5(10), 296-308.

Osburn, C. L., and Stedmon, C. A. (2011a). Linking the chemical and optical properties of dissolved organic matter in the Baltic–North Sea transition zone to differentiate three allochthonous inputs. Marine Chemistry, 126(1), 281-294.

Osburn, C. L., Wigdahl, C. R., Fritz, S. C., & Saros, J. E. (2011b). Dissolved organic matter composition and photoreactivity in prairie lakes of the US Great Plains. *Limnology and Oceanography*, *56*(6), 2371-2390.

Osburn, C.L., Boyd, T. J., Montgomery, M. T., Bianchi, T. S., Coffin, R. B, and Paerl, H. W. (2016) Optical Proxies for Terrestrial Dissolved Organic Matter in Estuaries and Coastal Waters. Front. Mar. Sci. 2:127. doi: 10.3389/fmars.2015.00127

Raymond, P. A., & Bauer, J. E. (2001a). Riverine export of aged terrestrial organic matter to the North Atlantic Ocean. *Nature*, *409*(6819), 497-500.

Raymond, P. A., & Bauer, J. E. (2001b). Use of 14 C and 13 C natural abundances for evaluating riverine, estuarine, and coastal DOC and POC sources and cycling: a review and synthesis. *Organic Geochemistry*, *32*(4), 469-485.

Raymond, P. A., & Saiers, J. E. (2010). Event controlled DOC export from forested watersheds. *Biogeochemistry*, *100*(1-3), 197-209.

Raymond, P. A., Hartmann, J., Lauerwald, R., Sobek, S., McDonald, C., Hoover, M., Butman, D. A., Striegl, R. G., Mayorga, E., Humborg, C., Kortelainen, P., Dürr, H., Meybeck, M., Ciais, P., & Guth, P. (2013). Global carbon dioxide emissions from inland waters. *Nature*, *503*(7476), 355-359.

Raymond, P. A., Saiers, J. E., & Sobczak, W. V. (2016). Hydrological and biogeochemical controls on watershed dissolved organic matter transport: pulse-shunt concept. *Ecology*, *97*(1), 5-16.

Runkel, R. L., Crawford, C. G., & Cohn, T. A. (2004). *Load Estimator (LOADEST): A FORTRAN program for estimating constituent loads in streams and rivers,* Tech. Meth., 4, chap. A5, 69 pp., U. S. Geol. Surv., Denver, Colo..

Senesi, N. (1990). Molecular and quantitative aspects of the chemistry of fulvic acid and its interactions with metal ions and organic chemicals. 2. The fluorescence spectroscopy approach. Analytica Chimica Acta, 232(1), 77-106.

Shen, Y., Chapelle, F. H., Strom, E. W., & Benner, R. (2015). Origins and bioavailability of dissolved organic matter in groundwater. *Biogeochemistry*, *122*(1), 61-78.

Singh, S., Inamdar, S., Mitchell, M., & McHale, P. (2014). Seasonal pattern of dissolved organic matter (DOM) in watershed sources: influence of hydrologic flow paths and autumn leaf fall. *Biogeochemistry*, *118*(1-3), 321-337.

Solomon, D. K., Genereux, D. P., Plummer, L. N., & Busenberg, E. (2010). Testing mixing models of old and young groundwater in a tropical lowland rain forest with environmental tracers. *Water Resources Research*, 46, W04518, doi:10.1029/2009WR008341.

Spencer, R. G., Hernes, P. J., Ruf, R., Baker, A., Dyda, R. Y., Stubbins, A., and Six, J. (2010). Temporal controls on dissolved organic matter and lignin biogeochemistry in a pristine tropical river, Democratic Republic of Congo. Journal of Geophysical Research: Biogeosciences (2005–2012), 115, G03013, doi:10.1029/2009JG001180.

Spencer, R. G., Butler, K. D., & Aiken, G. R. (2012). Dissolved organic carbon and chromophoric dissolved organic matter properties of rivers in the USA. *Journal of Geophysical Research: Biogeosciences*, *117*, G03001, doi:10.1029/2011JG001928.

Spencer, R. G., Aiken, G. R., Dornblaser, M. M., Butler, K. D., Holmes, R. M., Fiske, G., Mann, P. J. & Stubbins, A. (2013). Chromophoric dissolved organic matter export from US rivers. Geophysical Research Letters, 40(8), 1575-1579.

Stedmon, C. A., Markager, S., Tranvik, L., Kronberg, L., Slätis, T., & Martinsen, W. (2007). Photochemical production of ammonium and transformation of dissolved organic matter in the Baltic Sea. *Marine Chemistry*, *104*(3), 227-240.

Stedmon, C. A., & Bro, R. (2008). Characterizing dissolved organic matter fluorescence with parallel factor analysis: a tutorial. *Limnology and Oceanography: Methods*, *6*(11), 572-579.

Stubbins, A., Lapierre, J. F., Berggren, M., Prairie, Y. T., Dittmar, T., & del Giorgio, P. A. (2014). What's in an EEM? Molecular signatures associated with dissolved organic fluorescence in boreal Canada. *Environmental science & technology*, *48*(18), 10598-10606.

Stubbins A, Silva LM, Dittmar T and Van Stan JT (2017). Molecular and optical properties of tree-derived dissolved organic matter in throughfall and stemflow from live oaks and eastern red cedar. Front. Earth Sci. 5:22. doi: 10.3389/feart.2017.00022

Tieszen, L. L. (1991). Natural variations in the carbon isotope values of plants: implications for archaeology, ecology, and paleoecology. *Journal of Archaeological Science*, *18*(3), 227-248.

Wallace, J. B., Cuffney, T. F., Eggert, S. L., & Whiles, M. R. (1997). Stream organic matter inputs, storage, and export for Satellite Branch at Coweeta Hydrologic Laboratory, North Carolina, USA. *Journal of the North American Benthological Society*, *16*(1), 67-74.

Ward, N. D., Bianchi, T. S., Sawakuchi, H. O., Gagne-Maynard, W., Cunha, A. C., Brito, D. C., Neu, V., de Matos Valerio, A., da Silva, R., Krusche, A. V., Richey, J. E., & Keil, R. G. (2016). The reactivity of plant-derived organic matter and the potential importance of priming effects along the lower Amazon River. *Journal of Geophysical Research: Biogeosciences*, 121, 1522–1539, doi:10.1002/2016JG003342.

Weishaar, J. L., Aiken, G. R., Bergamaschi, B. A., Fram, M. S., Fujii, R., and Mopper, K. (2003). Evaluation of specific ultraviolet absorbance as an indicator of the chemical composition and reactivity of dissolved organic carbon. *Environmental Science and Technology*, *37*(20), 4702-4708.

Wiegner, T. N., Tubal, R. L., & MacKenzie, R. A. (2009). Bioavailability and export of dissolved organic matter from a tropical river during base-and stormflow conditions. *Limnology and Oceanography*, *54*(4), 1233-1242.

Wünsch, U. J., Murphy, K. R., & Stedmon, C. A. (2015). Fluorescence quantum yields of natural organic matter and organic compounds: Implications for the fluorescence-based interpretation of organic matter composition. *Frontiers in Marine Science*, *2*, 98.

Yamashita, Y., Maie, N., Briceno, H., Jaffe, R. 2010. Optical characterization of dissolved organic matter in tropical rivers of the Guayana Shield, Venezuela. J Geophs Res 115, G00F10.

Yamashita, Y., Scinto, L.J., Maie, N., Jaffe, R., 2010. Dissolved Organic Matter Characteristics Across a Subtropical Wetland's Landscape: Application of Optical Properties in the Assessment of Environmental Dynamics. Ecosystems 13, 1006-1019.

Yamashita, Y., Boyer, J.N., Jaffe, R. 2013. Evaluating the distribution of terrestrial dissolved organic matter in a complex coastal ecosystem using fluorescence spectroscopy. Continental Shelf Research 66, 136-144

Zanon, C., Genereux, D. P., & Oberbauer, S. F. (2014). Use of a watershed hydrologic model to estimate interbasin groundwater flow in a Costa Rican rainforest. *Hydrological Processes*, *28*(10), 3670-3680.

Deep groundwater-derived CO_2 as a source for plant photosynthetic uptake in a Costa Rican rainforest

Steven F. Oberbauer. [1], Diego Dierick[1,2], David P. Genereux[3], Christopher L. Osburn[3], Diana Oviedo-Vargas[3]

Abstract

The role of export of carbon via surface waters has been increasingly appreciated as an important component of ecosystem carbon budgets. However, the role of groundwater as an input of carbon to ecosystems is relatively poorly known. In a lowland rainforest in Costa Rica, inputs of geological (deep crustal) dissolved inorganic carbon (DIC) in regional groundwater greatly increase stream water carbon concentrations. Here we test if that groundwater-derived carbon represents a significant source of CO_2 for photosynthesis of riparian plants in the recipient watershed. We compared the isotopic signatures of air, plant tissue and soil near two weir-equipped streams with different inputs of high-DIC regional groundwater; the Taconazo has no inputs, and about 40% of stream discharge of the Arboleda is derived from regional groundwater. Concentrations of CO_2 in air along the Taconazo remained in the normal range of forest canopy CO_2 concentrations. In contrast, CO_2 concentrations in air along the Arboleda occasionally exceeded 1000 ppm and below the weir by the splash zone were often higher than 1500 ppm and occasionally exceeded 3000 ppm. Elevated CO_2 in air was also found at a small waterfall on the Quebrada Sura, the higher order stream into which the Arboleda flows. We found slightly higher $\delta^{13}C$-CO_2 in air above the Arboleda compared to the Taconazo, consistent with an enhanced flux of isotopically-heavy CO_2 from the Arboleda. Keeling plots of air samples taken at the Arboleda and Sura deviated from those over the Taconazo and clearly indicated a source of CO_2 other than atmospheric air and respiration. Measurements of ^{14}C-CO_2 in air near the Arboleda clearly revealed the presence of geological CO_2 derived from regional groundwater. $\delta^{13}C$ of leaf samples taken at the two streams were not strongly different, but ^{14}C measurement of leaves and soils indicate the presence of groundwater-derived carbon. Our data indicate that CO_2 dissolved in regional groundwater delivered from upslope catchments in the Central Cordillera to lowland watersheds supplements photosynthesis of riparian plants, especially near areas of turbulent water flow. This pathway represents another source of carbon for photosynthetic fixation in the ecosystem, in addition to the atmosphere.

[1]Department of Biological Sciences. Florida International University, Miami, FL 33199, USA. [2]Current address: La Selva Biological Station, Organization for Tropical Studies, Puerto Viejo de Sarapiqui, Costa Rica. [3]Department of Marine, Earth, and Atmospheric Sciences, North Carolina State University, Raleigh, NC 27695-8208, USA

Introduction

The role of export of carbon via surface waters has been increasingly appreciated as an important component of ecosystem carbon budgets (Richey et al. 2002, Mayorga et al. 2005, Cole et al. 2007, Dinsmore et al. 2010). The carbon (C) may be derived from ecosystem-derived sources such as dissolution of limestone (Plummer and Sprinkle 2001), export of soil respiration (Johnson et al 2008, Oquist et al. 2009), and breakdown of ecosystem carbon stores (Mayorga et al. 2005). Most research on this topic has focused on transport of C by shallow water arising from local rainfall within watershed. However, in some watersheds, C may be introduced from deep regional groundwater sources from upland recharge areas through interbasin groundwater flow (IGF, Genereux et al. 2005, Tóth 2009). In volcanic regions, this groundwater may be exposed to magmatic sources of CO_2 that may result in accumulation and transport of dissolved inorganic carbon (DIC) by the groundwater that ultimately mixes with surface derived water. The role of deep regional groundwater as a source of CO_2 into ecosystems is poorly known. Failure to correctly attribute these sources of the C to IGF rather than local shallow groundwater will result in erroneous estimates of carbon export from such watersheds (Genereux et al. 2013). Furthermore, the regional groundwater-derived carbon could potentially support increased stream productivity or, via degassing, terrestrial plant photosynthesis.

In a lowland rainforest in Costa Rica, inputs of elevated DIC in the form of dissolved CO_2 in regional groundwater greatly increase stream water carbon concentrations in some watersheds. At this site, DIC from IGF experiences little to no within-watershed sequestration and thus augments the C flux out of the watershed as stream flow and degassing flux from the stream. If IGF-derived CO_2 is a significant source to terrestrial plants, it should be included as a flux component in the ecosystem carbon balance that is not measured by eddy covariance methods. Here we compare concentration of CO_2 in air and the $\delta^{13}C$ and ^{14}C values of CO_2 in the air, plants, and soil adjacent to streams with and without regional groundwater inputs. We used a paired watershed approach comparing a stream without inputs of regional groundwater, the Taconazo, with a stream with 40% of its discharge derived from IGF, the Arboleda (Figure 1, Genereux et al. 2005, Zanon et al. 2014). We conducted additional measurements on the Quebrada Sura, the higher order stream fed by the Arboleda

Study site

The study was conducted at Organization for Tropical Studies La Selva Biological Station in the Atlantic lowlands of Costa Rica (10° 25′ 19″ N 84° 00 ′54″W, 35 to 135 m elevation). The forest is categorized at premontane tropical moist forest with an average annual rainfall of 4 m (Sanford et al. 1994). The study focused on a pair of watersheds, each equipped with v-notch weirs, with different inputs of high-DIC regional groundwater. The Taconazo watershed has no IGF, whereas about 40% of stream discharge of the Arboleda is a result of IGF (Genereux et al 2013). Secondary observations were made at the head waters of both of these streams; the headwaters of the Arboleda are above the zone of regional groundwater release and represent an area without regional groundwater inputs. Additional measurements were made at a small cascade in Quebrada Sura (Figure S1), the higher order stream the Arboleda joins about 250 m upstream of the cascade.

Groundwater-derived carbon in air above streams

Figure 1. Study site general location within Costa Rica (inset) and paired streams and sampling locations. Modified from Oviedo-Vargas et al 2015).

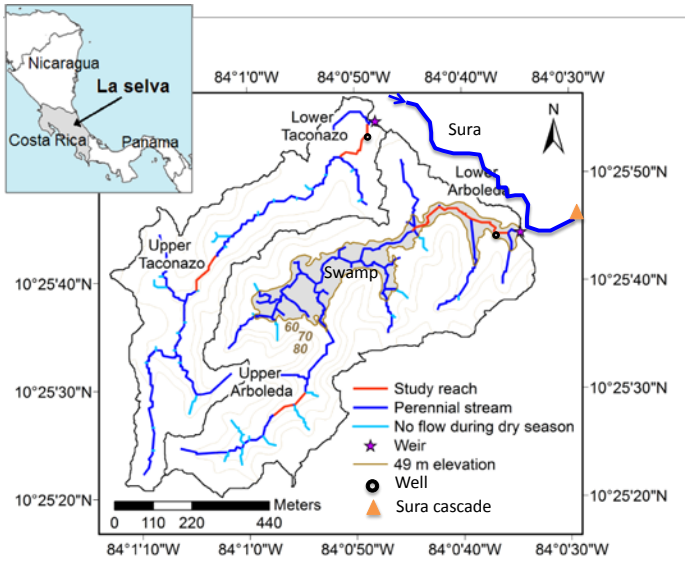

Fig. 2. Diel courses of concentration of CO_2 below the Taconazo weir (no input), the Arboleda weir (IGF input) and Sura cascade (IGF input).

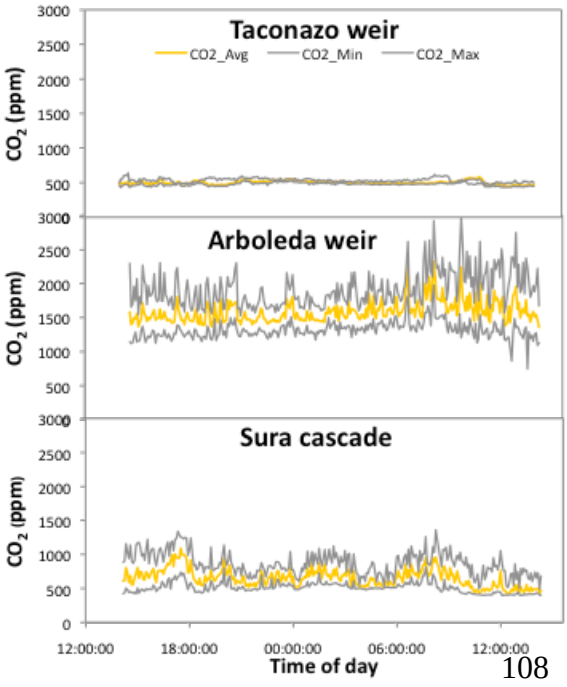

Concentrations of CO_2 in air along the Taconozo and at the weir remained in the normal range of forest canopy CO_2 concentrations (< 600 ppm, Figure 2A). Concentrations of CO_2 in air at the headwaters of the Arboleda, upstream of the zone of regional groundwater discharge, were similar to those at the headwaters and the weir of the Taconazo (data not shown). In contrast, concentrations of CO_2 in air just upstream of the Arboleda weir near calm water occasionally exceeded 1000 ppm and were generally above normal nighttime and early morning values of canopy storage of respiratory CO_2, and values below the weir by the splash zone were often higher than 1500 ppm and occasionally exceeded 3000 ppm (Figure 2B). A cascade on the Sura 250 m downstream of the confluence with the Arboleda (the source of the IGF) also showed elevated CO_2 (Figure 2C). These results are consistent with the high degassing rates estimated using tracers and flux chambers in previous studies by Oviedo-Vargas et al. (2015, 2016). Normalized by watershed area, an estimated 299 g C m^{-2} y^{-1} is lost from the Arboleda catchment compared to 48 g C m^{-2} y^{-1} for the Taconazo (Oviedo-Vargas et al. 2015).

The values $\delta^{13}C\text{-}CO_2$ in air above the Arboleda were somewhat enriched compared to those from the Taconazo, with values from the Sura intermediate (Figure 3A), but the differences were not significant in all cases and do not definitively indicate the presence of a source of $^{13}C\text{-}CO_2$ other than the bulk atmosphere and respired CO_2.

The $\delta^{13}C$ of CO_2 derived from regional groundwater at this site (-4.8 ‰, Genereux et al. 2013) is distinctly different from that of atmospheric air (-8.6 ‰). However, the CO_2 in air in the vegetation boundary layer layer is a typically a mixture of the background atmospheric CO_2 and the CO_2 from sources within the ecosystem, largely respiration of plants and soil organisms metabolizing organic matter derived from plants with the C_3 photosynthetic pathway (-20 to -31 ‰, Sternberg et a. 1989). Consequently, samples taken in the morning before air mixing occurs typically are more depleted than those taken in the afternoon when air throughout the canopy is well mixed with atmospheric air (Figure 3A).

Figure 3. Measurements indicate only a slight effect of regional groundwater on $\delta^{13}C$ of air, plant leaves, and soil at Arboleda and Sura sites compared to the Taconazo. Values are mean $\pm$ 1 SD, n = 5 for air and plants and n = 6 for soil).

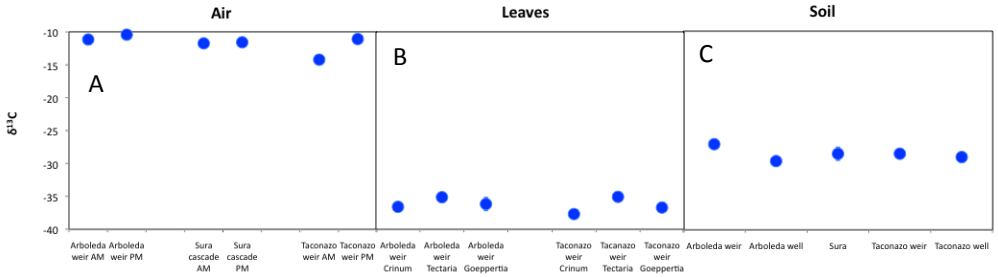

Figure 4. Plot of $\delta^{13}C$ of CO_2 vs. $1/[CO_2]$ for air in early morning (unmixed) and afternoon (mixed) above (calm) and below (splash zone) the Arboleda weir, below the Taconazo weir, the Sura cascade, and in the Arboleda swamp, where regional groundwater is upwelling.

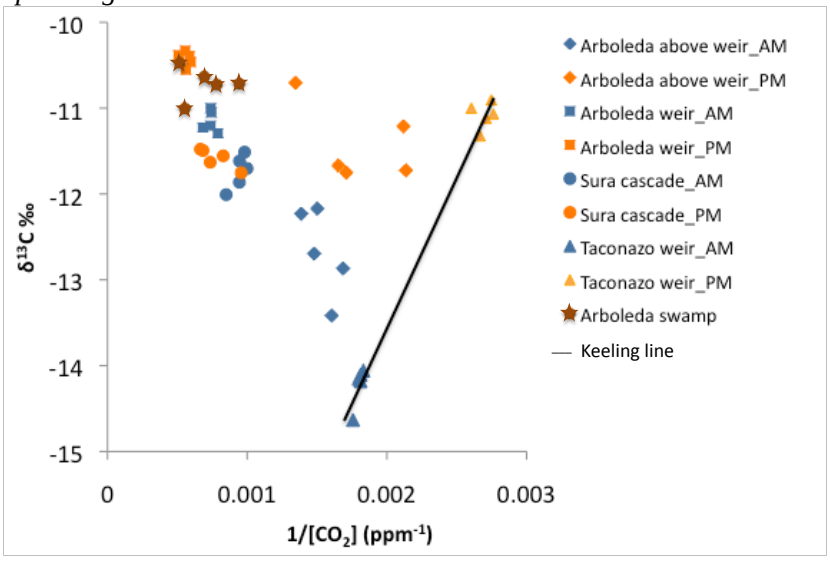

When $\delta^{13}C$ is plotted vs. $1/[CO_2]$, the IGF-derived CO_2 is readily apparent (Figure 4). If the only ecosystem source for CO_2 is respiration, as is the case for the air above the Taconazo, the result is a straight line (a Keeling plot, Keeling 1958, Pataki et al. 2003), with lower $\delta^{13}C$ at higher CO_2 concentrations and the y-intercept the $\delta^{13}C$ of the respired CO_2. In

contrast, the points for the Arboleda and Sura fall well off the Keeling plot line for the Taconazo because of their higher concentrations, indicating the additional source of degassed CO_2 from regional groundwater. The distance of the points from the respiratory/atmospheric line indicates the level of contribution of CO_2 from IGF. Sampling time significantly affected $\delta^{13}C$, with morning measurements generally lighter than afternoon measurements, likely a reflection of respiratory CO_2 build-up in mornings and mixing of boundary layer air with bulk atmosphere air in the afternoons.

As was the case for the ^{13}C-CO_2 analysis, air taken adjacent to the Arboleda and Sura for analysis of ^{14}C was strongly influenced by CO_2 from IGF. Samples for $\Delta^{14}CO_2$-C in air collected adjacent to the Arboleda weir in the unmixed layer early in the morning ranged from – 292 to -450 ‰, corresponding to 2710-4750 year bp (Figure 5A). Samples from the Sura cascade were -138 to -280 ‰, corresponding to 1140-2590 year bp. Samples upstream at the Arboleda well ranged from 0 to -58 ‰ (modern to 425 year bp). In contrast, samples collected at the Taconazo weir ranged from 9 to -26 (modern to 155 y bp, Figure 5a).

Figure 5. $\Delta^{14}C$ measurements indicated that regional groundwater carbon is found in air, plant leaves, and soil at Arboleda and Sura sites, but not the Taconazo. Values are mean $\pm$ 1 SD, n= 3 for air and leaves, n = 6 for soil.

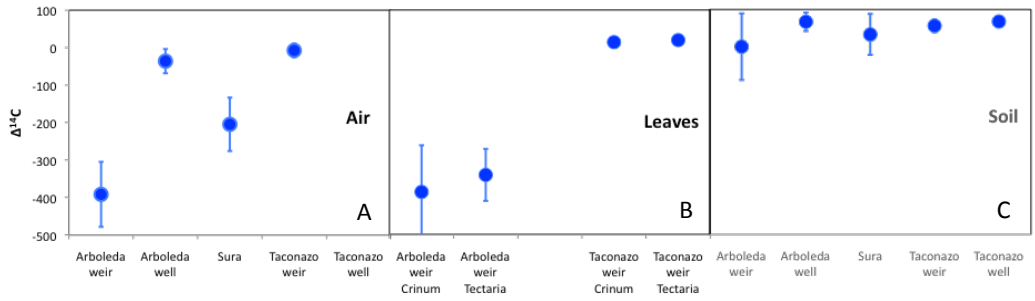

Groundwater-derived carbon in plant tissue

Leaf tissue samples from wet season and dry season all showed very light $\delta^{13}C$ values between -30 and -38 ‰ from all locations (Figure 4B). These signatures were found despite clear evidence that CO_2 enriched for ^{13}C is degassing from the Arboleda. Only one of the three species was significantly heavier at the Arboleda (*Crinum*). In principle, the influence of this air may be detectable through the $\delta^{13}C$ of carbon in plants growing near water bodies with regional groundwater inputs. If CO_2 from regional groundwater is released in forest understory under calm conditions, high concentrations of isotopically-heavy CO_2 should be available for photosynthetic uptake that would enrich leaf tissues for ^{13}C. That this signal was not clearly detectable is a result of several factors. First, the difference between the $\delta^{13}C$ of CO_2 from regional groundwater and that of the bulk atmosphere is small (-4.8 vs. -8 ‰). Second, photosynthetic uptake of CO_2 discriminates against ^{13}C, resulting in $\delta^{13}C$ of leaf tissue ranging from -20 to -31 ‰ for C_3 plants exposed to atmospheric air (Kohn 2010). In the forest understory where calm conditions

allow significant canopy storage of respiratory CO_2, plants may be taking up depleted CO_2 derived from C_3 plant tissue-based respiration, especially in the morning hours before canopy air mixing (CO_2 recycling; Sternberg et al. 1989), resulting in tissue as light as -38 ‰. The $\delta^{13}C$ of soil respiratory CO_2 measured at La Selva (in the same week as the data in Figure 4) near the canopy flux tower (Loescher et al. 2003) was 26.9$\pm$ 0.2 SE. Thus, recycling of respiratory CO_2 and build-up of regional groundwater derived CO_2 have opposing effects on leaf $\delta^{13}C$ and the recycling may mask the regional groundwater effect. The calm conditions that allow build up of IGF-derived isotopically heavy CO_2 also allow build up respiration-derived isotopically light CO_2. In contrast, in areas or at times where air is well-mixed during the day and photosynthesis is taking up regional groundwater CO_2 mixed with atmospherically-derived CO_2, the signature of plants should be heavier. Depending on the local conditions, open canopy over large stream with good mixing of atmospherically-derived CO_2 down to forest floor or closed canopy over small stream with little mixing, uptake of CO_2 derived from regional groundwater may or may not be detectable in the $\delta^{13}C$ of leaf tissue. $\delta^{13}C$ is also strongly indicative of plant water use efficiency in response to changes in soil moisture (Farquhar et al. 1989); under dry conditions, discrimination is reduced and leaf tissue values are enriched for ^{13}C. However, the dry season in the study region is relatively mild and not likely to be a major factor in these riparian habitats.

Leaf samples of two plant species taken adjacent to the weirs of the Arboleda and the Taconazo showed highly statistically significant differences in $\Delta^{14}C$ among sites (Figure 5B). Plants near the Arboleda weir contained old carbon (-245 – 484 ‰, 2200 to 5200 years bp), whereas those at the Taconazo had modern carbon (>modern). These results differ from those of the $\delta^{13}C$ of plant tissue that did not definitively show the heavier groundwater signal. This result can be attributed to the large difference between $\Delta^{14}C$ of CO_2 in modern air vs $\Delta^{14}C$ of the groundwater-derived CO_2 (~40 vs -400 ‰, respectively) compared to a difference in between IGF-CO_2 and bulk atmosphere CO_2 of about 4 ‰ and IGF-CO_2 and respiratory CO_2 of about 23‰.

Groundwater-derived carbon in riparian soil

We tested riparian soil for evidence of groundwater-derived carbon, which should be a more integrative measure of the importance of this carbon. Soil samples taken at the Arboleda weir and Sura cascade showed evidence of IGF delivered carbon in the soil carbon in the form of depleted $\Delta^{14}C$ levels (Figure 5C). However, the signal was much smaller than that of ^{14}C in leaf tissue of riparian plants and not statistically significant becaue of a mix of samples with clearly old carbon with samples with >modern carbon. The samples from the Arboleda well and the Taconazo weir and well were all modern (Figure 5C), and in fact, enriched ($\Delta^{14}C$ = 56-68‰) relative to the background measured for air and leaf tissue at the Taconazo (~20 ‰). The small signal of IGF carbon in the soil likely arises because most of the soil carbon is derived from overstory tree leaves and roots from CO_2 fixed at the canopy level that would not have been exposed to much of the IGF derived-CO_2. Also, the background level of soil carbon seen for the Taconazo weir and well corresponds to an enriched bomb ^{14}C background of soil carbon fixed approximately 10 y prior to the year of sample collection (2015). These values suggest a slow turnover of soil carbon resulting in all values shifted toward more enriched. In the

case of the Sura cascade, the site is subject to frequent floods that scour the rocky substrate preventing accumulation of deep soil at the site. As a result, there is little riparian vegetation growing in the area below the cascade although the site has nearly full canopy coverage in the overstory.

Our data conclusively show that dissolved carbon dioxide upwelling in water from a distant catchment supplements plant photosynthesis along a stream in Costa Rican rainforest. While CO_2 release from vents and springs directly adjacent to mantle outgassing are well known to affect plant growth both positively and negatively, Raschi et al 1997, Badiani et al 1999, in the present case the CO_2 is delivered via water flow from a catchment many kilometers distant. The quantity of carbon released from the study catchment is substantial, equivalent to 24 - 27% of annual soil respiration estimates for 2013 to 2015 (1119 to 1267 g $m^{-2}yr^{-1}$) and 8 – 11% of previous estimates of total ecosystem efflux (2670$\pm$260 to 3560$\pm$180 g $m^{-2}yr^{-1}$, Loescher et al. 2003, Cavaleri et al. 2008, respectively). As might be expected, degassing was more prevalent in high turbulence areas. Waters of the Arboleda are relatively calm, so degassing could potentially be much higher with different stream bed configurations. Spot measurements of $\delta^{13}C$ in a calm area of upwelling on the Arboleda, a nearly impenetrable swamp, suggest these areas may be releasing more CO_2 than the stream. Efflux rates at the points of upwelling require further study. Although leaf samples showed very strong $\Delta^{14}C$ signatures of IGF, soil samples were not suggestive of incorporation of large amounts of the IGF CO_2 into the ecosystem. Stream degassing occurs continuously, so much of the CO_2 released during nighttime may be vented or leave the watershed by advection without being taken up by photosynthesis.

The Arboleda is just one of several streams with inputs of IGF at the study site, and it is likely that IGF may be occurring throughout the region. Geological conditions under which IGF may be transporting C are quite common globally (Genereux et al. 2013), so ecosystem studies in these regions would be advised to evaluate the possibility of IGF delivery of CO_2.

Methods

Detecting groundwater-derived CO_2 in air

Groundwater-derived CO_2 can potentially be detected both from above-normal local atmospheric concentrations as well as from the carbon isotopic composition of the CO_2. Typical concentrations in the forest understory range from 400 to 500 ppm during the daytime and up to 600 ppm at night when mixing is reduced and soil and tree respiratory CO_2 builds up in the canopy (canopy storage, e.g., Loescher et al. 2003). Concentrations greater than 600 ppm can generally be assumed to be inputs from an additional source.

The $\delta^{13}C$ of CO_2 derived from regional groundwater at this site (-4.8 ‰, Genereux et al. 2009) is distinctly different from that of atmospheric air (-8.4 ‰). Similarly, $\Delta^{14}C$ of DIC in groundwater corresponds to an age of 2400 to 4000 year bp (Genereux et al. 2009) whereas $\Delta^{14}C$ of air is currently 40 ‰ and falling as atomic bomb testing elevated ^{14}C is incorporated into biomass.

Diel courses of CO_2 concentrations above streams

Concentrations of CO_2 in air near streams were recorded by a GMP343 CO_2 transmitter (Vaisala, Helskini, Finland) over multiple 24 hr periods in the upper headwaters of the streams, in waters near wells approximately 100 m above each of the weirs, near the pools above the weirs, in the splash zone below the weirs, as well as at the cascade on the Sura. Data were stored as 5 min averages with maxima and minimum using Campbell 21X or CR200 dataloggers (Campbell Scientific, Logan UT, USA).

Measurements of $\delta^{13}C$-CO_2 and $\Delta^{14}C$-CO_2 of air samples

Samples of air for $\delta^{13}C$-CO_2 were taken by 30 ml syringe from unmixed (early morning) and mixed (afternoon) air near the wells and weirs of each of streams and the Sura cascade and stored in 12 ml screw-capped Exetainer vials (Labco Limited, Ceredigion, United Kingdom) for analysis of [CO_2] and $\delta^{13}C$. Exetainers were prepared using two different approaches. Initially, sample vials were flushed three times with N_2 gas with a syringe and then pressurizeded with 20 ml of nitrogen prior to sampling. During sampling, the vials were flushed three times with sample air and then pressurized with a 20 ml of sampled air. For collection of sample air, a battery-operated pump (Model NMP015, KNF Neuberger, Trenton, NJ, USA) connected to at least 3 m of bev-a-line tubing with a weighted end pulled air from the desired sample location. Air was sampled from the tubing using a three-way valve and syringe with a one-way valve. Following sampling the one-way valve was closed, a needle installed on the valve, and the needle was flushed with excess sample prior to injection into the vial. Vials not pressured at the time of sampling were rejected for use. In later samples when a vacuum pump became available, vials were evacuated prior to use. During sampling the vials were flushed twice with the air sample and then filled with 20 ml of sample air. Vials not under vacuum at the time of sampling were rejected for use. Samples were shipped as soon as possible to the University of California Davis Stable Isotope Facility where they were measured by ThermoScientific PreCon-GasBench system interfaced to a ThermoScientific Delta V Plus isotope ratio mass spectrometer (ThermoScientific, Bremen, DE). Carbon dioxide concentrations were measured during sampling by drawing the sample air through a LI-840 infrared gas analyzer (LI-COR, Inc, Lincoln NE, USA) or Vaisala GMT 221 CO_2 transmitter with the calibration shroud (Vaisala, Inc, Helsinki, Finland). For some measurements, the sample tube inlet was placed adjacent to the sample space of a Vaisala GMP343 open path CO_2 transmitter and readings recorded at the time of sampling.

Samples for $\Delta^{14}C$-CO_2 of air were taken at the two well sites, below the two weirs, and at the Sura cascade (n = 3 for all but the Taconazo well site, n =2). For measurement of $\Delta^{14}C$-CO_2 in air samples, air was drawn through a molecular sieve (Alltech 13 X**)** for 5 min at ~1 lpm using a micropump (KNF Model NMP015) following procedures described by Schuur and Trumbore (2006). Carbon dioxide was desorbed from the sieves by heating, cryogenically trapped and purified and converted to graphite. A replicate for the Taconazo well was lost in the trapping process. Samples were sent for analysis to the National Ocean Sciences Accelerator Mass Spectrometry facility (NOSAMS, Woods Hole Oceanographic Institute, Woods Hole, MA, USA).

Soil respiration rates and $\delta^{13}C$-CO_2 of respiration

Soil respiration consistently represents one the largest components of ecosystem CO_2 efflux to the atmosphere, provides a good reference for assessing the scale of IGF delivery of CO_2, and is one of the simplest of the efflux components to measure. We measured soil respiration twice monthly from 2012 to 2016 across a subset of long-term study plots stratified for soil type and slope (Clark and Clark 2000). These plots are those measured by Schwendenmann et al. (2003) with the addition of three plots that improved representation of the range of the soil phosphorus levels. Soil respiration measurements were made using a static chamber system with a LI-COR 840 CO_2/H_2O infrared gas analyzer and a Campbell CR200 datalogger for data recording. Eight aluminum 20 cm internal diameter chamber bases at each plot were fitted with a PVC cap for 5 minutes of recording of the increase in CO_2 concentration that was used to calculate flux rates.

Keeling plots for determination of the $\delta^{13}C$-CO_2 of soil respiration were taken near the base of the ecosystem flux tower at the site (Loescher et al. 2003) in April 2014. For the measurements, a LI-COR 840 CO_2/H_2O infrared gas analyzer configured in a closed loop with 1 lpm flow rates was linked to an aluminum cap that was attached to 20 cm ID aluminum bases that had been placed in the soil more than 48 h prior to measurements. Measurements were conducted at night. Prior to the measurements, an auxiliary 3 lpm pump connected to a soda lime scrub tube was placed in a closed loop to remove all CO_2 except that derived from soil respiration. The pump was run for 12 min, sufficient time for the chamber air to run through the scrub at least 12 times and concentrations to drop below 150 ppm. Following scrubbing, the chamber was connected to the 1 lpm pump system and samples were taken by 30 ml syringe approximately every two minutes from an inline three-way valve and injected into previously evacuated 12 ml Exetainer vials following procedures described above for air samples. Three replicates were made with seven samples each spanning a range of over 300 ppm CO_2.

Detecting groundwater-derived CO_2 in plant tissue and soil

Measurement of $\delta^{13}C$ and $\Delta^{14}C$ of plant tissue

An exploratory set of leaves was collected at the weirs of the two streams as well as their headwaters, and at two other areas of groundwater upwelling. Later, a regular schedule of leaf sampling was instituted whereby leaf tissue of three species was collected at both sites in wet season and dry season of 2011, 2013, and 2014. Single leaves of each species were collected below the weir and at four locations upstream of the weir at approximately 50 m intervals. The ideal design would be to use replicate samples of the same species at both streams but that proved to be impractical because of the uneven distribution of the plants and small number of the plants at the stream bank access points. Two of the species were shared between the two sites, a lily, *Crinum erubenscens* and a fern (*Tectaria incisa*). The third species collected at each site was different (*Piper reticulatum* at the Arboleda and *Spathiphyllum leave* at the Taconazo). At the Taconazo, flooding after initial sampling reconfigured the stream bank removing some individuals of the fern, which was substituted with leaves of another species of fern at some of the upstream locations. A final collection of leaves was taken in the end of the dry season in May 2015 with six replicate leaves from three shared species at the Taconozo and Arboleda

weirs. These species were a *T. incisa*, *C. erubenscens*, and *Goeppertia micans.* A fourth species was collected but the species at the two sites differed (*Selaginalla* at Taconazo and *Cylcanthus* at the Arboleda). Leaf samples were collected, returned to the lab in Florida (permit DEVS 227-2015), cleaned of any mud or sediment, and oven dried at 65 C for 48 hr. Dried leaves were returned to the laboratory at Florida International University where samples were brushed off with a fine artists paintbrush to remove any loose soil or leaf particles and lightly rinsed with deionized water. A ~5 mg intact leaf blade sample without midrib was sent for analysis of ^{14}C to the NOSAMS facility at Woods Hole Oceanographic Institute (http://www.whoi.edu/nosams/home). The remainder of the leaf samples were ground with a Spex Certiprep for analysis for $\delta^{13}C$ at the Florida International University Stable Isotope Facility using a Finnigan Delta C EA-IRMS.

Measurements of $\delta^{13}C$ and $\Delta^{14}C$ of soil

Soil cores approximately 10 cm deep and 1.5 cm diameter were taken for $\delta^{13}C$ and $\Delta^{14}C$ analysis in November 2015 at the Arboleda and Taconazo weirs, approximately 100m upstream of both weirs, and at the Sura cascade. Soils at the Sura cascade were very thin as the stream passes through a rocky channel and flooding frequently scours the bank. Samples were air dried before shipping in sealed scintillation vials to a USDA-approved soils lab. Samples were sterilized by autoclave prior to pulverizing with a mortar and pestle. Powdered samples were shipped to the NOSAMS facility for $\delta^{13}C$ and ^{14}C analysis.

Literature Cited

Badiani M., Raschi A., Paolacci A. R. and Miglietta F. 1999. Plants responses to elevated CO_2; a perspective from natural CO_2 springs. - In: Agrawal S. B. and Agrawal M. (Eds.), Environmental pollution and plant response, pp. 45 - 81. - Lewis Pub., Boca Raton.

Cavaleri, M.A., Oberbauer, S.F. and Ryan, M.G., 2008. Foliar and ecosystem respiration in an old-growth tropical rain forest. *Plant, Cell & Environment*, *31*(4), pp.473-483.

Cole, J., Y. Prairie, N. Caraco, W. McDowell, L. Tranvik, R. Striegl, C. Duarte, P. Kortelainen, J. Downing, and J. Middelburg. 2007. Plumbing the global carbon cycle: integrating inland waters into the terrestrial carbon budget, *Ecosystems*, *10*, 172-185, doi:10.1007/s10021-006-9013-8.

Clark, D.B. and Clark, D.A., 2000. Landscape-scale variation in forest structure and biomass in a tropical rain forest. *Forest ecology and management*, *137*(1), pp.185-198.

Dinsmore, K. J., M. F. Billet, U. M. Skiba, R. M. Rees, J. Drewer, and C. Helfter (2010), Role of the aquatic pathway in the carbon and greenhouse gas budgets of a peatland catchment. *Global Change Biology*, doi:10.1111/j.1365-2486.2009.02119.x.

Farquhar, G.D., J.R. Ehleringer, and K.T. Hubick. 1989. Carbon isotope discrimination and photosynthesis. *Ann. Rev. Plant Physiol.* 40: 503-537.

Genereux, D. P., M. T. Jordan, and D. Carbonell (2005), A paired watershed budget study to quantify interbasin groundwater flow in a lowland rainforest, Costa Rica, *Water Resources Research*, 41, W04011, doi:10.1029/2004WR003635.

Genereux, D.P., M. Webb, and D.K. Solomon. 2009. The chemical and isotopic signature of old groundwater and magmatic solutes in a Costa Rican rainforest: evidence from carbon, helium, and chlorine. *Water Resources Research* 45, W08413, doi:10.1029/2008WR007630.

Genereux, D.P., Nagy, L.A., Osburn, C.L. and Oberbauer, S.F., 2013. A connection to deep groundwater alters ecosystem carbon fluxes and budgets: Example from a Costa Rican rainforest. *Geophysical Research Letters*, *40*(10): 2066-2070.

Johnson, M. S., J. Lehmann, S. J. Riha, A. V. Krusche, J. E. Richey, J. P. H. B. Ometto, and E. G. Couto (2008), CO_2 efflux from Amazonian headwater streams represents a significant fate for deep soil respiration, *Geophys. Res. Lett.*, 35, L17401, doi:10.1029/2008GL034619.

Keeling CD (1958) The concentration and isotopic abundances of atmospheric carbon dioxide in rural areas. *Geochimica et Cosmochimica Acta* 13:322–334.

Kohn, M.J., 2010. Carbon isotope compositions of terrestrial C3 plants as indicators of (paleo) ecology and (paleo) climate. *Proceedings of the National Academy of Sciences*, *107*(46), 19691-19695.

Loescher, H.W., Oberbauer, S.F., Gholz, H.L. and Clark, D.B., 2003. Environmental controls on net ecosystem-level carbon exchange and productivity in a Central American tropical wet forest. *Global Change Biology*, *9*(3), pp.396-412.

Mayorga, E., Aufdenkampe, A. K., Masiello, C. A., Krusche, A. V., Hedges, J. I., Quay, P. D., J. E. Richey.. and Brown, T. A. (2005). Young organic matter as a source of carbon dioxide outgassing from Amazonian rivers. Nature, 436(7050), 538-541.

Oquist, M. G., M. Wallin, J. Seibert, K. Bishop, and H. Laudon (2009), Dissolved inorganic carbon export across the soil/stream interface and its fate in a boreal headwater system, *Environ. Sci. Technol.*, 43, 7364–7369.

Plummer, L. N., and C. L. Sprinkle (2001). Radiocarbon dating of dissolved inorganic carbon in groundwater from confined parts of the Upper Floridan aquifer, Florida, USA, *Hydrogeology Journal*, 9: 127–150.

Raschi A., Miglietta F., Tognetti R. & Van Gardingen P. R. (Eds.) 1997. Plant responses to elevated CO2. - Cambridge University Press, Cambridge U K .

Richey, J. E., Melack, J. M., Aufdenkampe, A. K., Ballester, V. M., & Hess, L. L. (2002). Outgassing from Amazonian rivers and wetlands as a large tropical source of atmospheric CO_2. *Nature*, 416(6881), 617-620.

Sanford Jr, R.L., Paaby, P., Luvall, J.C. and Phillips, E., 1994. Climate, geomorphology, and aquatic systems. *La Selva: Ecology and natural history of a Neotropical rain forest*, pp.19-33.

Schuur, E.A. and Trumbore, S.E., 2006. Partitioning sources of soil respiration in boreal black spruce forest using radiocarbon. *Global Change Biology*, *12*(2), pp.165-176.

Sternberg, L.D.S.L., Mulkey, S.S. and Wright, S.J., 1989. Ecological interpretation of leaf carbon isotope ratios: influence of respired carbon dioxide. *Ecology*, *70*(5), pp.1317-1324.

Schwendenmann, L., Veldkamp, E., Brenes, T., O'brien, J.J. and Mackensen, J., 2003. Spatial and temporal variation in soil CO 2 efflux in an old-growth neotropical rain forest, La Selva, Costa Rica. *Biogeochemistry*, *64*(1), pp.111-128.

Tóth, J. A. (2009), Gravitational Systems of Groundwater Flow: Theory, Evaluation, Utilization, Cambridge University Press, New York.

Zanon, C., D. P. Genereux, and S. F. Oberbauer (2014), Use of a watershed hydrologic model to estimate interbasin groundwater flow in a Costa Rican rainforest, *Hydrological Processes*, 28: 3670–3680, doi:10.1002/hyp.9917.

Figure S1. Sura cascade approximately 250 m downstream of junction of Sura and the Arboleda.